‘What volume increase is needed for the management of raised intracranial pressure in children with craniosynostosis?’

R. William F. Breakey

Great Ormond Street Institute of Child Health

University College London

This dissertation is submitted for the degree of

Doctor of Philosophy

London, July 2020

DECLARATION

I, Richard William Francis Breakey, confirm that the work presented in this thesis is my own. Where information has been derived from other sources, I confirm that this has been indicated in the thesis.

01/07/20

ABSTRACT

Craniosynostosis describes a fusion of one or more sutures in the skull. It can occur in isolation or as part of a syndrome. In either setting, it is a condition which may lead to raised intracranial pressure. The exact cause of raised intracranial pressure in craniosynostosis is unknown. It may be due to; a volume mismatch between the intracranial contents and their containing cavity, venous hypertension, hydrocephalus or airway obstruction, which is often a sequela of an associated syndrome. At Great Ormond Street Hospital, after hydrocephalus and airway obstruction have been treated, the next surgical treatment of choice is cranial vault expansion. This expansion has been shown to reduce intracranial pressure, interestingly despite its success, the reasons behind its benefits are not fully understood. Using reconstructed 3-dimensional imaging, accurate measurement of cranial volumes can now be achieved. The aim of this project is to use the advances in 3-dimensional imaging and image processing to provide novel information on the volume changes that occur following cranial vault expansion. This information will be combined with clinical metrics to create a greater understanding of the causes of raised intracranial pressure in craniosynostosis, why cranial vault expansion treats them and whether there is an optimal volume expansion.

IMPACT STATEMENT

As a surgical subspecialty craniofacial surgery sits in the Reuleaux triangle of a Venn diagram containing plastic surgery, neurosurgery and maxillofacial surgery. The craniofacial team is however far broader than its surgeons, relying on the input of; optometrists, ophthalmologists, speech and language therapists, ear, nose and throat surgeons, clinical psychologists, specialist nurses, neuroradiologists and geneticists among many others. In its simplest form craniofacial surgery is used to correct a range of congenital and acquired abnormalities of the skull, face, and jaws. For the patient with a craniofacial syndrome, one of the most pressing concerns in early life is raised intracranial pressure. A dangerous clinical situation, that if left untreated can lead to blindness and ultimately death. One technique used to treat raised intracranial pressure is expansion of the cranial vault. This creates a greater intracranial volume thereby lowering the intracranial pressure.

Currently the aim is to create as much volume as reasonably possible, in order that intracranial pressure is reduced, the growing brain has space to develop and hopefully a further vault expanding procedure is avoided. With efforts being made to find ways of further increasing intracranial volume, new dynamic surgical techniques have been developed, which have the potential to greatly increase intracranial volume without adding to the surgical morbidity. The amount of volume that one of these techniques creates, and its effects on clinical outcomes has not yet been studied, nor have the techniques been directly compared.

To overcome this, provide information for all stakeholders involved, and assist in surgical planning, this thesis presents a multidisciplinary, multicentred analysis of cranial vault expansion by integrating clinical patient data with medical image analysis. A new command line script for automated intracranial volume measurement was developed and validated. This has the potential to be used both clinically and academically. Clinically, the rapid calculation of pre-operative intracranial volume can aid surgical planning and guide discussions with patients' families. Academically, this automated tool markedly reduces both the time taken to calculate intracranial volumes and human error, affording the craniofacial researcher time and peace of mind. The in-depth analysis of all dynamic cranial vault expansion procedures undertaken at Great Ormond Street Hospital again provides information useful for clinicians pre-operatively, intra-operatively and post-operatively. It is hoped that the findings presented in this thesis will influence craniofacial practice, clinical decision making and surgical planning, provide stimulus for future craniofacial research and ultimately improve patient quality of life.

ACKNOWLEDGEMENTS

The decision to undertake a PhD was not one I took lightly. I am not a traditional academic, being more used to an operating theatre than an academic laboratory. I therefore, would not have been able to produce this work without the support and encouragement of many others. This PhD was funded by the generous donors to the FaceValue charity and The Royal College of Surgeons of England. My supervisors Silvia Schievano, Owase Jeelani and David Dunaway were vital to this work; Silvia for her unwavering encouragement and attuned, critical eye, Owase for opening my eyes to bigger picture thinking and David for supporting me from day one and being a constant source of clinical and academic inspiration. I must also thank Prof. Hayward and Greg James for their help and council throughout this process.

The physical completion of this work would not have been possible without the technical knowledge, academic critique and overall support of Dr. Paul Knoops. I started with a colleague but gained a lifelong friend. The wider FaceValue group guided me through from junior doctor to junior academic and their help along the way was invaluable, many thanks Ale, Will, Naiara, Freida, Thanos, Lara and Selim. I thoroughly enjoyed my collaboration with the team at Seattle Children's Hospital and my time there was made very enjoyable by Dr. Ezgi Mercan Keremoglu and Dr. Richard Hopper.

Outside of the wider group, the support from my family and friends has been exceptional, thanks mum, dad, Liam and Josh. Lastly thank you to my wife Cattie, for keeping me going when I was sure I'd taken the wrong path. It seems that you can in fact give birth to an elephant.

TABLE OF CONTENTS

LIST OF FIGURES

LIST OF TABLES

LIST OF ABBREVIATIONS

2D	Two-dimensional
3D	Three-dimensional
BET	Brain extraction technique
CNS	Central nervous system
CPP	Central perfusion pressure
CT	Computed tomography
DICOM	Digital imaging and communications in medicine
FGFR	Fibroblast growth factor receptor
FI	Fractional intensity
FOA	Fronto orbital advancement
GOSH	Great Ormond Street Hospital for Children
HU	Hounsfield Unit
ICC	Interclass correlation
ICP	Intracranial pressure
IQ	Intelligence quotient
MRI	Magnetic resonance imaging
NCI	Neurocognitive impairment
NIfTI	Neuroimaging Informatics Technology Initiative
OFC	Occipitofrontal circumference
ONSD	Optic nerve sheath diameter
PACS	Picture archiving and communication system
PROMs	Patient reported outcome measures
PVE	Posterior vault expansion
RED	Rigid external distractor
RMS	Root mean square distance
ROI	Region of interest
SAPVE	Spring assisted posterior vault expansion
SD	Standard deviation
SCH	Seattle Children’s Hospital

SAS	Spring assisted surgery
TGF	Transforming growth factor

Chapter 1 **INTRODUCTION**

1.1 Introduction

Craniosynostosis describes a fusion of one or more sutures in the skull. It can occur in isolation or as part of a syndrome. The incidence of craniosynostosis as a whole is estimated at between 1 in 2,100 and 1 in 2,500 live births (Johnson & Wilkie, 2011). In either setting, it is a condition which may lead to raised intracranial pressure (ICP), a potential cause of insidious optic atrophy, visual loss and possible developmental delay (Marucci, Dunaway, Jones, & Hayward, 2008). The exact cause of raised intracranial pressure in craniosynostosis is unknown. Historical thinking in craniofacial surgery would argue that craniosynostosis *does* indeed lead to raised intracranial pressure and that *it should* be treated by expansion of the cranial vault. This dictum still holds true in many units as evidenced by treatment protocols (Spruijt, Joosten, et al., 2015). There are however clinical and surgical variables to consider and sadly it is not as simple as the opening statement might suggest. This research aims to investigate how craniosynostosis affects intracranial pressure and, when treating this by cranial vault expansion, how much extra volume should the surgeon aim to create.

The multidisciplinary field of Craniofacial surgery is relatively recently established. Its broad aim being to restore face shape and function by repositioning the cranium and facial bones. The vast progress in this area over the past 60 years is attributed to the work of Paul Tessier (1917-2008). Tessier in partnership with his neurosurgical colleagues, in particular Gerard Guiot, pioneered transcranial surgery, revolutionising the treatment of severe congenital deformity and, in doing so, created the new subspecialty of craniofacial surgery. Tessier was both a pioneer of craniofacial surgery and an

ambassador for it, travelling the world widely (including to Great Ormond Street Hospital) to train the first generation of craniofacial surgeons (Jones, 2008) (Figure 1.1).

Figure 1.1 Tessier consulting at UCLA circa 1980.

The modern-day craniofacial team has expanded beyond plastic and neurosurgery. In the UK it is now supra-regionally based and includes dentists, orthodontists, maxillofacial surgeons, speech and language therapists, ear, nose and throat surgeons, psychologists, ophthalmologists, optometrists, radiologists, geneticists and specialist nurses. The amalgamation of so many specialties reasonably reflecting the complexities faced by a patient with craniofacial problems. The expansion of the team to include myriad specialties has led to craniofacial research being extremely multifaceted. This thesis includes work with many of the aforementioned specialties and has been greatly helped by the advancement of 3-dimensional (3D) medical imaging.

1.2 Aims and objectives

Objective 1: Determine the optimal method of measuring intracranial volume

Cranial vault expansion procedures are carried out throughout the world in order to ameliorate raised intracranial pressure and to improve head shape in children who have craniosynostosis. At present, the optimal timing and technique for these procedures is unknown. The heterogenicity of craniosynostosis causing syndromes makes this decision process more difficult. The aim of this thesis is to utilise a multidisciplinary focus,

combining automated computer techniques with wide ranging clinical information in order to assess treatment techniques and improve management protocols.

The principal aim of this thesis is to provide an understanding of whether cranial vault expansion lowers intracranial pressure and use this understanding to inform on the optimal, patient specific, volume expansion, thereby improving surgical outcomes and patient quality of life.

In order that this principal aim is achieved, a number of objectives need to be met all of which requiring a sufficient amount of data, in particular 3D imaging. As a doctor I have undertaken my training with the dictum "*primum non nocere*" or "first do no harm" as a central ethical pillar. To apply this approach here means using currently available, clinically acquired, 3D imaging, and not exposing patients to any further radiation or anaesthesia. Once this data pool is established, the first objective is to investigate methods of measuring intracranial volume.

Objective 2: Generate ICV growth curves for individual craniofacial syndromes

Having determined the most effective method of measuring intracranial volume, I then propose to investigate the 'normal' intracranial volume, both in children affected by craniosynostosis as well as a control group of unaffected children. This investigation is made possible by the treatment protocol adopted by GOSH, whereby vault expansion surgery is performed on a reactive rather than the more widely adopted proactive basis (Forrest & Hopper, 2013). This makes 3D data available for a large age range of

unoperated skulls in children with craniosynostosis. This investigation serves two purposes: firstly, it describes the normal history of intracranial volume in unoperated skulls, which allows pre and post-operative comparisons and surgical assessment; secondly, the growth curves generated allow syndrome specific normalisation of growth when calculating volume changes between procedures. This approach to normalisation had been taken by Derderian et al. in 2015. The study included in this thesis expands on that work, increasing the number of data points and providing growth curves for syndromic craniosynostosis as well as control children (Derderian et al., 2015).

Objective 3: Understand the most advantageous ICV and how to achieve it

The third objective is to assess whether or not the volume expansion achieved by posterior vault expansion (PVE) has an advantageous effect. To do this requires volume change calculations from children undergoing PVE at GOSH and comparison of these changes to indicators of raised ICP. Once volume changes and outcomes following to PVE have been assessed, they are then compared to volume changes and outcomes achieved through other surgical methods.

1.3 Outline of the thesis

This thesis has the following structure:

Chapter 2 provides a background to craniosynostosis, intracranial pressure and cranial vault expansion.

Chapter 3 analyses and compares different methods of calculating intracranial volume in an effort to gain a thorough understanding of measurement techniques.

Therefore, allowing critical appraisal of other authors' volumetric work, and providing a framework of personal techniques going forward.

Chapter 4 provides reference growth curves for ICV and occipitofrontal circumference (OFC). This data is then used for the normalisation of growth in later cohort studies, whilst also providing a clinical tool whereby the ICV can be estimated from the OFC. This useful tool could be used in the outpatient clinic to perform a simple assessment of ICV and avoiding the need for further imaging.

Chapter 5 presents an ICV change analysis of consecutive spring assisted PVE (SAPVE) cases at GOSH. This data is accompanied by full clinical data to provide an analysis of the safety and efficacy of SAPVE in syndromic craniosynostosis.

Chapter 6 investigates the use of optic nerve sheath diameter (ONSD) measurement as an assessment of ICP. Non-invasive methods of assessing ICP can provide an immediate snapshot of the current intracranial pressure. ONSD is one such non-invasive method and has previously been used in adult trauma assessment, it is based on the presence of an enlarged optic sheath suggesting raised ICP transmitted intraorbitally.

Chapter 7 compares the operative parameters and volume expansion of three different techniques of posterior cranial expansion performed at two centres (GOSH and Seattle Children's Hospital (SCH)). This chapter's aim was to determine if there was an optimal surgical technique to achieve the required volume expansion.

Chapter 8 provides a summary of the main findings and outlines the contribution of these findings to the field of craniofacial surgery. Final conclusions are drawn and opportunities for further research are discussed.

Chapter 2 **BACKGROUND**

This chapter provides an overview of craniosynostosis, intracranial pressure, the relationship between craniosynostosis and intracranial pressure, and the history of the surgical procedures undertaken to address these problems.

2.1 Craniosynostosis

2.1.1 Background

The word craniosynostosis wonderfully describes the underlying condition it refers to, ‘cranio’ meaning skull, ‘syn’ meaning united and ‘osto’ meaning bone; the skull has united bones. Craniosynostosis covers a wide spectrum of disease involving the bones of the skull, and, whilst it is simple in its etymology, the condition that it defines is not.

Clinical descriptions of craniosynostosis date back to the time of Galen and Hippocrates; however, the first published reference appears to be Plutarchus’ (46-127 AD) description of the Greek statesman Pericles (495 – 429 BC) as ‘squill headed’ (a squill being a plant in the lily family with an elongated bulb) (Cunningham, Seto, Ratisoontorn, Heike, & Hing, 2007). Two thousand years later, Andreas Vesalius illustrated a series of specific skull shapes associated with the absence of various cranial sutures (Cunningham et al., 2007) (Figure 2.1).

Figure 2.1 Early illustration of specific skull shapes. From De Humani Corporis Fabrica, Andreas Vesalius (1552). Here skulls are depicted with absent sutures and abnormal shapes, interestingly the centre image on the top row appears to show a coronal synostosis but a scaphocephalic head shape. (Source: Cunningham et al., 2007)

A description of the growth restriction in craniosynostosis was published by Virchow in 1851 in his work entitled *Über den Cretinismus, namentlich in Franken, and über patholigische Schadelformen*, (Cretinism, Particularly in Franconia and Pathological Skull Forms) (Virchow, 1851). In his work he published the first organised descriptions of the various skull shapes associated with craniosynostosis (Figure 2.2). Virchow was the first to describe a skull containing a fused suture being growth restricted in a perpendicular vector to the suture, and that compensatory growth would take place via the remaining sutures.

Figure 2.2 Virchow schematic. Showing an axial view of the skull. Thick line – oxycephaly skull, thin line – dolichocephalic skull, dashed line – sphenocephalic skull. (Source: Persing et al., 1989)

2.1.2 Brief biological background

Since the time of Virchow's seminal paper, where he describes patients with craniosynostosis as 'changelings and monsters exchanged by Satan for the right children'

the causes of craniosynostosis have become far better understood (Persing et al., 1989). Understanding of the biological processes underpinning cranial sutures and skull vault growth has continued to improve. Cranial sutures are fibrocellular structures which allow deformation of the skull during passage through the birth canal and, in addition, they allow skull growth to occur in coordination with the rapid development of the brain in foetal life and early infancy.

There now exists an understanding that both environmental and genetic factors can predispose to craniosynostosis. In modern medicine, initial theories regarding the aetiology of craniosynostosis revolved around intrauterine constraint. Graham et al. published a brief clinical communication on the subject in 1979 and a case report detailing intrauterine constraint caused by a bicornuate uterus and triplet caught between the hips of its two siblings (Figure 2.3) (Graham, deSaxe, & Smith, 1979; Graham & Smith, 1980). Lakin et al. added weight to this argument with their 2012 twin study suggesting a 2.62 times great incidence of craniosynostosis in twins than unaffected controls ($p = <0.0001$), whilst also commenting on the role of foetal constraint in breech presentation (Lakin, Sinkin, Chen et al., 2012).

Figure 2.3 Drawing to show foetal head lodged in the left horn of the bicornuate uterus alongside the placenta. Thought in this case to have cause metopic craniosynostosis. (Source: Graham & Smith, 1980)

However contradictory evidence was later presented when studies using elongation of gestation rather than externally applied pressure found a higher prevalence

of fused sutures. In June 2000, Bradley et al. showed that after mini-plate compression of a foetal lamb skull, which avoided disruption of the normal suture dura interface, skulls had deformational changes rather than suture fusion, more closely representing positional plagiocephaly than a true craniosynostosis.(Bradley et al., 2000). Kirschner et al. in 2002 induced foetal constraint in mouse models by performing uterine cerclage and thus causing foetuses to grow for 2.5 days longer than their usual gestation period; this resulted in a spectrum of coronal and squamosal suture closure from narrowing to complete ossification. It also caused an upregulation of transforming growth factor (TGF) ß1 and a downregulation of TGF-ß3 (Figure 2.4 A and B) (Bradley et al., 2000; Kirschner et al., 2002).

Figure 2.4. A (left) Immunohistochemical staining of TGF-ß1. Top image shows non-constrained control and minimal staining at osteogenic front (of) and of the dura (d). Bottom image shows 2.5 days of foetal constraint and intense staining in the dura and in the overlying bone (arrowheads). **B** (right) Immunohistochemical staining of TGF-ß3. Intense staining in the non-constrained control (above), minimal staining in the 2.5 days constrained (below). (Source: Kirschner et al., 2002)

The transforming growth factors are part of a larger family of growth regulatory proteins which play a role in the regulation of bone formation and are involved in both normal and pathological suture closure, as shown by Opperman, Nolen, and Ogle (1997) and Roth et al. (1997). Other reported environmental factors include maternal valproate ingestion, hypophosphataemia and hypophosphataemia linked to excessive use of antacids in children (Jentink et al., 2010; Pivnick, Kerr, Kaufman, Jones, & Chesney, 1995; Roy, Iorio, & Meyer, 1981). Unproven, but observationally linked contributory factors may include maternal cigarette smoking and thyroid disease (Hackshaw, Rodeck, & Boniface, 2011; Rasmussen et al., 2007).

The genetic basis for craniosynostosis had a paradoxical start. Whilst a chromosomal region had been mapped for Saethre-Chotzen in 1992 (7p2), a specific causative gene was not found until 1993 when Jabs et al. presented a missense mutation of the *MSX2* gene in a single three generational family (Brueton, Van Herwerden, Chotai, & Winter, 1992; Jabs et al., 1993). This discovery held much promise and injected further energy into the search for a molecular genetic basis of craniosynostotic disease. Interestingly, however, *MSX2* mutations leading to craniosynostosis have not been further reported in the literature and Wilkie et al. in 2000 published a letter in Nature Genetics suggesting that *MSX2* mutations were more likely to cause skull ossification defects rather than craniosynostosis (Wilkie et al., 2000). Following the discovery of *MSX2,* many specific genes have been identified as the cause of craniofacial syndromes. These discoveries include the fibroblast growth factor receptor family *FGFR1, FGFR2, FGFR3,* the *TWIST1* genes (of which Saethre-Chotzen was later attributed to), *POR* mutations in Antley-Bixley syndrome, *EFNB1* mutations in craniofrontonasal syndrome and more recently *ERF* (which encodes a negative regulator of ERK1/2, the key signal transducer at the base of the pathway from growth factor receptors through RAS-MAP kinase) and *TCF12* which encodes a partner protein of TWIST1 (Twigg & Wilkie, 2015; Wilkie, 1997; Wilkie et al., 2006). Isolated forms of craniosynostosis are less often associated with genetic mutations and are more likely to occur spontaneously (Fearon, 2014; Morris, 2016).

FGFR2, FGFR3 and TWIST1 were the most commonly mutated genes found to cause syndromic craniosynostosis in a ten year analysis by Johnson and Wilkie (Johnson & Wilkie, 2011), and are the causative mutations in the majority of syndromes concentrated upon in this thesis. The FGFR2 gene encodes a transmembrane receptor

tyrosine kinase which comprise an extracellular ligand-binding region (immunoglobulin like domains IgI, IgII and IgIII), a single pass transmembrane region and split tyrosine kinase domain (TK1 and TK2). Heterozygous mutations of FGFR2 cause three classical craniosynostosis syndromes, those of Apert, Crouzon and Pfeiffer. There is phenotypical overlap with all exhibiting the Crouzonoid facial appearance. Localised recurrent missense substitutions, which encode proteins with gain of function properties are encoded for by FGFR2 and FGFR3. These lead to complex cellular changes with enhancement of proliferation, differentiation and apoptosis of osteoblast adjoining suture mesenchyme. It is believed that premature differentiation is probably the most important factor leading to craniosynostosis (Iseki, Wilkie, & Morriss-Kay, 1999).

The majority of Apert syndrome cases are caused by missense mutations of FGFR2, either Ser252Trp (66%) or Pro253Arg (32%) (Johnson & Wilkie, 2011). The Ser252Trp substitution is associated with a higher frequency of cleft palate, but milder syndactyly. Both Ser252Trp and Pro253Arg mutations result in enhanced binding to FGF2. Ser252Trp mutation displays a greater increase in affinity over the Pro253Arg mutation for most FGF ligands (Ibrahimi et al., 2005). Furthermore, Apert syndrome mutations appear to cause a loss of ligand binding specificity (Pro253Arg more so than Ser252Trp), with the greater loss of ligand binding specificity mirroring the severity of syndactyly in patients with Apert Syndrome. This explains the genotype – phenotype correlation seen in patients with Apert syndrome (Ibrahimi et al., 2005).

FGFR2 mutations in Pfeiffer syndrome overlap those in Crouzon syndrome, but the majority of severe cases are caused by a small subset of substitutions encoding Trp290Cys, Tyr340Cys, Cys342Arg or Ser351Cys (Lajeunie et al., 2006). The distribution of mutations causing Pfeiffer and Crouzon syndromes in FGFR2 has

considerable overlap with some authors referring to Crouzon-Pfeiffer together as part of a spectrum (Cunningham et al., 2007). Virtually all of the mutations associated with the phenotypes of Crouzon and Pfeiffer, are within the Ig-III domain of FGFR2c. The vast majority represent missense mutations however a small number of deletions and insertions have also been described. Twenty-one of the 52 missense mutations reported in the Ig III domain of FGFR2c result in either a gain or loss of a cysteine residue. The loss of a cysteine residue at position 342 (C342Y) is associated with a classic Crouzon phenotype (Mangasarian et al., 1997).

The domain structure of the protein encoded by FGFR3 is similar to that of FGFR2, and whilst its mutations are usually associated with bone dysplasia there are two heterozygous mutations relevant to craniosynostosis. One, a Pro250Arg substitution causes Muenke syndrome and the other, an Ala391Glu substitution cause a subtype of Crouzon syndrome; Crouzon syndrome with acanthosis nigricans. The Pro250Arg substitution in Muenke syndrome is the exact equivalent to the Apert Pro253Arg substitution in FGFR2, and also causes ligand dependent gain of function (Ibrahimi et al., 2004).

Mutations in the TWIST1 gene cause Saethre-Chotzen syndrome. These loss of function mutations include nucleotide substitutions (missense and nonsense), deletions, insertions, duplications, and complex rearrangements. They lead to functional haploinsufficiency of the basic helix-loop-helix transcription factor TWIST1. Unlike Apert syndrome there has been no genotype–phenotype correlation described, although in their 1998 paper Johnson et al. did find that large deletions are associated with learning disability (Johnson et al., 1998).

The brain will triple in volume over the first year of growth, reaching two thirds of its adult size. Rapid growth continues for the next two years before slowing to a steadier more gradual growth. Full adult size is reached between 6 and 10 years of age. Skull vault growth is facilitated by intracranial pressure, which produces tensile strains both directly upon the suture itself and indirectly upon the dura mater (a tough fibrous membrane which adheres to the inner surface of the skull vault and separates this from the brain); these strains drive bone deposition at the suture site (Herring, 2008). Cranial sutures are described as 'major' or 'minor'. The major sutures include the sagittal, coronal, metopic and lambdoid. The minor sutures include the squamosals, mendosal and intraoccipital among others (Figure 2.5)

Figure 2.5 3D reconstruction to show the normal cranial sutures. Shown from both axial and lateral views (**A** & **B**). Metopic (m), coronal (c), sagittal (s), lambdoid (l), squamosal (sq) and anterior fontanelle (af). (Source: Governale, 2015)

In line with Virchow's law, the fused suture or combination of fused sutures will result in a different head shape. The resultant head shapes of the major suture synostoses are described below.

2.1.3 Craniosynostosis described by fused suture(s)

Sagittal synostosis (Figure 2.6) causes a growth restriction perpendicular to the main midline suture of the skull. This results in compensatory growth through the remaining major sutures in the anterior and posterior areas of the skull. Posteriorly,

growth at the lambdoid sutures results in posterior dolichocephaly (often termed an occipital 'bullet') and anteriorly, growth at the coronal and metopic sutures results in frontal bossing. Both anterior and posterior growth contribute to an overall elongation and narrowing of the skull. Most commonly this head shape is referred to as scaphocephaly.

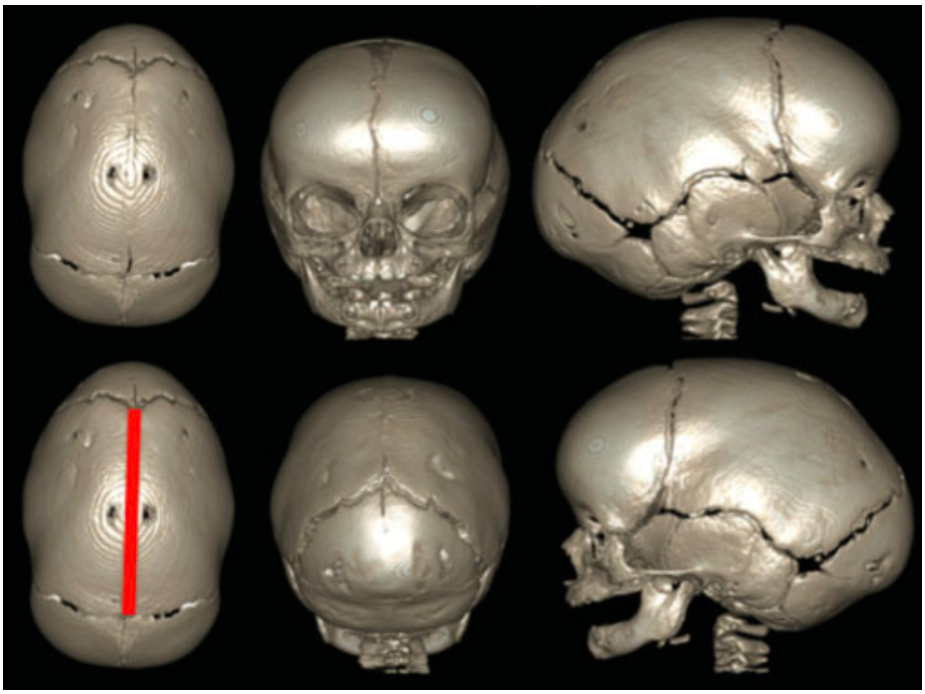

Figure 2.6 3D reconstruction to show the scaphocephalic head shape found in sagittal craniosynostosis. There is a long narrow skull, with frontal bossing and reduced posterior skull height (fused suture indicated by bold red line). (Source: Morris, 2016)

Coronal synostosis is more commonly found unilaterally (Figure 2.7) but can in some cases be bilateral (Figure 2.8). In a unilateral case, coronal synostosis results in an ipsilateral forehead flattening and elevation of the ipsilateral superior orbital rim. This can cause contralateral shift of the anterior fontanelle, and ipsilateral deviation of the

nasal root. In counteracting the restricted growth on one side of the forehead, the other coronal suture compensates, causing contralateral frontal bossing. This head shape is referred to as anterior plagiocephaly. In a bilateral case, the resultant head is shortened and widened. This is known as brachycephaly and, due to its multisuture nature, should prompt a search for a syndromic diagnosis (Governale, 2015), however with a genetic cause found in 17.5% of unilateral cases, these must also be fully investigated (Johnson & Wilkie, 2011).

Figure 2.7 3D reconstruction showing right sided unicoronal craniosynostosis. Flattening of the ipsilateral forehead, deviation of the nasal root towards the affected side, elevation of the supraorbital rim and contralateral forehead and temporal bossing are all illustrated (fused suture indicated by bold red line). (Source: Morris, 2016)

Figure 2.8 3D reconstruction to show bicoronal craniosynostosis. There is heightening and shortening of the calvarium giving turribrachycephaly. The lateral orbital rims are elevated and there is widening of the temporal regions (fused suture indicated by bold red line). (Source: Morris, 2016)

The metopic suture is of interest, in that unlike other the other major cranial sutures it is normal for it to be fused in infancy. CT based studies in children unaffected by craniosynostosis have shown children to develop radiological evidence for metopic suture fusion between 3 to 9 months with 100% showing fusion by 9 months (Weinzweig et al., 2003).

Indeed, prenatal 3D ultrasound studies have shown closure of the metopic suture in the glabella region at 32 weeks' gestation which then continues to progress superiorly towards the anterior fontanelle before birth (Faro, Benoit, Wegrzyn, Chaoui, & Nicolaides, 2005).

It is important to recognise that metopic suture fusion in childhood can be part of a normal process and instead it is the effects that an abnormal fusion may have on the remainder of the skull which requires intervention.

Abnormal metopic synostosis (Figure 2.9) causes a reduction in the width of the anterior section of the skull. Compensatory growth occurs at lambdoid and sagittal sutures leading to an increased width in the posterior section of the skull. Overall, this creates (when viewed from above) a triangular appearance of the skull, known as trigonocephaly. The forehead growth restriction can lead to varying degrees of hypotelorism (Fearon, Kolar, & Munro, 1996).

Figure 2.9 3D reconstruction to show metopic craniosynostosis. A vertical forehead or metopic ridge is shown, as is the posterior widening, giving the characteristic triangular shape skull known as trigonocephaly (fused suture indicated by bold red line). (Source: Morris, 2016)

Craniosynostosis of a lambdoid suture (Figure 2.10) is rare and results in an ipsilateral occipital flattening and reduction in skull height. There is compensatory growth from the contralateral lambdoid suture and the sagittal suture, resulting in contralateral posterior bossing. This head shape is called posterior plagiocephaly. It is interesting to

note here that this head shape can mimic the much more common head shape of positional plagiocephaly, which is a result of a baby lying repeatedly on one section of the skull. It is important to differentiate this from a craniosynostosis caused plagiocephaly as the positional form will correct itself once the child grains sufficient motor function to lie on a different part of the skull.

Figure 2.10 3D reconstruction to show left sided lambdoid craniosynostosis. There is ipsilateral occipital flattening and contralateral parietal and frontal bossing. There is a trapezoid shape rather than the parallelogram seen in positional plagiocephaly (fused suture indicated by bold red line). (Source: Morris, 2016)

2.1.4 Classification of craniosynostosis

To classify craniosynostosis effectively requires that all forms are considered. Craniosynostosis can be either isolated where one single suture is fused, or it can present as multi-suture synostosis where more than one suture is fused. Isolated craniosynostosis is more common and is further described by the suture that is fused. It leads to the characteristic head shapes described above. Multi-suture synostosis can be described as either ‘complex craniosynostosis’ when no other anomalies exist or as ‘syndromic synostosis’ when associated with anomalies outside of the skull. The incidence of craniosynostosis as whole is estimated at between 1 in 2,100 and 1 in 2,500 live births (Johnson & Wilkie, 2011). This varies greatly dependent on the type of craniosynostosis, with the incidence of multi-suture synostosis being considerably lower.

Of the multi-suture synostoses, the complex cases with no extra cranial anomalies occur less frequently than the syndromic cases and most do not appear to be associated with specific gene mutations (Czerwinski, Kolar, & Fearon, 2011). Regarding these cases, few retrospective studies exist; however, these studies suggest that the most common bi-suture fusions are of the metopic plus sagittal or a unilateral coronal and sagittal. The tri-sutural fusions are mainly of the sagittal and both lambdoid sutures, which gives a Mercedes Benz pattern. More recently this suture fusion pattern has begun to be associated with ERF related craniosynostosis and therefore may be part of a syndromic diagnosis (Glass et al., 2019). Fusion of the unilateral coronal, sagittal and contralateral lambdoid gives a Z-pattern. (Czerwinski et al., 2011; Greene, Mulliken, Proctor, Meara, & Rogers, 2008).

Although still rare, syndromic synostoses occur more frequently than their complex counterparts. Each individual syndrome is composed of a well-defined clinical pattern, that exists on a spectrum severity. Regardless of the severity, when compared to single suture synostoses, they impose a far greater challenge on the multi-disciplinary management team, requiring care from many different clinical specialties. Syndromic craniosynostosis tends to be genetic in nature and may demonstrate autosomal dominant, autosomal recessive and x-linked patterns of inheritance. Multiple different syndromes have been identified. The most commonly found include Muenke (variable incidence but may affect up to 20% of coronal synostosis patients), Crouzon (1 in 65,000), Saethre-Chotzen (1 in 25,000 -50,000), Pfeiffer (1 in 100,000) and Apert (1 in 100,000) (Forrest & Hopper, 2013). Of these five most common craniosynostotic syndromes, all but Saethre-Chotzen are associated with a gain of function mutation in the *FGFR* gene, with a loss-of-function mutation in the *TWIST* gene responsible for Saethre-Chotzen

(Cunningham et al., 2007). The pattern of fused sutures in syndromic craniosynostosis often involves the 'coronal ring', that being the coronal sutures bilaterally, the frontosphenoid and the sphenoethmoidal sutures (Forrest & Hopper, 2013). This results in a classic, tall or tower shaped head known as turribrachycephaly (Figure 2.11). There is often phenotypic overlap in cases of syndromic craniosynostosis and, therefore, diagnosis may rely on radiological and genetic investigations.

Figure 2.11 3D reconstruction to show turribrachycephaly. The tall, broad, tower shaped head of turribrachycephaly, caused by bicoronal synostosis and involvement of the coronal ring is shown. (Source: Forrest & Hopper, 2013)

Muenke syndrome differs from the other eponymous syndromes in that the name is derived from Muenke et al.'s 1997 paper describing a genetic mutation rather than a phenotype. The mutation is a pro250Arg mutation in *FGFR-3* on chromosome 4p (Muenke et al., 1997). Consistent features of Muenke syndrome include craniosynostosis of the coronal sutures, hearing loss, developmental delay and thimble like middle phalanges (Figure 2.12). Males tend to demonstrate a higher incidence of unicoronal synostosis than females; however bicoronal synostosis remains the dominant pattern (Honnebier et al., 2008).

Figure 2.12 Brachydactyly of the hands and feet in Muenke syndrome. Image from the original Muenke paper. (Source: M Muenke et al., 1997)

Crouzon and Pfeiffer syndromes are predominantly caused by mutations in the *FGFR-2* gene (a smaller percentage of Pfeiffer is caused by mutations in *FGFR-1* and exhibits a less severe phenotype) (Cornejo-Roldan, Roessler, & Muenke, 1999; Maximilian Muenke et al., 1994). Both are inherited in an autosomal dominant pattern. The overlapping of the *FGFR* mutations in Crouzon and Pfeiffer syndromes has led to them being thought of as part of a 'Crouzon-Pfeiffer' spectrum and they may now be referred to as Crouzon-Pfeiffer Syndrome. Whilst it exists on a spectrum of severity, Crouzon syndrome can present as the mildest of the *FGFR-2* associated craniofacial disorders, with characteristic Crouzonoid facial features of shallow orbits, midface hypoplasia, (Figure 2.13) a high arched palate and an anterior open bite. This is combined with an absence of limb anomalies and typically normal intelligence. Bicoronal synostosis is the most common craniosynostotic finding; however, pan-synostosis can be a late finding. The *FGFR-3* related, and often severe subtype of Crouzon syndrome is Crouzon Syndrome with acanthosis nigricans.

Figure 2.13 Crouzanoid features. A severe example of midface retrusion in a girl with Crouzon syndrome, this has necessitated a tracheostomy. (Source: Forrest & Hopper, 2013)

As with all craniofacial syndromes, Pfeiffer exhibits a variable pattern of severity. It is usually characterised by broad, radially deviated thumbs and / or great toes. Cohen proposed a classification of Pfeiffer in his 1993 paper. He designated 3 clinical subtypes: Type 1 described the classical Pfeiffer features of turribrachycephaly, midface hypoplasia, exorbitism, broad thumbs and great toes, and varying degrees of soft tissue syndactyly, in association with hypertelorism, strabismus, down slanting palpebral fissures, class III malocclusion and a beaked nose. Type 2 is more severe including a cloverleaf skull (Kleeblattschädel), and Type 3 is more severe again, with severe ocular proptosis; however, the cloverleaf skull is not present (Figure 2.14) (M Cohen, 1993). In 2009, Fearon and Rhodes published a review of treatment of patients with Pfeiffer syndrome outcomes in a single institution and indicated that the incidence of Type 1 was 61%, Type 2 was 25%, and Type 3 was 14%.

Figure 2.14 Pfeiffer features on CT scan. Severe exorbitism, shallow orbits and globe protrusion beyond the lateral orbital wall seen in Pfeiffer. (Source: Forrest & Hopper, 2013)

Saethre-Chotzen is the most commonly found syndromic craniosynostosis not associated with an *FGFR* mutation (Twigg & Wilkie, 2015). It exhibits a heterogeneous pattern of craniosynostosis, in line with its wide range of phenotypic severity in presentation. Caused by a mutation in the *TWIST-1* gene in chromosome 7p21.2, it is inherited in an autosomal dominant pattern (el Ghouzzi et al., 1997). Saethre-Chotzen is caused by a loss of function mutation in 7p21.2, however there is a subgroup that have

microdeletions of 7p21.1 which can be associated with significant learning difficulties (Johnson et al., 1998). Most patients with Saethre-Chotzen present with bicoronal synostosis (45-76%), with unicoronal synostosis found in 18-27% and multisuture synostosis found in 6-18%. In addition to the calvarial dysmorphology, patients with Saethre-Chotzen usually present with a low frontal hairline, ptosis, downward slanting palpebral fissures, prominent superior transverse crus, depressed nasal bridge, overall facial asymmetry and an incomplete syndactyly of the index and middle fingers and third and fourth toes (de Heer et al., 2004; Foo et al., 2009; Saethre, 1931).

Apert syndrome is found in around 1 in 100,000 births. This eponymous syndrome is named after French physician Eugene Apert following his publication De l'acrocephalosyndactylie in 1906 (Apert, 1906). Whilst the Apert name has remained attached to this syndrome since that time, the collection of findings had actually been published 20 years earlier by Troquart (Perlyn, Nichols, Woo, Becker, & Kane, 2009). During the development of the skull in a patient with Apert syndrome many factors combine to present a hyperacrobrachycephalic head shape (Cohen & Kreiborg, 1996). The cranial malformation is primarily due to coronal suture synostosis, but there is synostosis of multiple sutures. This is combined with abnormal fusion of the skull base sutures, namely the spheno-frontal, spheno-occipital and petro-occipital, to leave a shortened skull base and a small, crowded posterior fossa. To a varying degree, patients with Apert syndrome will suffer from exorbitism due to a widened cribriform plate and a shortened anterior fossa (Breik et al., 2016). The phenotype is characterised by turribrachycephaly, mid face hypoplasia and a symmetrical syndactyly of both feet and hands, which usually results in a mid-digital mass due to fusion of index, middle and ring fingers. Patients with Apert syndrome tend to have more severe midface hypoplasia than

those with Crouzon syndrome, leading to a concave midface, shallow orbits and ocular proptosis, mild hypertelorism and downward slanting palpebral fissures (Derderian & Seaward, 2012). Other facial features that patients may also exhibit include a depressed nasal bridge with downturned nasal tip, a high arched or sometimes cleft palate and an anterior open bite (Figure 2.15) (Derderian & Seaward, 2012). It is an autosomal disorder with gain-of-function mutations of the *FGFR-2* being responsible in 98% of cases (Cohen et al., 1992; Ibrahimi, Chiu, McCarthy, & Mohammadi, 2005). As described previously the majority of Apert syndrome cases are caused by missense mutations of FGFR2, either Ser252Trp (66%) or Pro253Arg (32%), with each mutation leading to a particular phenotypical presentation. Those patients with Ser252Trp mutation present more commonly with a cleft palate, whilst those with Pro253Arg present with a more severe degree of syndactyly (Ibrahimi et al., 2005).

Figure 2.15 A photograph showing a one-month old girl with Apert Syndrome. Midface concavity, turribrachycephaly, hypertelorism and downward slanting palpebral fissures are all shown. (Source: Derderian & Seaward, 2012)

As alluded to previously, children with multi-suture synostosis provide a more complex management challenge to the multidisciplinary team, and from here on this thesis will concentrate solely on these cases. The complexity of the challenge is due to the complexity of presenting craniofacial dysmorphia and the presence of extracranial anomalies. Treatment needs to be coordinated between many surgical teams (including craniofacial, ear, nose and throat, hand, cleft lip and palate, maxillofacial and dental),

nurse specialists, speech and language teams, and psychology specialists among others. Of the dangers associated with multi-suture synostosis, the most concerning are raised intracranial pressure, airway obstruction and exorbitism. It is accepted that raised intracranial pressure in craniosynostosis can contribute to optic atrophy and, therefore, visual impairment and potentially blindness; however debate exists regarding the contribution of raised intracranial pressure to neurocognitive impairment (Forrest & Hopper, 2013; Tay et al., 2006).

2.2 Intracranial pressure

Intracranial pressure (ICP) is a dynamic state driven by the volume of the intracranial contents and the force that their enclosing vault places upon them. Normal intracranial contents include the brain parenchyma (80%), blood (10%), and cerebrospinal fluid (CSF) (10%). Abnormal contents include space occupying lesions such a haematomas, abscesses and tumours. The modified Munro-Kellie doctrine states that the sum of all intracranial contents remains constant, i.e., an increase in one component must be offset by a decrease in another. In non craniosynostotic children, the unfused sutures allow for progressive expansion of the intracranial contents without increases in the ICP. If calvarial growth is disrupted, craniocerebral disproportion may occur. Here the enlarging intracranial contents are unable to be accommodated by the calvarium and ICP rises accordingly. ICP rises exponentially, with initial compensation provided by buffering mechanisms such as a lowering of CSF volume. Once these mechanisms become exhausted, ICP can rise rapidly, eventually leading to hindbrain herniation through the foramen magnum, which if left uncorrected can lead to death (Hott

& Rekate, 2014). Raised intracranial pressure has been extensively reported in children with syndromic craniosynostosis, with Tamburrini et al. documenting a 30-40% prevalence in their 2005 review, and also in non-syndromic craniosynostosis, although with a lower incidence of 15-20% (Tamburrini, et al., 2005; Thompson et al., 1995).

2.2.1 Normal intracranial pressure

One of earliest and most important publications from the craniofacial field regarding intracranial pressure in craniosynostosis was from Renier, Sainte-Rose, Marchac, and Hirsch in 1982. In this paper, the authors investigated relationships between neurocognitive impairment and raised ICP, and also changes in ICP following craniofacial surgery (Renier et al., 1982). Renier states that a definition of "normal" or "abnormal" ICP in children raises a problem as it is imprecisely defined; however, they considered ICP to be normal when below 10mmHg, abnormal above 15mmHg and borderline when in between. Hayward, Britto, Dunaway, and Jeelani questioned this assumption in 2016, quoting an Avery et al. study of opening pressures in 197 children, where the lower limit of normal was 8.5mmHg and the upper limit of normal was found to be higher at 20.6mmHg (Avery et al., 2010; Hayward et al., 2016). This study used lumbar punctures, performed with the patient in a lateral position, in a series of children aged between 1-18 years of age. Using a lumbar puncture to measure or asses ICP is an indirect method, as it is actually a measure of neuraxis CFS pressure (Wiegand & Richards, 2007). In Avery's study, no significant association was found between age and opening pressure, even when patients were grouped as 10 years or more or 10 years or less. The most commonly used levels remain those adopted by Renier et al. in 1982 and outlined above; however they have wide boundaries, making the detection of minor

changes difficult and many children present in the borderline category (Eide, Helseth, Due-Tønnessen, & Lundar, 2002). Another reported way of assessing whether a patient has normal ICP is to monitor the occurrence of Lundberg A and B waves. These are rises in ICP over 50 mmHg for durations of over 5 minutes or between 0.5 to 2 minutes in duration respectively. Again, difficulty exists when assessing borderline patients and further difficulty exists in the interpretation of the B waves (Eide et al., 2002). Overall, the upper limit of normal ICP being 15mmHg has continued to hold in craniofacial circles, but with more studies such as that by Avery et al., this may begin to change.

2.2.2 Causes of raised ICP in syndromic craniosynostosis

2.2.2.1 Craniocerebral disproportion

Several factors contribute to a rise in ICP in syndromic craniosynostosis and the dynamic nature of ICP may be matched by the dynamic nature of those factors able to cause it. It is unlikely that any one such factor acts alone, rather that all can act in concert or alone throughout the child's life. Perhaps the simplest concept is one of an object (the brain parenchyma) outgrowing its available space (the fused and growth restricted calvarium); it was this lack of volume or craniocerebral disproportion that was initially given a causative attribution (Renier et al., 1982). It is, however, not the only cause. The importance of this brain / calvarium volume mismatch has been challenged by studies by Gault, Renier, Marchac, and Jones (1992) and Fok, Jones, Gault, Andar, and Hayward (1992), where the relationship between intracranial pressure and intracranial volume was investigated. Gault et al. (1992) concluded that "restricted skull volume contributes to intracranial pressure, but this is not the only factor responsible for intracranial hypertension." Indeed, a lack of volume is difficult to attribute as the cause of raised

intracranial pressure in Apert syndrome, where children have a larger than average skull volume (Gosain, McCarthy, Glatt, Staffenberg, & Hoffmann, 1995). The other contributing factors are venous hypertension, airway obstruction and hydrocephalus.

2.2.2.2 Venous hypertension

Venous drainage of the brain and bony skull is collected by the dural venous sinuses, which are found between the periosteal and meningeal layers of the dura mater. There are 11 venous sinuses in total, draining the collected blood into the internal jugular vein. Stenosis or occlusion of these drainage channels can lead to venous hypertension and, therefore, contribute to raised ICP, and has been found in between 70 and 75% of children with syndromic craniosynostosis (Figure 2.16) (Hayward, 2005; Rollins, Booth, & Shapiro, 2000).

Figure 2.16 A lateral view during venography of the internal jugular vein. The vein is patent but there is high grade stenosis at the skull base (arrow). (Source: Rollins et al., 2000)

Potential causative reasons include abnormal bony growth leading to outflow constriction (especially of the jugular foramen) or abnormal growth of the sinuses themselves (perhaps driven by the same mutated genes as their underlying syndrome). Jugular foramen anatomy in syndromic craniosynostosis was studied in more detail by Florisson et al. They found that whilst the jugular foramen diameter was smaller in those with craniosynostosis, there was no difference in diameter between craniosynostotic

children who did or did not have raised ICP (Florisson et al., 2015). This was at odds to the findings of Rich et al. who found narrower jugular foramina in children with raised ICP (Rich, Cox, & Hayward, 2003). Florisson et al. also showed, in agreement with other authors, that patients with syndromic craniosynostosis had developed prominent collateral venous networks, especially in the occipital area. They hypothesise that this venous collateral development is to reduce intracranial blood volume and thereby lower ICP (Florisson et al., 2015; Hayward, 2005). Much of the work investigating venous hypertension with raised ICP in craniosynostosis has been linked to work produced on raised ICP in children with achondroplasia. Achondroplasia is known to be caused by a mutation in *FGFR-3*, and can lead to venous hypertension and hydrocephalus (Pierre-Kahn, Hirsch, Renier, Metzger, & Maroteaux, 1980). The raised ICP is also known to settle spontaneously, and this has added weight to the hypothesis that raised ICP in syndromic craniosynostosis may do likewise. This would likely occur at around 6 years of age when sufficient collateral venous channels have been developed. This is also the upper age limit at which Renier et al. in 1982 felt patients would be safe from raised ICP (Renier et al., 1982). Venous hypertension may lead to a reduction in the mean cerebral perfusion pressure (CPP) simply due to a 'back pressure' effect. This CPP reduction is likely to harm the more vulnerable areas of the central nervous system (CNS) i.e. the optic nerves, which have less of an ability to autoregulate their blood flow than the rest of the CNS (Hayward, 2005).

2.2.2.3 Airway obstruction

The previously alluded to Lundberg A waves (ICP rises of over 50mmHg for longer than 5 minutes) can often be observed at times of respiratory obstruction in a child

with craniosynostosis. With both physical airway obstruction due to facial anomalies and obstructive sleep apnoea more prevalent in children with syndromic craniosynostosis, they are at a high risk of respiratory obstruction (Driessen et al., 2013). In 2005, Hayward and Gonsalez suggested that during active sleep, the relaxation of pharyngeal muscle tone around a deformed airway leads to an aggravation of the respiratory compromise, which in turn leads to an increase in retained CO_2 and hypoxia, an increase in ICP, and a decline in CPP. Then the compensatory mechanisms, which are necessary for the preservation of sufficient cerebral blood flow to protect cerebral function, react to the hypoxia by producing a state of cerebral vasodilation, which in turn further increases ICP (Hayward & Gonsalez, 2005). From the same unit, Liasis et al.'s case study of 2005 further illustrates the effect of airway obstruction on ICP when the authors showed reversible deterioration of visual evoked potentials following adenoid-tonsillectomy (airway opening) in a child with sagittal synostosis (Liasis et al., 2005). Possible aetiologies include occlusion of the veins of the neck, increased intrathoracic pressure caused by exhaling against an obstructed airway, and an airway obstruction associated rise in cerebral carbon dioxide levels causing vasodilation and further venous hypertension. This cycle of active sleep, obstruction, vasodilation, venous hypertension and rising ICP continues until the child is woken and recovers their blood gases and airway patency. As such airway obstruction in syndromic craniosynostosis seems a reasonable contributing factor to an overall state of potentially raised ICP.

2.2.2.4 Hydrocephalus

Progressive hydrocephalus is the outcome of either the production of too much CSF or a reduction in its absorption and outflow. Ventricular dilatation is known as hydrocephalus

when it is progressive and ventriculomegaly when it is stable (Collmann, Sörensen, & Krauß, 2005). It was not until the 1980's, when the use of computed tomography (CT) and magnetic resonance (MR) imaging became more common, that hydrocephalus in craniosynostosis was able to be studied carefully. Many patients with Apert and Crouzon syndrome have a degree of ventricular dilatation (Figure 2.17), whilst in Muenke and Saethre-Chotzen syndromes it is rarely seen (Cinalli et al., 1998). Shunting is more commonly required in Crouzon and Pfeiffer syndrome whilst, in Apert syndrome, most cases remain stable without a shunt. In their review of hydrocephalus in craniosynostosis, Collmann and colleagues suggest two pathogenic factors which may act in isolation or together:

1. Constriction of the posterior fossa leading to mechanically increased CSF outflow resistance.
2. Impaired CSF absorption due to venous outflow obstruction (Collmann et al., 2005).

The theory regarding constriction of the posterior fossa marries well with the evidence that Crouzon (and therefore perhaps Pfeiffer) syndrome is more likely to need shunting, as they are more likely to exhibit tonsillar herniation than Apert syndrome; this is possibly due to their earlier fusion of the lambdoid suture (Cinalli et al., 1995). That posterior fossa constriction and increased CSF outflow resistance may not be the sole cause of hydrocephalus is supported by studies showing failure of posterior fossa decompression to restore normal CSF circulation and that the presence of hindbrain herniation does not always lead to hydrocephalus (Cinalli et al., 1998; Taylor et al., 2001; Thompson, Harkness et al., 1997). Most authors favour a multifactorial cause, assuming that CSF absorption is reduced by venous hypertension, which concurrently causes brain

swelling and herniation of the tonsils and, therefore, mechanical obstruction also (Thompson, Harkness et al., 1997). In children with single suture craniosynostosis abnormal dilatations of the subarachnoid spaces are a common finding and may be caused by a disturbance in CSF absorption (Thompson et al., 1995). The scaphocephalic head shape seen in sagittal synostosis can compress the superior sagittal suture and may cause impaired CSF absorption at normal ICP levels. These findings, whilst not contributing a novel cause of raised ICP in craniosynostosis do bolster the evidence for hydrocephalous being a causative factor.

Figure 2.17 An MR image of a 6-month-old child with Crouzon's syndrome. Dilated ventricles and herniated cerebellar tonsils are shown. (Source: Collmann et al., 2005)

2.2.3 The deleterious effects of raised ICP

Raised ICP requires a prompt diagnosis, as prolonged periods of elevated pressure may lead to neurocognitive delay, Chiari Type 1 malformation and to optic atrophy, which may progress to blindness if left untreated (Hayward et al., 2016; Liasis, Thompson, Hayward, & Nischal, 2003). The evidence for raised ICP causing visual loss in children with craniosynostosis is stronger than for that of it causing neurocognitive delay. Whilst visual loss may be attributed to raised ICP, patients with syndromic craniosynostosis are more likely to have correctable causes such as amblyopia and ametropia. Tay et al. in 2006 studied 63 patients with syndromic craniosynostosis and

found that of 55 who had their visual acuity tested at first presentation 35.5% had a unilateral visual impairment. Of this 35.5%, 9.5% could be attributed to raised ICP as indicated by papilloedema, which resolved following decompressive surgery (Tay et al., 2006). These findings are consistent with those of other authors, who found amblyopia to be the most common finding. Gray, Casey, Selva, Anderson, and David (2005) found 4/56 (7%) of patients with Crouzon syndrome studied to have optic atrophy and Hertle, Quinn, Minguini, and Katowitz (1991) found optic atrophy to account for 7% of visual loss in their study of 43 craniosynostotic patients.

Chiari malformation, a herniation of the hindbrain down through the foramen magnum is often seen in patients with syndromic craniosynostosis, with a reported 70% incidence in Crouzon syndrome (Cinalli et al., 2005). It appears to be a progressive condition, that is frequently seen in conjunction with raised ICP. It occurs within the first few months of life and develops due to the disproportion between small posterior fossa and the growing hindbrain (Forrest & Hopper, 2013).

Neurocognitive impairment (NCI) due to raised ICP is often suggested as a sequela of the syndromic craniosynostoses; however, evidence for this claim is less striking than for that of visual impairment (Derderian & Seaward, 2012). Renier et al.'s 1982 paper was the first to objectively link raised ICP and NCI. They studied IQ level and ICP before surgery in 55 children with craniosynostosis. They state: "This study suggests such a relationship but does not prove it definitively." They are also careful to add a caveat that "increased ICP and low IQ [could be] two consequences of a third variable" (Renier et al., 1982). Further studies into NCI in relation to raised ICP in syndromic craniosynostosis have been not been forthcoming. In their review of the subject, Hayward et al. (2016) concluded that "the evidence that [ICP] levels frequently

accepted as elevated can be responsible (in the absence of hydrocephalus) for cognitive impairment is weak at best." In support of there being a different cause of NCI, other than raised ICP, is Raybaud and Di Rocco's 2007 paper which links the L1 cell adhesion molecule (*L1CAM*) gene to defects in *FGFR* gene. *L1CAM* is needed for normal development of the white matter and it requires an interaction with *FGFR* to operate correctly. They postulate that it is logical to attribute both skull changes and white matter changes to defects in the *FGFR* gene (Raybaud & Rocco, 2007).

2.2.4 Measurement of intracranial pressure

Clinical judgement, non-invasive measures and invasive measures all play a part in the assessment of raised ICP. Clinical judgement revolves around symptoms and signs suggestive of an increase in ICP such as headaches, vomiting, lowered levels of consciousness, failure to thrive and patient reported visual changes. Unfortunately, sensitivity and specificity for these tests is low and it can be difficult to elicit the history from children (Derderian & Seaward, 2012; Tamburrini et al., 2005). ICP measurements can be performed either invasively or non-invasively, with advantages and disadvantages to both. Direct monitoring of ICP is invasive and requires the placement of a device within the cranial cavity and transducing the underlying pressure to give a reading. The original method describes ventricular cannulation, where a ventricular catheter is placed in the lateral ventricle. Its advantage is that CSF can be therapeutically drained during the procedure; its disadvantage is that CSF leak can lead to falsely low readings (Wiegand & Richards, 2007). Intraparenchymal device use has become more commonplace. These devices measure the ICP within the brain parenchyma itself, they are easier to place and cause fewer complications (Anderson et al., 2004). Whilst these methods are the gold

standard for accurate ICP measurement, they both require hospital admission and 24-48 hours of monitoring in a specialist unit.

The search for a reliable non-invasive method is an important one. Efforts to discover useful modalities have explored methods which assess both structural and functional changes. The study of structural changes includes imaging of the brain, cranium, optic disc, optic nerve and the ventricles. Investigations into functional changes have included cerebral blood flow and nerve conduction analysis.

2.2.4.1 Measuring structural and functional changes

Imaging modalities that provide static or dynamic images of the brain, skull, optic disk, optic nerve or ventricles have been studied in relation to ICP. For the brain, MRI can provide information on cerebral blood flow, CSF velocity through the aqueduct and elastance index, as well as being used to measure ONSD. The published cohorts for MRI studies are mainly adult patients with idiopathic intracranial hypertension, whereas CT studies mainly include adult traumatic brain injury patients (Alperin, Lee, Loth, Raksin, & Lichtor, 2000; Muehlmann et al., 2013; Xu, Gerety, Aleman, Swanson, & Taylor, 2016). CT is widely available and has been used to investigate whether thumb printing of the skull, effacement of the ventricles, midline shift or reduction in size of the basal cisterns correlates to ICP. Mizutani et al. used multiple regression analysis to investigate the relationship between CT findings and ICP and provided an equation which predicted ICP within 10mmHg of the recorded ICP in 80% of those studied (Mizutani, Manaka, & Tsutsumi, 1990). Fewer studies include children, and those which have provide less confidence in the use of static CT imaging to assess ICP. Kouvarellis et al. (2011) concluded that open basal cisterns could not rule out raised ICP, and Bailey, Liesemer,

Statler, Riva-Cambrin, and Bratton (2012) found a raised ICP on invasive monitoring in seven out of nine children with a head CT reported as normal following traumatic brain injury. As with MRI, CT can also be used to measure ONSD.

When utilising the eye as a window through which to measure ICP, methods which use structural changes rely on the assumption that the eye and the optic tract are a direct extension of the CNS. Traditionally, ophthalmoscopy had been used to examine the dilated fundus in search of papilloedema. Tuite et al. when studying the relationship between raised ICP and papilloedema in children with craniosynostosis showed that whilst papilloedema is specific for raised ICP in all ages, it had a low sensitivity in children under 8 years of age (Tuite et al., 1996). This was purportedly due to a number of reasons; the greater compliance of the unfused sutures in the younger infant may buffer the effect of raised ICP on the optic nerve; difficult ophthalmological examination in the younger infant may have under or over reported papilloedema; the optic nerve subarachnoid space in younger infants may be less communicative with the subarachnoid space surrounding the brain and therefore CSF pressure; venous congestion and axoplasmic stasis would not be transmitted to the optic nerve as effectively; or that optic nerve axons are more resilient in younger children and provide a degree of protection against raised ICP to the optic nerve (Tuite et al., 1996). A study by Nazir et al. of papilloedema in patients with shunt failure added further evidence to the poor sensitivity of papilloedema in raised ICP, finding that even children with severe ICP elevations may show flat optic discs (Nazir et al., 2009). More recently the idea that CSF flow is continuous between the general subarachnoid space and the optic nerve subarachnoid space has been challenged by Killer et al. who described a lack of contrast loaded CSF in the optic nerve subarachnoid space as compared to the intracranial subarachnoid space

following contrast computed cisternography (Killer et al., 2007). With the usefulness of papilloedema being questioned, interest has grown in other non-invasive methods which utilise the eye and optic tract such as optical coherence tomography and the ONSD (Haredy et al., 2018; Skau, Milea, Sander, Wegener, & Jensen, 2011).

Measurement of the ONSD relies again on the theory of the optic nerve being surrounded by a subarachnoid space in continuation with that of the brain. It has been studied in both traumatic brain injury patients as well as more recently in children with craniosynostosis (Haredy et al., 2018; Helmke & Hansen, 1996). Haredy et al. (2018) showed comparable results between MRI and CT measured ONSD. In their study of patients over one year of age, an ONSD over 6mm had a sensitivity of 71.4% and a specificity of 89.7% for detecting raised ICP. However, they advise a cautionary interpretation of these results due to the small patient population studied. Padayachy, Padayachy, Galal, Gray, and Fieggen (2016) studied 174 children, with 56 below one year of age and 118 above one year but less than four years of age. They found ONSD thresholds of 4.97mm and 5.49mm for detecting ICP over 15mmHg, with a sensitivity of 86.4% and a specificity of 82.4% in the under ones, and a sensitivity of 93.7% and a specificity of 77.4% in those over one year of age (Haredy et al., 2018; Padayachy et al., 2016).

Functional modalities can also be used as non-invasive methods of detecting raised ICP. At GOSH, the assessment of visual evoked potentials by the ophthalmology team is the most commonly used functional non-invasive measure of ICP. Visual evoked potentials are the electrical signals generated by the occipital lobe when responding to visual stimuli. Evaluation of these signals gives an impression of the visual pathway from optic nerve to visual cortex. Measuring a VEP tracing involves placing electrodes onto

the scalp before presenting flash or patterned visual signals to the patient. The shapes and latencies of the returning waveforms are assessed and correlated to ICP values (York, Pulliam, Rosenfeld, & Watts, 1981). Flash VEPs can be performed on most patients regardless of their level of consciousness, whereas pattern evoked VEPs require an alert (and cooperative) subject, which, much like the assessment of visual acuity and papilloedema, can be challenging in infants.

Transcranial doppler ultrasound measures the velocity of blood flow through intracranial vessels during systole and diastole. When ICP rises the diastolic blood flow velocity is reduced more so than the blood flow during systole. The ratio created is used to predict ICP (Klingelhöfer, Conrad, Benecke, Sander, & Markakis, 1988). The use of transcranial doppler ultrasound in craniosynostosis was first reported by Iqbal, Hockley, Wake, and Goldin in 1994, who rather than use it to predict ICP, utilised it as a measure of success following craniofacial surgery. Govender et al. found that transcranial doppler ultrasound findings correlated poorly with ICP measurements inferred from lumbar puncture. They, and others suggest that transcranial doppler ultrasound can be a useful monitoring tool post cranial decompression surgery rather than as a measure of ICP (Govender, Nadvi, & Madaree, 1999; Spruijt et al., 2016). Whilst transcranial doppler ultrasound appears to have useful potential as a non-invasive measure of ICP in craniosynostosis, its use has not been widely adopted.

Whether raised ICP in syndromic craniosynostosis causes neurocognitive impairment, and is due to craniocerebral disproportion, venous hypertension, hydrocephalus or airway obstruction remain up for debate. That prolonged periods of raised ICP causes detriment to the visual pathway is not. Children with syndromic craniosynostosis will therefore likely need some form of intervention.

2.3 Cranial vault expansion

Treatment protocols for syndromic craniosynostosis vary from unit to unit. The over-riding theme is that all patients should be managed in a tertiary referral centre where there is access to the plethora of specialist services required for their complex treatment. Treatment goals are wide and range from operative management of associated co-morbidities to clinic-based treatment of speech and language problems. Surgically there is a fine balance between restoring craniofacial function, ameliorating raised ICP and improving the psychosocial well-being and appearance of the patient. Algorithms for operative timing also differ between specialist units, with some choosing to perform prophylactic surgery before one year of age, and other choosing to wait until signs of raised ICP appear (Marucci et al., 2008; Spruijt, Joosten, et al., 2015). Before undergoing expansion of the cranial vault, most units will address hydrocephalus (with ventriculoperitoneal shunting) and airway obstruction (with adeno-tonsillectomy or tracheostomy if required) primarily (Forrest & Hopper, 2013; Marucci et al., 2008). It is the transcranial operative management of raised ICP, by means of cranial vault expansion that this thesis will concentrate on.

The history of cranial vault expansion dates to the 1890's, shortly after Virchow's landmark paper on aberrant skull growth in craniosynostosis. The first reported surgical procedures for craniosynostosis were by Lannelongue in Paris in 1890 and L.C. Lane in San Francisco in 1892 (Lane, 1892; Lannelongue, 1890). Both performed strip craniectomies, with Lannelongue retaining the sagittal suture and Lane removing it (Mehta, Bettegowda, Jallo, & Ahn, 2010). These early interventions were adopted by many surgeons at the time. However, when Jacobi reviewed the outcomes of a series of

33 children surgically treated for craniosynostosis, he found a mortality rate of 15/33. His famous speech at the American Academy of Paediatrics halted the progress of craniosynostosis surgery for the next 3 decades:

> *"The relative impunity of operative interference accomplished by modern asepsis and antisepsis has developed an undue tendency to, and rashness in, handling the knife. The hands take too frequently the place of brains…Is it sufficient glory to don a white apron and swing a carbonized knife, and is therein a sufficient indication to let daylight into a deformed cranium and on top of the hopelessly defective brain, and to proclaim a success because the victim consented not to die of the assault? Such rash feats of indiscriminate surgery…are stains on your hands and sins on your soul. No ocean of soap and water will clean those hands, no power of corrosive sublimate will disinfect the souls"* (Jacobi, 1894)

By the 1940's, strip craniectomies and suturectomies had made a resurgence. New difficulties were faced with reossification requiring difficult revision surgery. Attempts to counter this were made by Simmons and Peyton, who inserted tantalum foil between the cut edges of the bone (Simmons & Peyton, 1947). The technique was not widely taken up due to reports of failure. As the 20th century progressed, surgeons realised the need for procedures more complex than the strip craniectomies. Jane and colleagues developed the pi procedure, removing part of the sagittal, bilateral coronal and lambdoid sutures, before greenstick fracturing the parietal bones laterally to increase skull width (Figure 2.18) (Jane, Edgerton, Futrell, & Park, 1978).

Figure 2.18 An illustration of the site and shape of bone removed during Jane et al.'s pi procedure. (Source: Mehta et al., 2010)

Further significant advances came from the contributions of Paul Tessier in the 1960s and 70s. It was Tessier who developed many of the principles and surgical

instruments that craniofacial surgeons employ today, performing the first successful intracranial approaches to the midface and interorbital region. His collaborative approach to treating craniofacial problems continues today. As understanding of the pathophysiology of craniosynostosis has evolved, surgical techniques and technologies have evolved alongside it. With cranial vault expansion employed to counter raised ICP.

Children with syndromic or multisuture craniosynostosis often present with turribrachycephaly or severe brachycephaly predisposing them to an underdeveloped, small posterior cranial fossa (Thomas et al., 2014). These patients are at risk of developing raised ICP, as well as hydrocephalus or a Chiari type 1 malformation (Cinalli et al., 2005). Traditionally, to overcome these problems, cranial vault expansion was undertaken via the anterior route. This was thought to be the optimal first step, as it offered both volume expansion and protection for the eyes (Choi, Flores, & Havlik, 2012; Steinbacher, Skirpan, Puchała, & Bartlett, 2011). The technique of choice was FOA, however, this was found to be prone to relapse and, therefore, patients would require secondary vault expansion surgery. Wall et al. further evidenced this in 1994 when reporting a mean reoperation rate of 8.2% raising to 16.7% in Apert syndrome. They also showed a markedly higher rate of reoperation when FOA was performed before 6 months of age (Wall et al., 1994). The posterior route for expansion of the calvarium was first reported by the Craniofacial Team in Birmingham, UK in 1996 (Sgouros, Goldin, Hockley, & Wake, 1996). Following a successful rigid posterior approach to a skull releasing procedure in two patients with cloverleaf skull, they noted that no further operative intervention was required, and thereafter switched their practice to performing PVE as the initial procedure, purporting that it reduces pressure from the growing brain on the orbits and allows FOA to be delayed. Since this time the posterior route has become

increasingly favoured among craniofacial surgeons. It avoids the frontal orbital region, therefore leaving this area undisturbed should frontal facial procedures be required later, is reported to deliver greater increase in ICV, and in patients with Chiari malformation it may avoid the need for foramen magnum decompression (Choi et al., 2012; Levitt, Niazi, Hopper, Ellenbogen, & Ojemann, 2012; Spruijt, Rijken, et al., 2015). Surgical technique has evolved to now offer gradual expansion through the use of implantable distraction devices.

Current surgical techniques for posterior vault expansion therefore include the traditional posterior cranial vault remodelling (PCVR) and the novel, less invasive methods which allow for gradual expansion via the use of springs or distractors. A free-floating parieto-occipital cranial vault release is the traditional and more invasive of the techniques. It has the advantage that can be used in very young children with thin calvarial bones, which might not be able to withstand the forces placed upon them by metal hardware. It is disadvantaged by its invasive nature, the risk of skin breakdown and that the patient is required to lie in a lateral position postoperatively.

The use of distraction osteogenesis (Figure 2.19) to manipulate the craniofacial skeleton was pioneered by McCarthy in New York in the early 1990s (McCarthy, Schreiber, Karp, Thorne, & Grayson, 1992). The technique is based on gradual distraction of the callus formed at healing fracture sites. Standard distraction protocols were devised by Ilizarov who suggested a 5-7 day latency period following fracture and a 1mm/day distraction rate (Ilizarov, 1990). The first use of distractors for cranial vault expansion was in an anterior direction by Sugawara in Tokyo (Sugawara, Hirabayashi, Sakurai, & Harii, 1998). Posterior distraction was undertaken by White et al. from the Birmingham UK group, citing ease of scalp closure, greater volumetric increase and less posterior

relapse when compared to tradition techniques as their reasons for this choice (White et al., 2009). This technique has been accepted by many other units (Derderian, Bastidas, & Bartlett, 2012; Goldstein et al., 2013; Saiepour, Nilsson, Leikola, Enblad, & Nowinski, 2013; Thomas et al., 2014). Disadvantages of distractor devices are that they break the skin barrier, forming a communication between the calvarium and the environment, potentially increasing infection rates.

Figure 2.19 (Left and Centre) Plain radiographs to show distraction devices in situ, before and during distraction. (Right) Photograph to show distractor protruding through the skin. (Source: Steinbacher et al., 2011)

Spring assisted surgery (SAS) was introduced by Lauritzen's team in Sweden in 1997. They developed a technique to use a single piece of stainless steel wire, that when bent into an omega shape, would gradually spread outwards once released (Lauritzen, Davis, Ivarsson, Sanger, & Hewitt, 2008). Initially used to treat scaphocephaly, the use of springs has evolved and they are now commonly used in posterior vault distraction (De Jong, Van Veelen, & Mathijssen, 2013). The operative technique for spring assisted PVE (SAPVE) undertaken at GOSH is further discussed in Chapter 5. With refinement of this technique has come refinement of the springs themselves. The original design, constituting a bent wire form rather than a spring in its purest sense, made standardisation difficult. To overcome this difficulty GOSH designed a standardised torsional spring with a 10-millimetre diameter central helix and a 60-millimetre opening distance at rest (Figure 2.20). Due to the rapid speed of spring opening, they do not perform distraction

osteogenesis as such, instead the springs produce large bone gaps quickly (primary distraction) with osteogenesis occurring in the space created (secondary osteogenesis). Potential advantages include the correction being guided by the expanding springs rather than by rigid reorganisation of bony pieces, no break of the skin barrier, reduced surgical time, blood loss, cost and in-patient stay. Disadvantages lie in the need for two operations, lack of control over expansion vectors and spring related complications such as dislodgment (Lauritzen et al., 2008; Nowinski et al., 2012; Serlo et al., 2011).

Figure 2.20 3D reconstruction to show posterior vault expansion with springs (as modified by Jeelani; from an omega shape to one which includes a central helix).

2.4 Summary

This chapter has given a brief overview of craniosynostosis, its various forms, the problems it can cause, and the current techniques used to overcome these problems. This started with the ground-breaking work done by Virchow in 1851 and progressed to modern theories of suture biology. A description of the suture positions within the skull and the shape changes that occur when they are fused was provided. Both single suture, multi-suture and syndromic craniosynostosis were discussed, as well as the novel genetic research done by Andrew Wilkie and his laboratory in Oxford. Multi-suture and syndromic craniosynostosis were focused upon, with the still rare but most common syndromes and their sequalae being described in more detail. One such sequalae is raised ICP, which was introduced and discussed further. This discussion included the difficulty in measuring ICP and finding a consensus on what a normal childhood ICP is. Causes of raised ICP were considered, including craniocerebral disproportion, venous hypertension, airway obstruction and hydrocephalus. Finally, this chapter concluded with an examination of the various techniques used to overcome raised ICP in craniosynostosis and their evolution over time; from an anterior approach to a posterior one and a single stage invasive procedure to a two stage less invasive procedure using implantable distractors or springs.

The following chapter begins this thesis's investigation into ICV. It examines the difficulties in measuring intracranial volume and reviews three different techniques that can be used to measure it.

Chapter 3 **INTRACRANIAL VOLUME MEASUREMENT**

Part of the work described in this chapter has been published in the *Journal of Craniofacial Surgery*:

- Breakey, R. W. F., Knoops, P. G. M., Borghi, A., Rodriguez-Florez, N., Dunaway, D. J., Schievano, S., & Jeelani, N. U. O. (2017). Intracranial volume measurement: A systematic review and comparison of different techniques. *Journal of Craniofacial Surgery,* 28(7), 1746-1751.

This work was presented at the 15th Congress of the International Society of Craniofacial Surgery in Tokyo, Japan, September 14th – 18th, 2015

Chapters 1 and 2 introduced the use of cranial vault expansion to increase ICV and in doing so ameliorate raised ICP. In order to answer the central question to this thesis 'what volume increase is needed to manage raised ICP', it was first necessary to review and investigate different ways of measuring ICV. This chapter examines three ICV measurement techniques.

3.1 Introduction

CT and MR imaging allow for accurate measurement of ICV (Kamdar et al., 2009; Sgouros, Hockley et al., 1999). This information is increasingly used by craniofacial teams to analyse and formulate treatment strategies for patients, allowing them to better understand pathologies of ICP disturbances and to quantify the operative change in volume achieved by craniofacial surgeries, such as vault expansion (Abbott et al., 2000). This wide-ranging utility makes both CT and MR imaging useful tools in the craniofacial team's armamentarium. Prior to the availability of 3D imaging, OFC measured in clinic and the cephalic index measured from plain films were relied upon to assess cranial proportion and monitor growth (Edler, Abd Rahim, Wertheim, & Greenhill, 2010). ICV measurement is performed through a process of segmentation and post processing of 3D images. This can be done manually or automatically on contiguous head image stacks. Manual segmentation involves a time-consuming process of outlining the intracranial area within each slice throughout the image stack, from the foramen magnum to the vertex. Semi-automatic techniques require thresholding of Hounsfield Units (HU) followed by the use of automated region growing methods, whilst fully automatic techniques involve thresholding and brain extraction techniques coded to allow automatic

calculation of ICV (De Jong, Rijken, Lequin, Van Veelen, & Mathijssen, 2012; Muschelli et al., 2015). Fully automatic techniques have been extensively investigated in MR studies (Wang et al., 2014) and only more recently in CT imaging (Muschelli et al., 2015). Each technique has advantages and disadvantages in terms of the time taken to execute each measurement and their reliability. There are commercial and freeware options available for each technique. In the context of craniosynostosis, there is currently no standardised protocol for ICV measurements. A systematic literature search of material published by craniofacial centres worldwide showed that fully automatic methods of ICV measurement are yet to be adopted, with the majority of craniofacial units preferring semi-automatic techniques (Table 3.1).

The purpose of this chapter was therefore to compare manual, semi-automatic and fully-automatic segmentation techniques for ICV measurement from CT images. The manual technique was assumed as the gold standard, this presumed that the clinician would provide expert outlining of the intracranial cavity. The systematic literature review revealed that a semi-automatic technique was the mainstay of most centres measuring ICV, and thus its inclusion in this study. Finally, a fully-automatic method was assessed due to its potential as a time saving and non-biased technique, which to our knowledge has not, as of yet been applied to patients with craniosynostosis.

3.2 Methodology

3.2.1 Systematic review

A systematic literature search using the PubMed database was undertaken to investigate the various methods of intracranial volume measurement published by different craniofacial centres worldwide. Search terms were restricted to those papers published between 1996 and 2016, using a search string of "Craniosynostoses"[Majr] AND “intracranial” AND “volume”, which resulted in 86 papers. Studies were required to:

1. Have used an imaging modality that provided views of the intracranial vault rather than that of the outer surface of the head, including the soft tissues
2. Have been restricted to human subjects
3. Explain their method of volume calculation
4. Have measured the entire intracranial volume
5. Provide 3D volume measurements as generated by their measurement technique not mathematical estimations based on elliptical volumes.

3.2.2 Patient population and ICV measurements

The pre and post-operative CT scans from 13 patients with Apert syndrome (9 male, 4 female, average age at operation = 9.5 months, range 3.6 – 16.1) who underwent spring assisted PVE at GOSH between 2008 and 2014 were retrospectively considered for this study. Each patient had full CT data sets. patients with Apert syndrome were chosen for this study as they present with complex skull bone distribution and, with the

pre- and post-vault expansion data, a wide variation of head volumes would be captured. The full head volume, from foramen magnum to vertex, was included in each CT scan and the images did not present obstructive artefacts caused by the springs. The scans had a constant slice thickness of 1mm.

All measurements on the 26 scans (13 pre-operative and 13 post-operative) were performed by the same operator (the primary author) using three separate techniques; a fully manual segmentation, a semi-automatic segmentation and finally a fully automatic segmentation. The fully manual segmentation technique was taken as the gold standard as it should provide the most user control, however given the potentially protracted length of time taken to perform fully manual segmentation a semi-automatic and a fully automatic technique were developed. The semi-automatic technique utilises a series of on the go user chosen commands to create a closed skull vault, the volume of which can then be measured. This will not offer the same level of user control as the fully manual technique, reducing both the time taken to compute a volume and also the operator bias. The fully automatic technique uses a pre-determined (by the user) command line code to compute an ICV. These techniques are further detailed below, with their advantages and disadvantages expanded upon in this chapter's discussion.

1. Fully manual segmentation with the freely available OsiriX software (OsiriX v4.1, Pixemo; Geneva, Switzerland), running on a MacBook with Mac OS X 10.6.8 (Apple Computer, Inc., Cupertino, CA, U.S.A). Digital Imaging and Communications in Medicine (DICOM) images were windowed with an OsiriX derived bone window level and width (Scolozzi & Jaques, 2008). As the skull vault is open ended at its inferior aspect a cut-off point at which to stop the volume measurement was required. The inferior extreme of the foramen magnum was

chosen as the most inferior plane between the clivus and the occipital bone (Francisca et al., 2015). The bone-brain interface, which was identifiable by the tonal change in the images, was manually outlined in each of the contiguous CT coronal sections using a digital pen (Wacom Bamboo, Kazo, Japan) and the OsiriX pencil tool to create the region of interest (ROI) on each slice, from foramen magnum to vertex. At the end of the segmentation process all ROIs were grouped and the volume was computed by OsiriX as the sum of the contained voxels (Scolozzi & Jaques, 2008) (Figure 3.1).

Figure 3.1 Coronal view of a mesh created by manual tracing of the inner table of the cranium using OsiriX and a digital pen.

2. Semi-automatic segmentation using the commercial software Simpleware Scan IP (Simpleware Ltd., Exeter, UK), running on 64-bit Operating System with Intel

Xeon CPU E3-1270 and Windows 7 Enterprise, Service Pack 1 (Microsoft Corporation).

DICOM images were loaded into Simpleware then rotated and cropped to include foramen magnum (cut off as above) to vertex. The image threshold was set at -55HU to 117HU for all scans, similar to other threshold levels published in the literature (Leikola, Koljonen, Heliövaara, Hukki, & Koivikko, 2014); these parameters were found visually to provide the most reliable soft tissue range for the first 'mask', highlighting the region of interest to be created. It is then necessary to separate the intracranial contents from the surrounding tissues using a region growing operation (known as 'flood fill' in Simpleware); here the software fills in connected regions of the mask using a seed point and the given threshold. After this, the spill of the mask from the skull base foramina was assessed and corrected through a series of open and close morphological operations. Any remaining spill that could not be solved using the morphological operations was then removed manually by closing any remaining cranial defects. This produced a final mask that best filled the intracranial cavity across axial, sagittal and coronal views. The volume of this mask was calculated, based on mask statistics in Simpleware, using the voxel information within the mask (Figure 3.2).

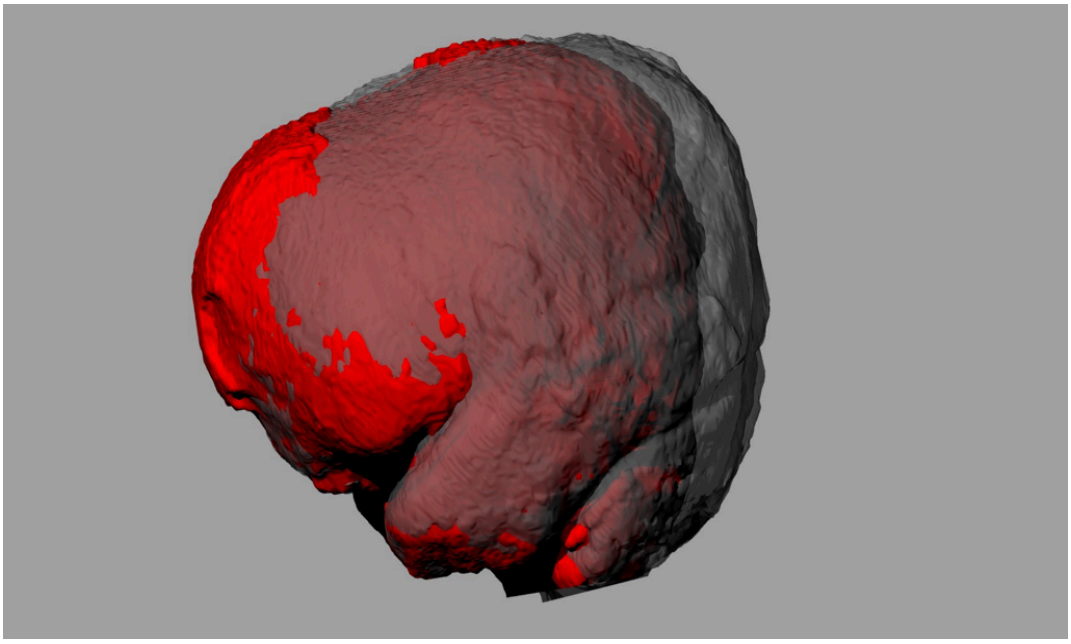

Figure 3.2 3D volume render showing a pre and post-operative Apert skull following PVE. 3D volume renders created in Simpleware using a semi-automatic method. Overlay performed in Rhinocerous (McNeel Europe, Barcelona, Spain).

3. Fully automatic method with FSL neuroimaging software (Analysis Group, FMRIB, Oxford, UK), freely available, running on MacBook Pro 2 GHz Intel Core i5 with macOS Sierra 10.12.1 (Apple Computer, Inc., Cupertino, CA, U.S.A).

   DICOM images were converted to the Neuroimaging Informatics Technology Initiative (NIfTI) format using ITK-SNAP (Yushkevich et al., 2006). An example bash script for the initial FSL command-line (FSL_Muschelli) can be downloaded from http://bit.ly/CTBET_BASH (Muschelli et al., 2015). The description in Muschelli et al. (5), was followed for each scan: images were thresholded using a range of 0 to 100HU and then smoothed using a 3-dimensional Gaussian Kernel (σ = 1mm^3). Smoothing is a process by which data points are

averaged with their neighbours in a series, this usually has the effect of blurring any sharp edges. Smoothing requires a 'kernel' this kernel defines the shape of the function that is used to take the average of the neighbouring points. A Gaussian kernel is a kernel with the shape of a Gaussian (normal distribution) curve. These settings have been shown to increase performance of the automatic measurement algorithm (Muschelli et al., 2015). Brain extraction technique (BET) was then applied using a pre-set fractional intensity (FI) parameter, which determines the edge of the extraction (Rorden, Bonilha, Fridriksson, Bender, & Karnath, 2012). FI values lie between 0 and 1 with smaller values providing larger volumes (Smith, 2002). Following BET, holes were filled using the 'fill holes' command, a mask was created, and the volume measured. When using the automatic method, the result is influenced by two main variables – the degree of Gaussian smoothing applied to the image and the FI at which the brain is extracted. These variables were assessed by altering the FI parameter in a step-wise manner from 0.01 to 0.99 with a constant smoothing setting of 1 and vice-versa altering the smoothing from 0.1 to 1 with the FI set at 0.01 (Muschelli et al., 2015).

It was found that a number of the extractions were failing to remove the entire intracranial volume, with holes being found in the extraction. The command line was altered due to this finding (FSL_Altered) to use initial threshold levels of 5-100HU, include re-thresholding of the images at 5-100 HU after smoothing, and a different pipeline order (Figure 3.3). An example bash script for the FSL_Altered command-line can be downloaded from http://bit.ly/2cCEBIu and is detailed in Appendix B.

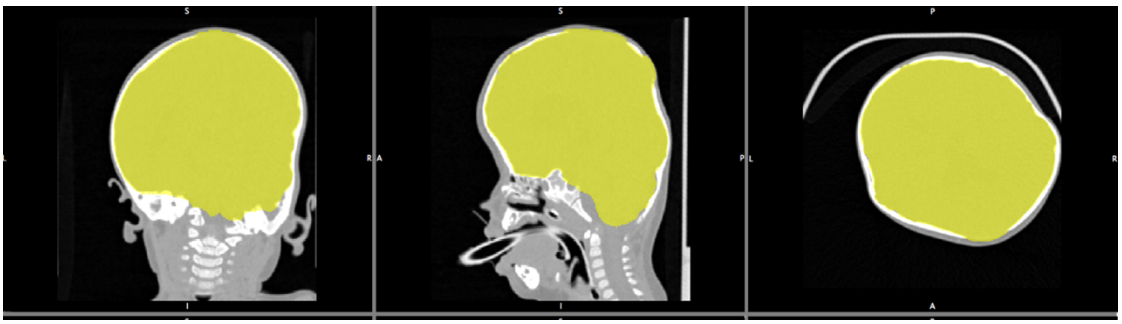

Figure 3.3 Automatic ICV extraction using FSL's brain extraction technique.

The post-operative scans were used to assess observer reliability in all post op scans by calculating volumes three times when using the manual and semi-automatic techniques. The average values between these repeated measurements were used for the comparison between methods.

In addition, a further small study was undertaken to assess the number of slices (or amount of CT scan data) required to obtain clinically accurate volume measurements. This was undertaken after realising that in the past CT scanners often acquired information with larger slice thicknesses and that old CT scan repositories only hold a fraction of the full number of slices. To assess this the CT slice number of each post-operative scan was reduced in a step wise manner. Thus, half, quarter, and an eighth of the original number of slices were re-measured to calculate ICV using the semi-automatic technique (Figure 3.4).

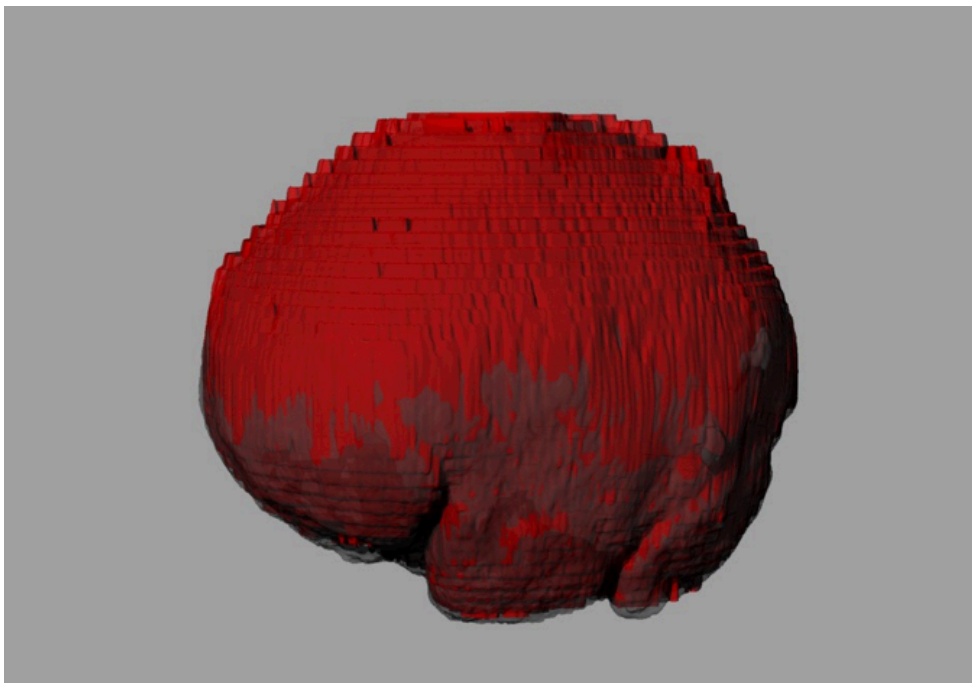

Figure 3.4 3D reconstruction of a CT scan which has been down sampled to include half the original number of slices.

When considering that wide-spread adoption of any measurement technique would be partly determined by the time taken to perform the process, it was felt important to analyse the average time to perform the segmentation and extract ICV. As such time taken for each method was estimated as an important factor in assessing the quality of each technique.

3.2.3 Data analysis and statistics

Data analysis was performed using R statistical software (v. 3.2.5, R Foundation for Statistical Computing, Vienna, Austria). Relationships between manual, semi-automatic and fully automatic techniques (with the initial and altered scripts), and the influence of the number of CT slices was assessed using the coefficient of determination

(R^2) and Bland-Altman plots. When assessing intra-observer reliability, the interclass correlation (ICC) was performed, and root mean squared error (RMSE) and maximum error were calculated as percentages between each measurement and the average of three measurements.

3.3 Results

3.3.1 Systematic review

The semi-automatic method of ICV calculation was shown to be the most popular. Twenty-nine studies from 14 centres met the inclusion criteria for the analysis with all but one utilising a semi-automatic method of ICV calculation. The included centres used a mixture of proprietary, paid for and free software. One study used the fully manual method in OsiriX (Nowinski et al., 2012) (Table 3.1).

Table 3.1 Craniofacial centre and reported method (manual, semi-automatic or fully automatic) used to calculate intracranial volume (ICV) from magnetic resonance imaging or computed-tomography data.

Centre	Author	Method	Program	Modality
Erasmus	De Jong T	Semi-automatic	Brainlab (BRAINLAB AG, Feldkirchen Germany)	MR
Berlin	Schulz M	Semi-automatic	BrainLab (BRAINLAB AG, Feldkirchen Germany)	MR
Missouri	Hill CA	Semi-automatic	Analyze 9.0 (AnalyzeDirect, Inc. KS, United States)	MR
CHOP	Derderian CA	Semi-automatic	Mimics (Materialise, Leuven, Belgium)	CT
Australian Craniofacial Centre	Abbott A	Semi-automatic	Proprietary	CT
Yale	Heller JB	Semi-automatic	Scion Image (Informer Technologies Inc.) / Image J (– National Institutes of Health)	CT
Gothenburg	Fischer S	Semi-automatic	MATLAB (MathWorks, MA, United States)	CT
Helsinki	Leikola J	Semi-automatic	Volume Share 2 (– GE Healthcare)	CT
Helsinki	Ritvanen AG	Semi-automatic	Proprietary	CT
Paris	Nowinski D	Manual	OsiriX (Pixemo, Bermex, Switzerland)	CT
Wisconsin	Deschamps -Braly J	Semi-automatic	Amira (FEI,)	CT
Seoul	Park DH	Semi-automatic	Lucion (MEVISYS, Seoul, Korea)	CT
Columbia Med Centre	Kamdar MR	Semi-automatic	Amira 3.0 (FEI,)	CT
Birmingham Children's Hospital	Sgouros S	Semi-automatic	N/A	CT

3.3.2 Intracranial volume measurement

All twenty-six scans were measured using the manual and semi-automatic technique. The fully-automatic technique provided ICV measurement for all 26 scans when using the altered script (FSL_Altered as detailed in section 3.2.2) (Figure 3.5 A). Only 12 scans were successfully extracted when using the original Muschelli pipeline (FSL_Muschelli) (Figure 3.5 B).

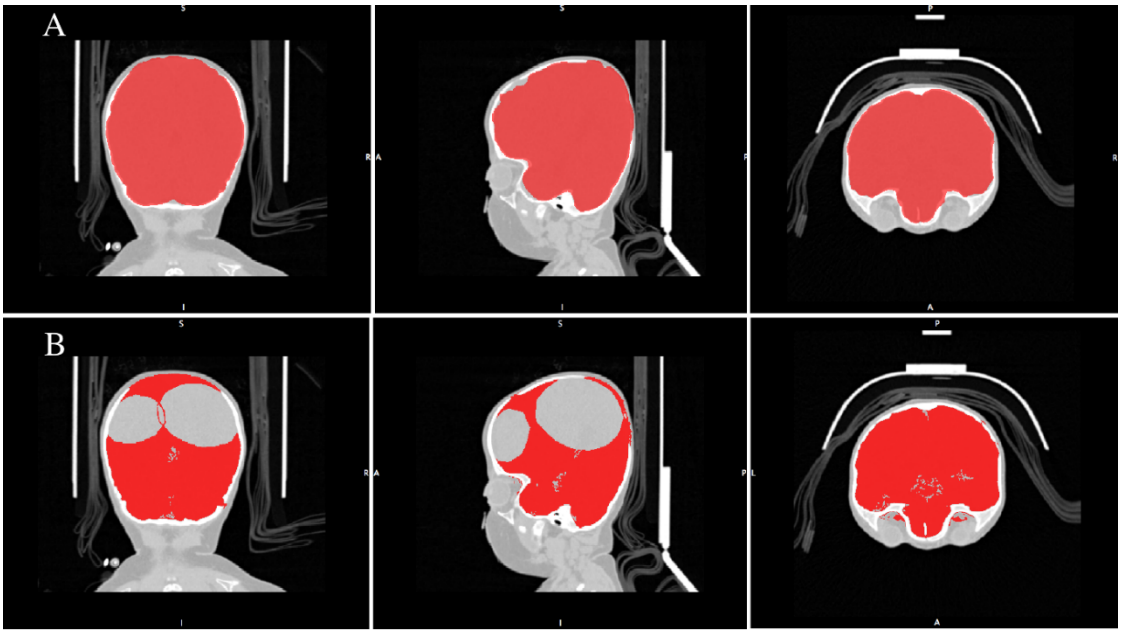

Figure 3.5 An example of successful brain extraction using FSL_Altered, showing that complete extraction of the cranial vault can be achieved by altering the Hounsfield units and fractional intensity in panel **A** (HU range = 5-100, σ= 1, FI = 0.35) and failed extraction showing an incomplete extraction of the cranial vault using FSL_Muschelli pipeline in panel **B** (HU range = 0-100; σ= 1; FI = 0.01).

Volume measurements for all patients across all techniques are shown in Table 3.2. The manual technique had an ICC of 0.997 (RMSE: 1.27%, maximum error: 3.82%).

The semi-automatic technique had an ICC of 0.993 (RMSE: 2.02%, maximum error: 5.32%). Altering the FI and smoothing parameters in the fully automatic technique gave a volume range of 336.6–6673.4 cm^3 and 1112.1–3629.2 cm^3 respectively (Table 3.3).

All volume measurements, manual against semi-automatic (OsiriX against Simpleware) and manual against automatic (OsiriX against FSL_Muschelli) showed a high linear correlation (R^2=0.993 and R^2=0.995 respectively) (Figure 3.6 A-B). This was similar for the fully automatic method once the command line had been altered (OsiriX against FSL_Altered)(R^2=0.978) (Figure 3.6 C).

Table 3.2 Calculated ICV (cm^3) for all scans across all methodologies. FSL_Altered returned uniformly larger ICVs, This was due to the mask overlaying the skull in parts, leading to a larger mask and therefore a larger volume, as shown in Figure 3.9.

Patient	OsiriX	Simpleware	FSL_Muschelli	FSL_Altered
Pre-op				
1	1559.4	1513.6		1659.6
2	706.3	714.9	702.7	764.0
3	689.6	719.9	710	781.7
4	767.7	758.5		845.7
5.0	794.3	779.5	813.1	962.0
6.0	824.6	795.2	823.7	883.9
7.0	882.3	859.7	902.5	984.2
8.0	916.1	908.6	942.9	1013.9
9.0	996.2	1006.3		1053.7
10.0	1070.0	1019.9	1083.4	1148.1
11.0	1202.0	1196.7	1234	1288.4
12.0	1376.1	1391.1		1458.0
13.0	1354.1	1374.8		1499.3
Post-op				
1.0	1705.5	1715.3		1818.0
2.0	1543.2	1559.2	1543.1	1648.9
3.0	1086.5	1123.7		1220.3
4.0	1151.2	1145.6		1218.8
5.0	1619.7	1609.9		1789.1
6.0	1067.8	1076.0		1129.0
7.0	1215.3	1173.8	1199.9	1259.0
8.0	1544.6	1543.6		1694.7
9.0	1438.3	1359.5		1393.6
10.0	1390.9	1363.4	1354.3	1420.4
11.0	1539.7	1504.8	1491.5	1564.5
12.0	1646.1	1620.9		1671.0
13.0	1755.0	1718.5		1805.8

Table 3.3 Differences in the measurement of intracranial volume (ICV) using the fully automatic technique with altered fractional intensity (FI) and Gaussian Smoothing (Smoothing) parameters.

FI	ICV (CM^3)	Smoothing	ICV (CM^3)
0.01	1083.4	0.10	1112.1
0.05	1082.5	0.20	3629.2
0.10	1080.8	0.30	1069.2
0.15	1079.7	0.40	1068.7
0.20	1078.0	0.50	1083.4
0.25	1076.6	0.60	1083.4
0.35	1067.2	0.70	1083.5
0.50	6673.4	0.80	1083.7
0.75	1875.3	0.90	1083.6
0.99	366.6	1.00	1083.4

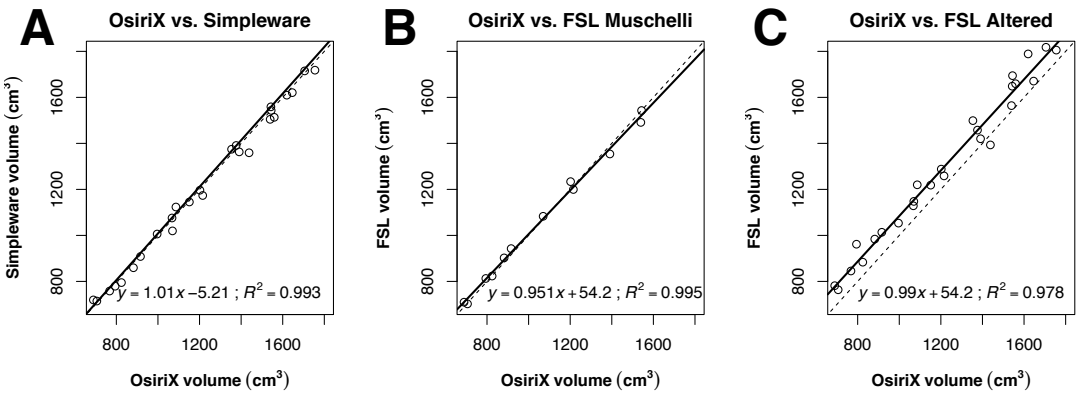

Figure 3.6 Correlation of volume across different methodologies. Dashed line shows 1:1 correlation, solid line shows correlation between the two techniques.

Limits of agreement were similar for Simpleware and FSL_Muschelli (Figure 3.7 A-B): mean difference and 95% confidence intervals (CI) for Simpleware was 11.1 cm^3 (95%CI: -42.5; 64.7 cm^3) and for FSL_Muschelli was -2.2 cm^3 (95%CI: -51.5; 47.0 cm^3).

However, for FSL Altered (Figure 3.7 C), a larger positive bias was found with a mean difference of -82.0 cm^3 (95%CI: -177.3; 13.2 cm^3).

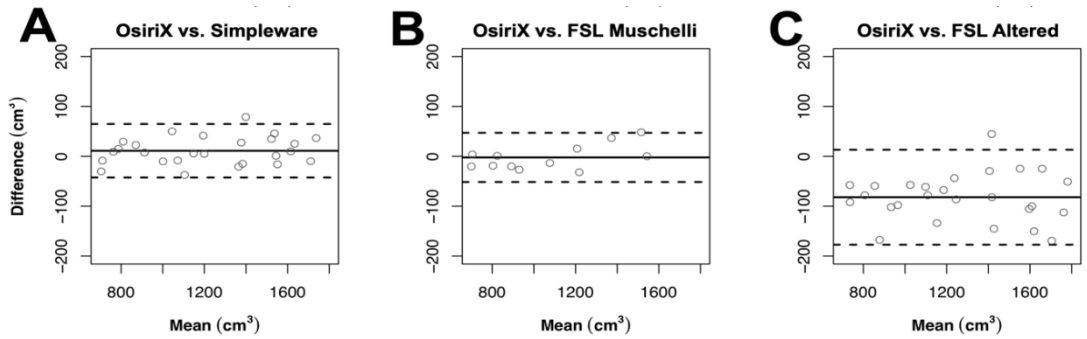

Figure 3.7 Bland Altman plots of technique comparisons. Dashed lines show 2SD from the mean, solid line shows the mean.

Time spent to perform the segmentation and extract ICV was recorded; the manual technique took an average of 44 minutes per scan, the semi-automatic technique, approximately 20 minutes, and the fully-automatic method 2 minutes.

The coefficient of determination for full scan versus half scan, full scan versus quarter scan and full scan versus eighth scan when analysed with the semi-automatic method were $R^2 = 0.98$, 0.96 and 0.94, respectively (Figure 3.8 A-C). However, the limits of agreement increased with a decreasing number of slices (Figure 3.8 D-F): mean difference and 95% CI for full versus half were -9.9 cm^3 (95%CI: -77.3; 57.4 cm^3), full versus quarter 2.6 cm^3 (95%CI: -81.5; 86.8 cm^3), and full versus eighth -5.8 cm^3 (95%CI: -113.4; 101.9 cm^3).

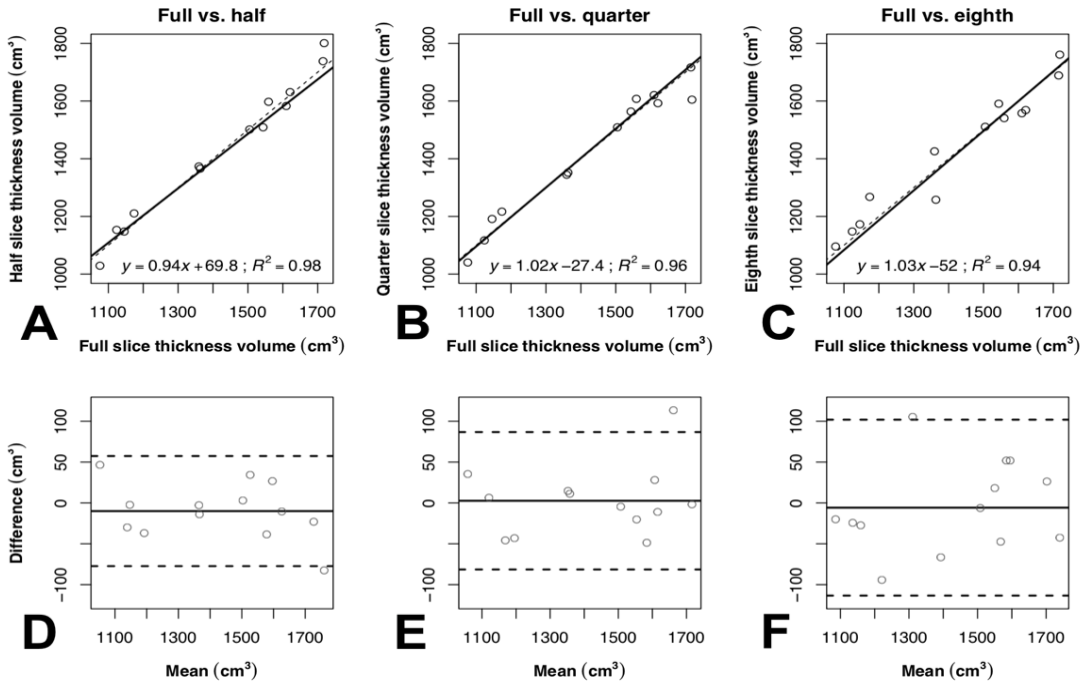

Figure 3.8 (A-C) Correlation of volume across slice number including full versus half scan, quarter scan and eighth scan. Dashed line shows 1:1 correlation, solid line shows correlation between the two techniques. **(D-F)** Bland Altman plots showing decreasing agreement as slice number decreases. Dashed lines show 2SD from the mean, Solid line shows the mean.

3.4 Discussion

Accurate measurement of intracranial volume (ICV) is useful in many settings: anthropometrically it can be used to provide normative data on skull vault volumes and in neurology it can be used in conjunction with measures of brain volume to assess disease driven volumetric changes (Dinomais et al., 2016; Kamdar et al., 2009). To the craniofacial surgeon it provides information for management paradigms, for pre-operative planning and for post-operative evaluation of surgical outcomes, allowing for

quantifiable, objective measurements to be made (Arab et al., 2016). These data driven outcome measurements are important in a time of rapid innovation of surgical techniques.

Since Gault's early work on the study of ICV from CT scans and then application of this technique to Apert syndrome by Gosain et al., many authors have investigated this objective measure (Anderson et al., 2004; Gault, Brunelle, Renier, & Marchac, 1988; Gosain et al., 1995). The results presented in this study suggest that different methods available to the craniofacial investigator give broadly similar results. Despite the cohort being made up of complex patients with Apert syndrome, each technique has been shown to manage volume extraction in both small paediatric skulls and enlarged post-operative skulls, which often contained bone holes due to the syndrome.

The use of different image post-processing techniques to manipulate and analyse CT data to provide ICV calculation in the setting of craniosynostosis has been shown here to give significantly similar results. The limits of agreement were similar for both manual and semi-automatic, and manual and fully automatic when using the Muschelli technique. When using the fully automatic method with the altered command line there was a positive bias, with uniformly higher values generated by the fully automatic method, due to the mask overlying the skull vault in places.

Manual and semi-automatic techniques provide varying degrees of user control whilst a fully automatic technique performs ICV calculation through command line instructions alone. There remains an inherent degree of human control in this technique, manifest through the values chosen for fractional intensity and Gaussian smoothing. A fully manual technique provides the user with a high degree of control. Using a digital pen, the outline of the intracranial cavity can be accurately traced from foramen magnum to vertex. However, this technique is time costly, which may limit the size of the studies

in which it can be used. It is noted that the OsiriX software is free to download and this technique should be reproducible in other craniofacial centres. This study used the measurement techniques to calculate the volume of the entire cranial vault. Due to the size of the measured space, the manual method is time consuming. This technique may become more useful when measuring smaller objects such as intracerebral lesions or specific spaces such as cerebral ventricles or orbital volumes.

The semi-automated technique utilises thresholding and region growing to segment the intracranial contents from the skull. This technique, whilst not providing the same control as the manual method does offer other advantages. It is possible to manipulate the images in 3D and have a constantly updated 3D visual of the extraction (Figure 3.2). Alongside the 3D visualisation of the intracranial vault extraction, it is possible to produce and view segmentations of the various components of the head in general. This allows for investigation of dead spaces, cerebrospinal fluid (CSF) spaces and other areas discernible on a CT scan. With practice, this technique is less time consuming than the fully manual technique. Whilst Simpleware Scan IP is commercial software, there are other programs freely available such as 3D Slicer (http://slicer.org) and ITK snap (http://www.itksnap.org/) that work in a similar way.

A fully automated technique is not a panacea. It requires a rudimentary knowledge of command line programming, and the user has less control over the results. In our first attempt, fourteen of the twenty-six scans failed to extract. This gave a failure rate of 53.8%, which compares unfavourably to Muschelli's failure rate of 5.2% (Muschelli et al., 2015). We hypothesise that this failure was in part caused by the presence of cranioplasty springs in some of the post-operative scans as, in nine of the failed scans, springs were still in situ. In the scans that were successful, there remained a scattering of

holes in the mask, which were not filled by the fill holes command. This led to marginally lower ICV values when compared to the manual method. The altered command line gave a 100% success rate, however the ICV values were uniformly larger than those from the manual and semi-automatic methods. This was due to the mask overlaying the skull in parts, leading to a larger mask and therefore a larger volume (Figure 3.9).

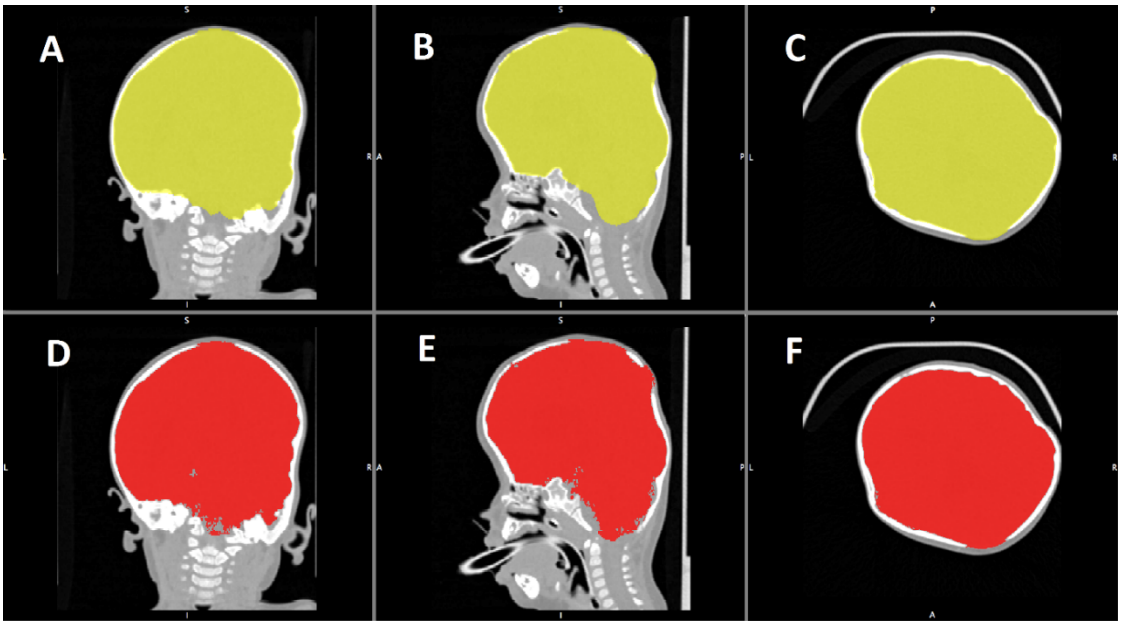

Figure 3.9 Example FSL outcomes. Showing an altered command line extraction (FSL Altered) in which there has been a slight over estimation in the volume (panels **A-C**). FSL_Muschelli command line shown in panels **D-F** with a slight under estimation due to holes in the mask. HU range =, 5-100, 0-100; σ= 1; FI =,0.35, 0.01respectively.

The fully automatic method has the advantage of being faster to use, the speed of which could be advantageous when programming entire cohorts to undergo the same pipeline at once. This would however require knowledge of the scripting process, not always available in every unit. In addition, this method removes user dependency, in that

by running one pipeline of commands for every study image, unbiased results can be obtained. Obtaining uniformly larger volume results may not be problematic depending on the intended use of the tool. For example, when comparing pre- and post-operative volume change, or calculating ICV in a large cohort using the fully automatic method will give rapid, unbiased results.

The comparison of CT scans with full, half, quarter and an eighth number of slices analysed using the semi-automatic method has shown that the linear relationship between full and an eighth of the number of slices remains high, but that the limits of agreement increase with a decreasing number of slices. We postulate this is due to the uniformity in calvarial shape and the averaging effect. The number of slices in the 'eighth category' ranged from 26 to 40 and our analysis shows that this number of slices may be utilised to provide a meaningful result with good concordance to the 1mm slice thickness volumetric data.

Whilst correlations between measurements have been provided and show good agreement, we would recommend that where possible one technique is used throughout to ensure the highest accuracy.

3.5 Summary

When measuring ICV in craniosynostosis, the most commonly used method reported in the literature is a semi-automatic one. Similar results can be obtained using manual, semi-automatic or automatic techniques with decreasing amount of time taken to perform each method. Command line instructions have been provided to perform

automatic ICV calculations from CT data. When calculating ICV in the remainder of the thesis, the semi-automatic and automatic methods outlined in this chapter are used.

Chapter 4 **INTRACRANIAL VOLUME AND HEAD CIRCUMFERENCE**

Part of the work described in this chapter has been published in *Plastic and Reconstructive Surgery*:

- Breakey, R. W. F., Knoops, P. G. M., Borghi, A., Rodriguez-Florez, N., O'Hara, J., James, G., . . . Jeelani, N. U. O. (2018). Intracranial volume and head circumference in children with unoperated syndromic craniosynostosis. *Plastic and Reconstructive Surgery, 142*(5), 708e -717e.

This work was presented at the 17th Congress of the International Society of Craniofacial Surgery in Cancun, Mexico, October 24th – 28th, 2017

To calculate the ICV change following cranial vault expansion requires pre and post-operative ICV measurement. The volume change that can be calculated from pre to post-operative scans however accounts for both ICV increase due to surgery and patient growth that has occurred in the time between the two scans. In order to correct for this and assess the effects of surgery alone, growth curves for unoperated children need to be created so that the expected change in volume attributed to growth can be subtracted from the post-operative ICV. This chapter describes the use of the semi and fully automatic ICV measurement techniques analysed in Chapter 3 to generate growth curves for an unaffected control group as well as for the most common craniofacial syndromes.

4.1 Introduction

As described in chapter 2, craniosynostosis includes a range of skull growth abnormalities due to the premature fusion of the cranial sutures that can lead to multiple functional and aesthetic problems, with one of the earliest and most important being raised intracranial pressure ICP.

ICV measurements, whilst not providing direct information about ICP, can provide information about the space available for the growing brain and give an indication as to whether craniocerebral disproportion may be present (Fok, Jones, Gault, Andar, & Hayward, 1992). They can also be used to assess the change in volume gained by operative interventions (Serlo et al., 2011); however, as pre- and post-operative scans are often taken with significant time intervals, it may be necessary to take into account the underlying growth. Due to the current lack of syndrome specific growth curves, the underlying growth used in these cases is often taken from healthy children's reference

curves, which may not always be a true representation of syndromic growth (Derderian et al., 2015).

A variety of measurement techniques to determine ICV have been described in the literature, from early efforts relying on mathematical estimations (Bray, Shields, Wolcott, & Madsen, 1969; Sgouros, Goldin et al., 1999; Tng, Chan, Hagg, & Cooke, 1994) to more reliable, current practice methods based on 3-dimensional imaging from CT or MR scans. However, exposure to ionising radiation during CT scans and the potential deleterious effects of a general anaesthetic required for a young child in MR, combined with lengthy image post-processing analysis, make regular surveillance of ICV in the same patient impractical. Francisca et al. in 2015 illustrated the correlation between OFC and ICV; they suggested that OFC could be used as a marker of ICV, therefore overcoming the above problems (Francisca et al., 2015). Whilst promising, the number of patients per syndrome in the study were small.

At GOSH, treatment for raised ICP is reactive rather than prophylactic. Thorough surveillance of ICP via ophthalmology including fundal examination and electrodiagnostic tests (visual evoked potentials) are included in the patient protocol (Liasis et al., 2003). Any deterioration, in concert with clinical evaluation indicating raised ICP would necessitate a vault expansion. Due to the reactive management of raised ICP at GOSH, there is a large cohort of unoperated children with syndromic craniosynostosis.

The aim of this chapter is twofold:

1. To provide syndrome specific reference growth curves to enable monitoring of ICV over time and allow for like-with-like comparison
2. To provide evidence for the use of OFC as an indicator of ICV

4.2 Methodology

4.2.1 Patient population

All pre-operative CT scans from GOSH patients with a diagnosis of Apert, Crouzon-Pfeiffer or Saethre-Chotzen syndrome were considered for this study. Crouzon and Pfeiffer syndrome patients were grouped together due to their shared FGFR2 mutations and the consideration that they can be phenotypic variations of the same genetic defect (Cunningham et al., 2007; Rutland et al., 1995). Scans were available from 2004 onwards. Exclusion criteria were scans with slice thickness >3mm, incomplete scans that did not include the full region between the vertex and the foramen magnum, and scans that were obstructed by artefacts from shunt devices.

A cohort of non-craniofacial children was selected from the GOSH PACS database as control group. These patients underwent scanning in the period between January 2015 and January 2017. Other than those children with no known disease, diagnoses included haematological malignancies, epilepsy, extra cranial carcinomas, diabetic ketoacidosis and immune deficiencies. The CT scans were carried out to investigate a number of presentations including infection, haemorrhage, arterio-venous malformations, headaches, intracranial extension of dermoid cysts, cerebral oedema and craniosynostosis. None of the control patients had a history of head or craniofacial trauma. All control group scans were reported as normal by GOSH consultant radiologists, with no intracranial abnormalities. These scans were also required to be of a slice thickness <3mm and to include the vertex through to the foramen magnum.

4.2.2 Intracranial volume measurement

ICV was calculated using the semi-automatic and automatic methods discussed in chapter 3. The majority were calculated automatically using FSL (Analysis Group, FMRIB, Oxford, UK) (Muschelli et al., 2015). In those cases where the automatic technique failed to extract the entire cranial vault, the semi-automatic approach using Simpleware ScanIP (Simpleware Ltd., Exeter, UK) was adopted. As shown in chapter 3 both techniques have been shown to be reliable methods of ICV measurement, producing significantly similar results (Breakey et al., 2017).

4.2.3 Occipitofrontal circumference measurement

OFC was performed on the same CT scan as the ICV measurement using CAD software Rhinocerous (McNeel Europe, & Associated, Seattle, WA, USA). In Rhinocerous, a cutting plane can be visually selected at the level of maximal head circumference. The head circumference is then measured from the glabella to the occipital protuberance. This process is undertaken three times to closely reflect the technique for measuring OFC in a clinical setting (Figure 4.1).

Figure 4.1 OFC measurement. Measured using Rhinocerous with a technique that closely matches clinical measurement.

4.2.4 Data analysis and statistics

Correlation between IVC and OFC was studied in MATLAB (MathWorks, Natick, MA, USA), with logarithmic fits accompanied by 95% confidence intervals as well as a coefficient of determination (R^2) in all patient groups. The R^2 is used as a statistical measure of how close data are to a fitted regression line. In general, the higher the R^2 the better the model fits the data. The strength of the correlation can be described according to the guide produced by Evans (Evans, 1996) which suggests:

- 0.00-0.19: “very weak”
- 0.20-0.39: “weak”
- 0.40-0.59: “moderate”

- 0.60-0.79: “strong”
- 0.80-1.0: “very strong”

Normality of the data was assessed using the Shapiro-Wilk test. Two tailed Student t-test results were considered significant for p values <0.05. Statistical analyses were performed using IBM SPSS Version 25.

4.3 Results

There were 229 syndromic patients suitable for this study. Of these, 147 patients had 243 pre-operative CT scans. 221 of the scans remained eligible for inclusion. The study group comprised 93 Apert scans (M:F 50:31), 117 Crouzon-Pfeiffer scans (M:F 67:45), and 33 Saethre-Chotzen (M:F 15:13) scans. The children with Pfeiffer’s syndrome included in the study were either Type I or Type II / III, with 10/15 being type I. The older Pfeiffer syndrome children were all Type I (the oldest Type II / III child was 7 months old) (M Cohen, 1993). The control group consisted of 56 patients with 58 eligible scans (M:F 33:25) (Table 4.1).

Table 4.1 Available numbers of scans in the GOSH PACS depository. Where available, multiple scans taken at different time points for the same patient were used.

	Apert	Crouzon-Pfeiffer	Saethre-Chotzen	Control	Totals	Syndrome totals
Patients	71	127	31	56	285	229
Patients with scans	53	71	23	56	203	147
Total Scans	93	117	33	62	305	243
Usable Scans	81	112	28	58	279	221
Male : Female	50:31	67:45	15:13	33:25	165:114	132:89

In the Apert cohort (n=71); one patient had a shunt in situ at the time of their scan, this was not excluded because the shunt had not caused any artefact and therefore did not affect the volume calculation, 6 patients later had a shunt inserted. 18 patients have not required vault expansion for raised ICP, 35 patients have had posterior vault expansion after the scan used for ICV measurement.

In the Crouzon-Pfeiffer cohort (n=127); six patients had shunts in situ at the time of their scan, five were not excluded because the shunt had not caused any artefact and therefore did not affect the volume calculation, seven patients went on to have a shunt after the scan used for ICV calculation. Following the scan used for ICV measurement; 37 patients required cranial vault expansion, 15 required Monobloc and Rigid external distractor (RED) frame, three required a Le Fort III procedure, one patient underwent FOA and 15 have had no procedures to date.

In the Saethre-Chotzen cohort (n=31); no patients required shunting, seven required cranial vault expansion, eight required FOA and eight patients have yet to require a craniofacial procedure.

The mean age across all syndromic groups was 2.4 years (range 1 day to 17.5 years), whilst for the control group the mean age was 5.4 years (range 6 days to 15.7 years). For easier comparison, patients were further subdivided into 6 age ranges: 0 – 1year, 1 – 2year, 2 – 4year, 4 – 8year, 8 – 12year, 12 – 18year (Francisca et al., 2015) (Table 4.2).

Table 4.2 Age group demographics and study numbers across all syndromes. Where available multiple scans, taken at different time points for the same patient were used.

Age group	Apert	Crouzon-Pfeiffer	Saethre-Chotzen	Control	Syndrome totals
0-1 yr.	44	52	12	12	108
1-2 yr.	10	21	8	9	39
2-4 yr.	11	17	4	9	32
4-8 yr.	7	11	3	8	21
8-12 yr.	4	5	0	13	9
12-18 yr.	5	6	1	7	12
Mean age, yr. Mean Age (years)	2.6	2.45	2.1	5.4	
Minimum Age (yr.)	0.0	0.0	0.2	0	
Maximum Age (yr.)	17.2	17.5	12.7	15.7	

Best fit logarithmic curves were assessed for ICV and OFC against time in all syndromes and divided for gender (Figures 4.2 – 4.11). IVC growth curves for each syndrome (black) and control (blue) are shown with the solid lines representing the fitted logarithmic curve and the dashed line representing the 95% confidence interval. The equations shown in Figure 4.6 provide the ICV in cm^2 when given age (x) in days. The equations shown in Figure 4.11 provide the OFC in cm when given age (x) in days.

For ICV, mean R^2 for the syndromic groups was 0.75, for the control group R^2 was 0.8. For OFC, mean R^2 for the syndromic groups was 0.76 and control group R^2 was 0.86 (Figures 4.2 – 4.11).

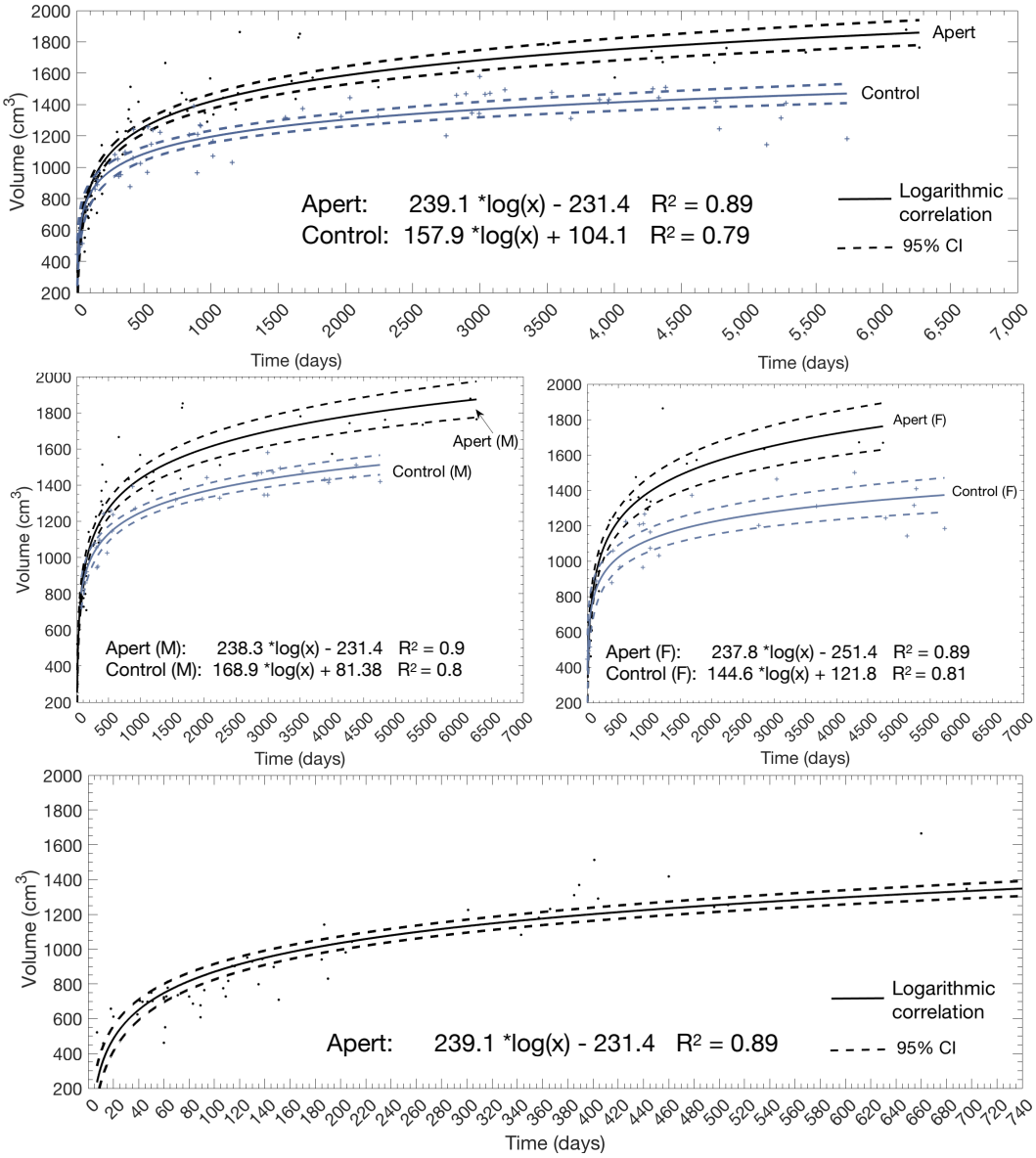

Figure 4.2 Apert ICV growth curves (**A**) All Apert ICV against time, (**B**) male Apert ICV against time, (**C**) female Apert ICV against time, (**D**) all Apert ICV against time, highlighting first 2 years of life.

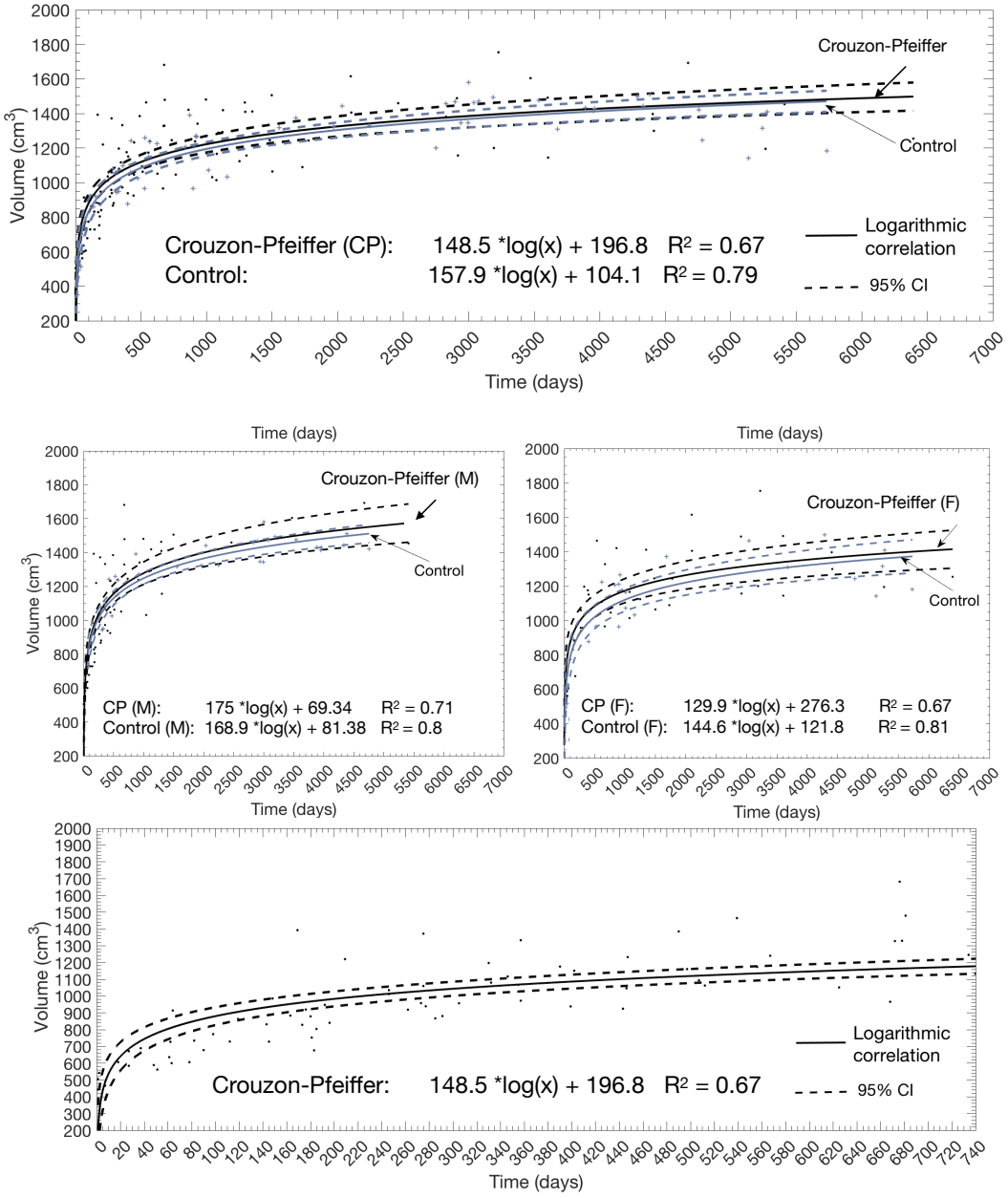

Figure 4.3 Crouzon-Pfeiffer ICV growth curves (**A**) All Crouzon-Pfeiffer ICV against time, (**B**) male Crouzon-Pfeiffer ICV against time, (**C**) female Crouzon-Pfeiffer ICV against time, (**D**) all Crouzon-Pfeiffer ICV against time, highlighting first 2 years of life.

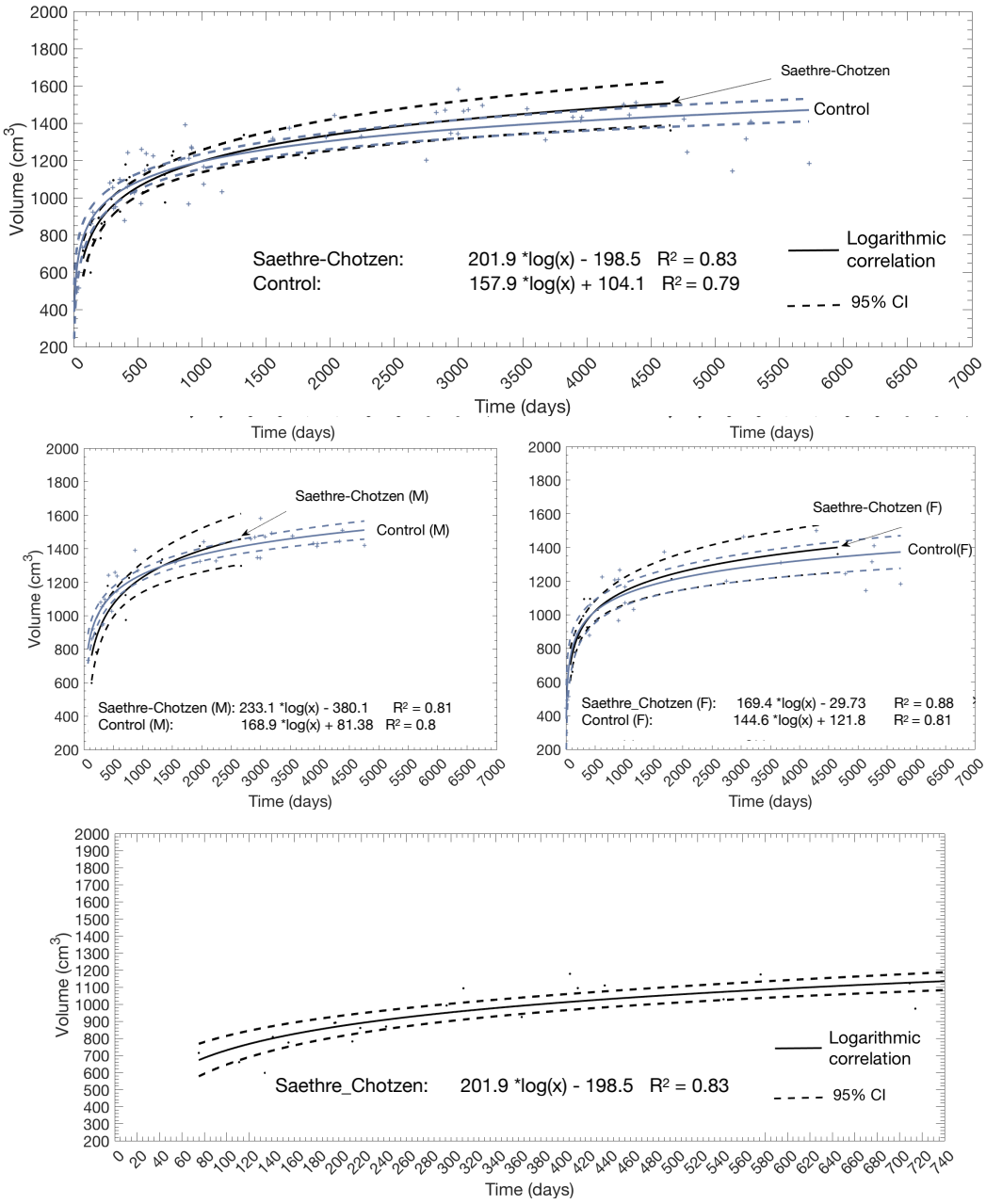

Figure 4.4 Saethre-Chotzen ICV growth curves (**A**) All S-C ICV against time, (**B**) male S-C ICV against time, (**C**) female S-C ICV against time, (**D**) all S-C ICV against time, highlighting first 2 years of life.

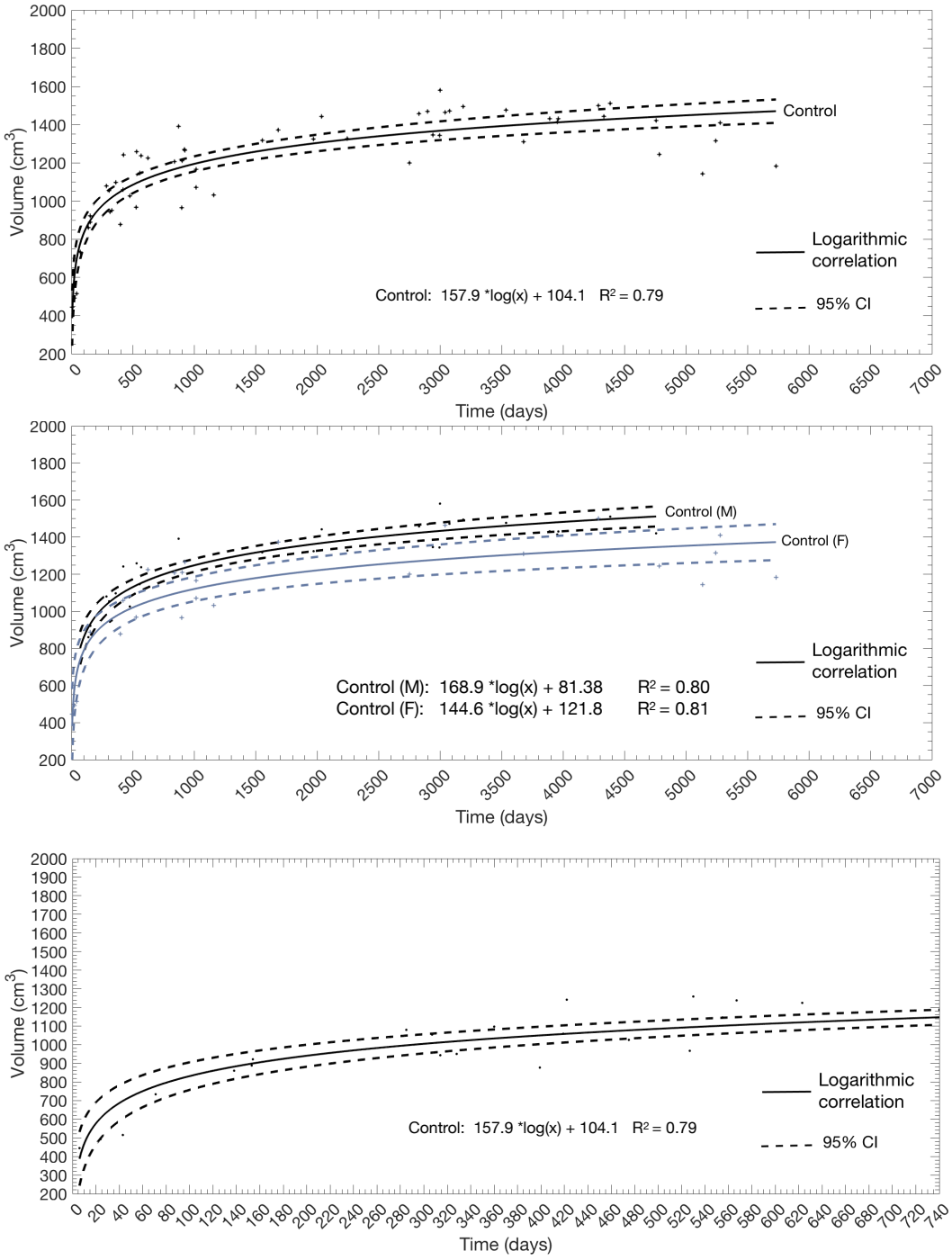

Figure 4.5 Control ICV growth curves (**A**) All control ICV against time, (**B**) male and female control ICV against time, (**C**) all control ICV against time, highlighting first 2 years of life.

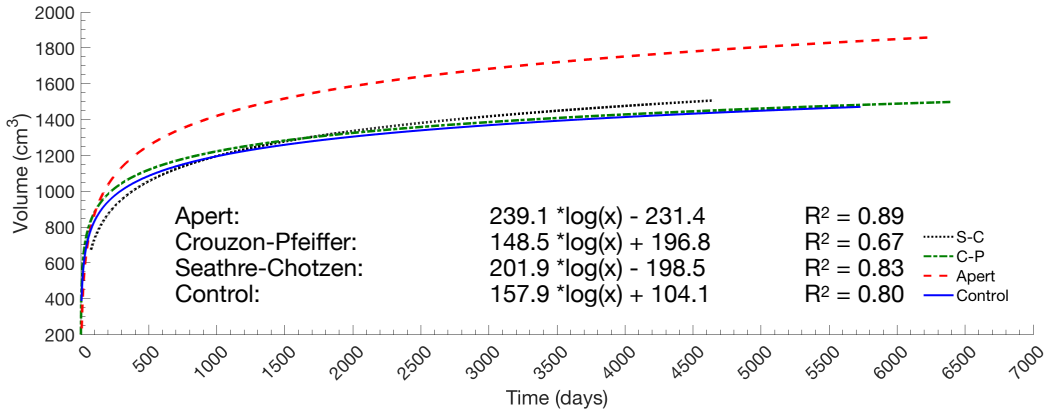

Figure 4.6 All groups ICV growth curves. All Syndromic groups and control volume (cm^3) against time.

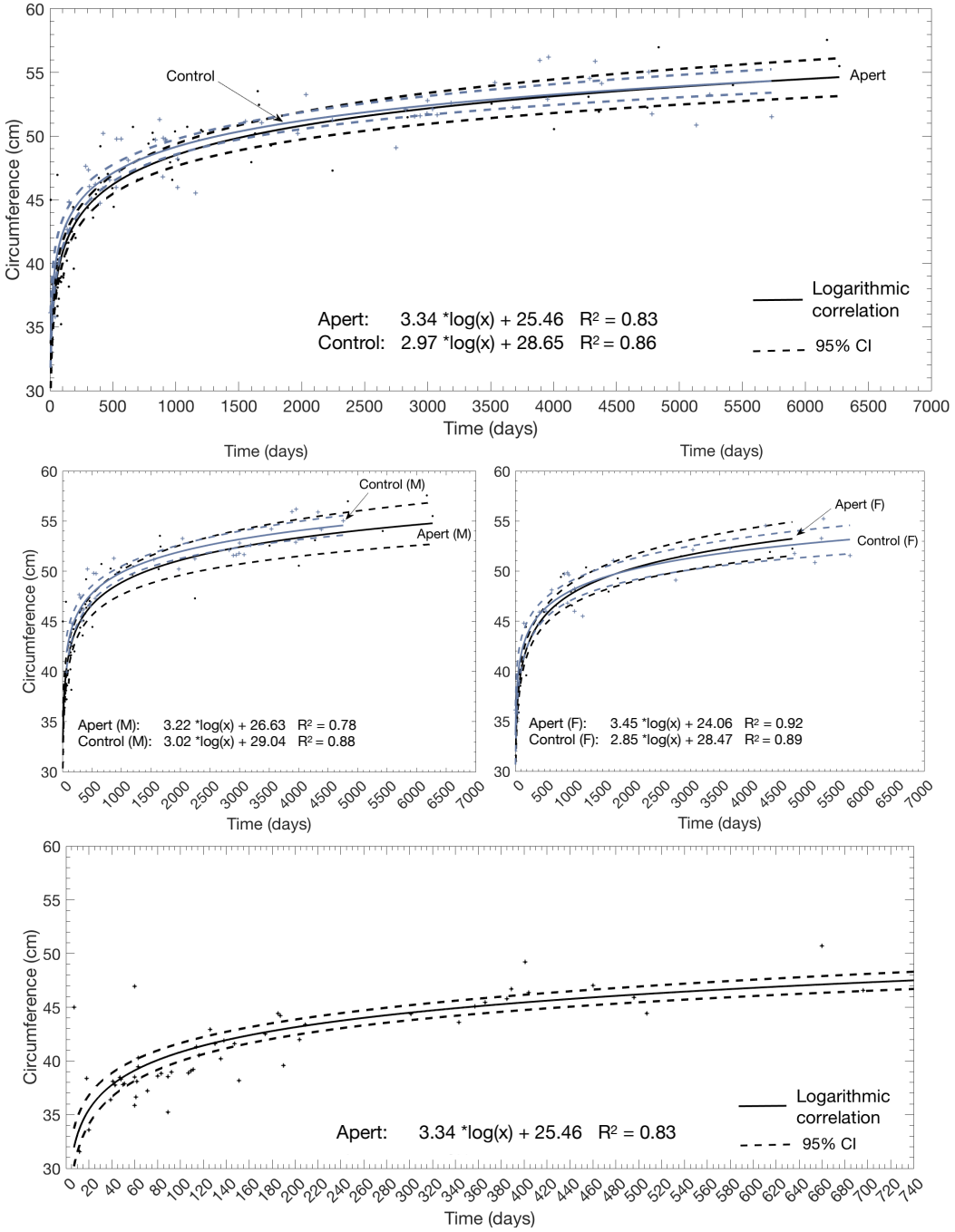

Figure 4.7 Apert OFC growth curves (**A**) Apert and control OFC against time, (**B**) male Apert OFC against time, (**C**) female Apert OFC against time, (**D**) all Apert OFC against time, highlighting first 2 years of life.

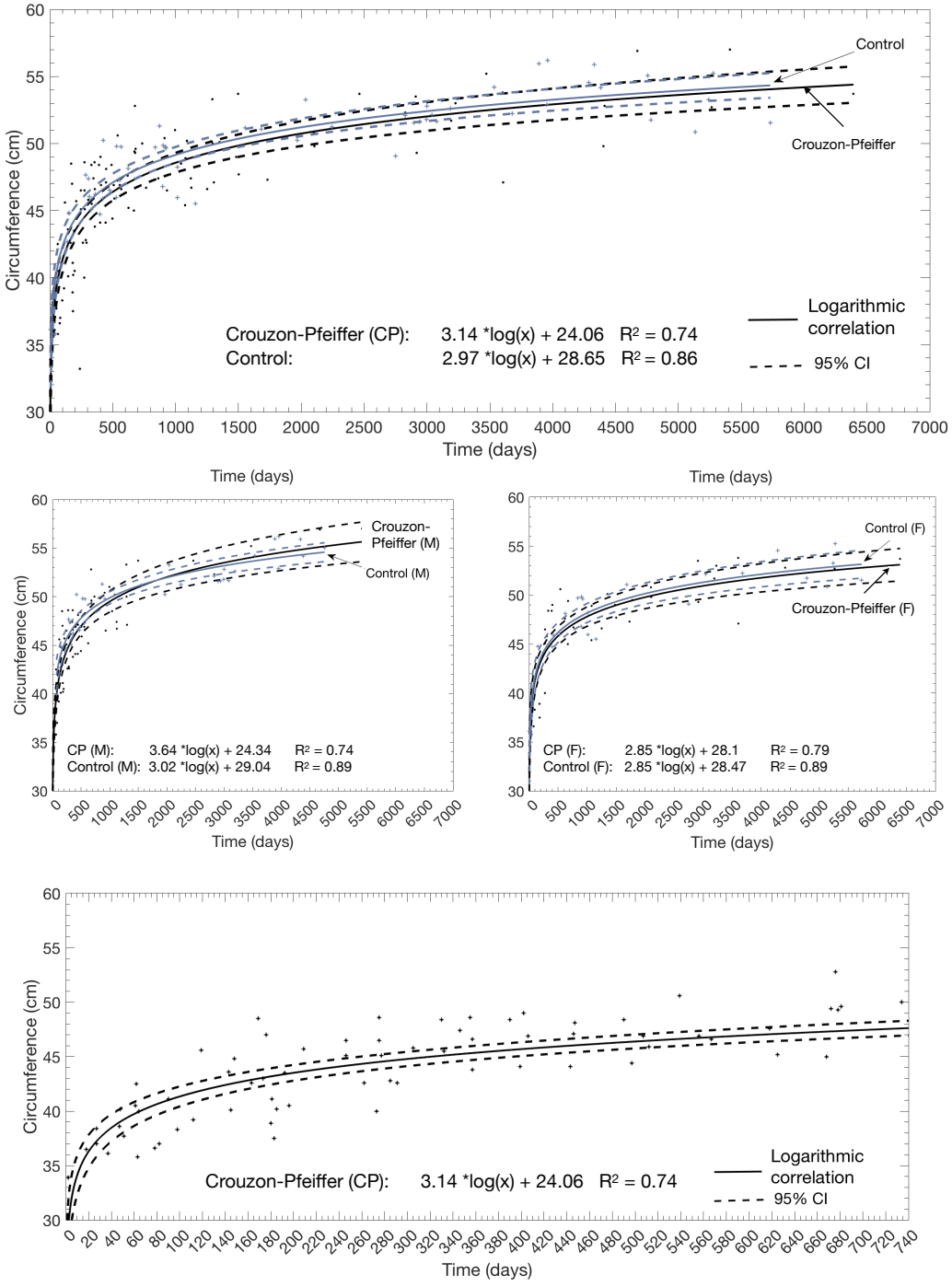

Figure 4.8 Crouzon-Pfeiffer OFC growth curves (**A**) Crouzon-Pfeiffer and control OFC against time, (**B**) male Crouzon-Pfeiffer OFC against time, (**C**) female Crouzon-Pfeiffer OFC against time, (**D**) all Crouzon-Pfeiffer OFC against time, highlighting first 2 years of life.

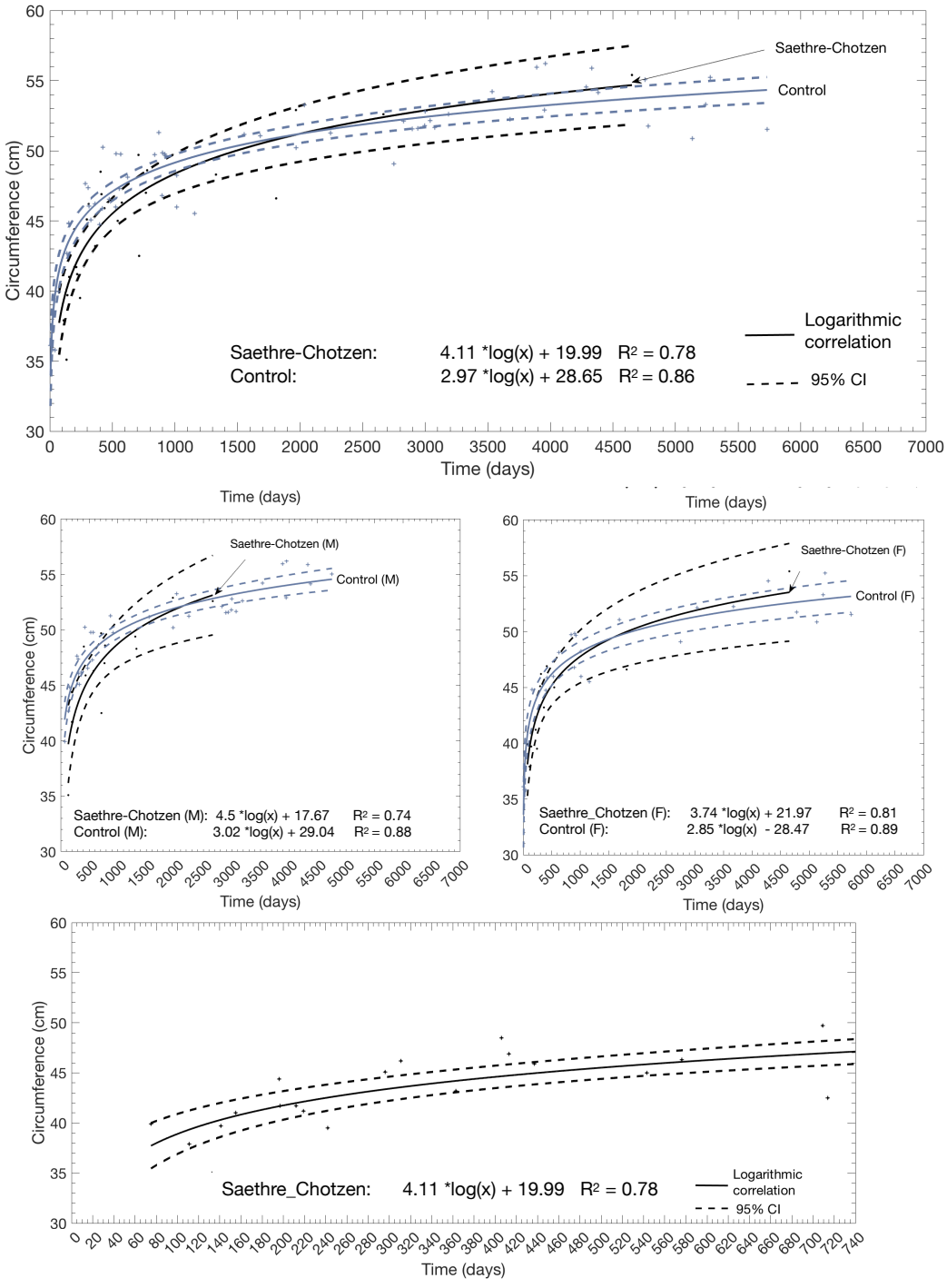

Figure 4.9 Saethre-Chotzen OFC growth curves (**A**) Saethre-Chotzen and control OFC against time, (**B**) male Saethre-Chotzen OFC against time, (**C**) female Saethre-Chotzen OFC against time, (**D**) all Saethre-Chotzen OFC against time, highlighting first 2 years of life.

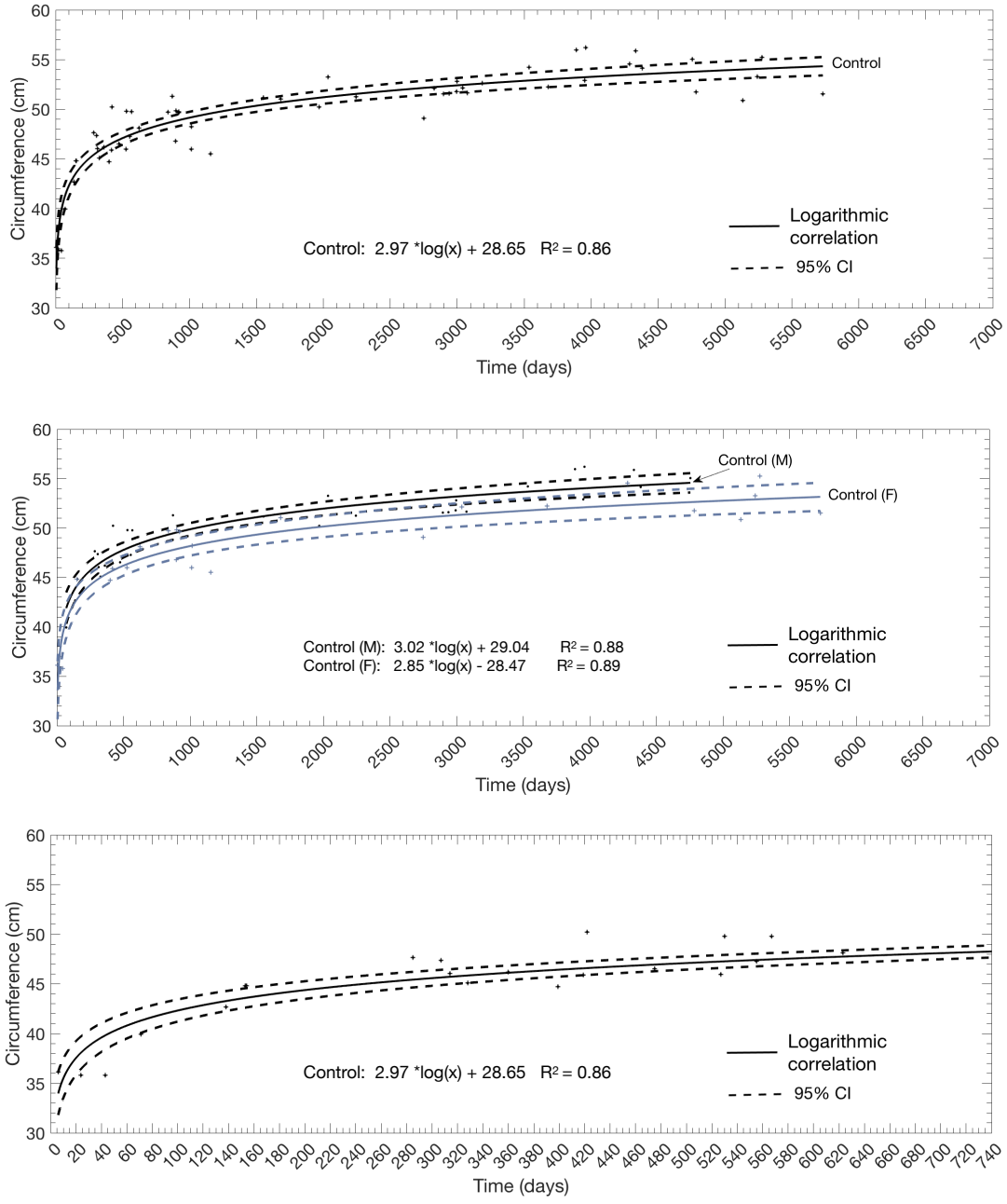

Figure 4.10 Control OFC growth curves (**A**) All control OFC against time, (**B**) male and female control OFC against time, (**C**) all control OFC against time, highlighting first 2 years of life.

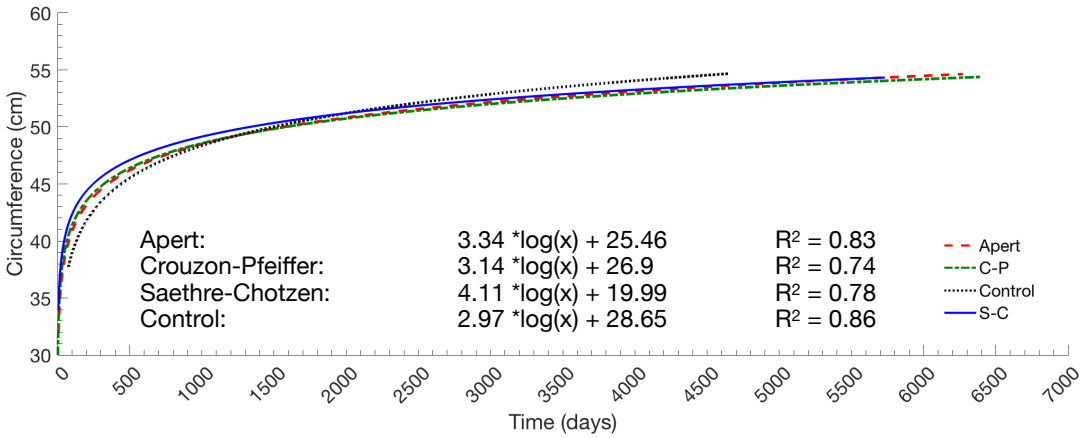

Figure 4.11 All groups OFC growth curves. All syndromic groups and control circumference (cm) against time.

The correlation coefficient between ICV and OFC for all syndromes combined was $R^2 = 0.87$, (male $R^2 = 0.85$, female $R^2 = 0.87$) for the control group $R^2 = 0.91$ (male $R^2 = 0.88$, female $R^2 = 0.93$) (Figures 4.12 – 4.15). A summary figure is shown in Figure 4.16.

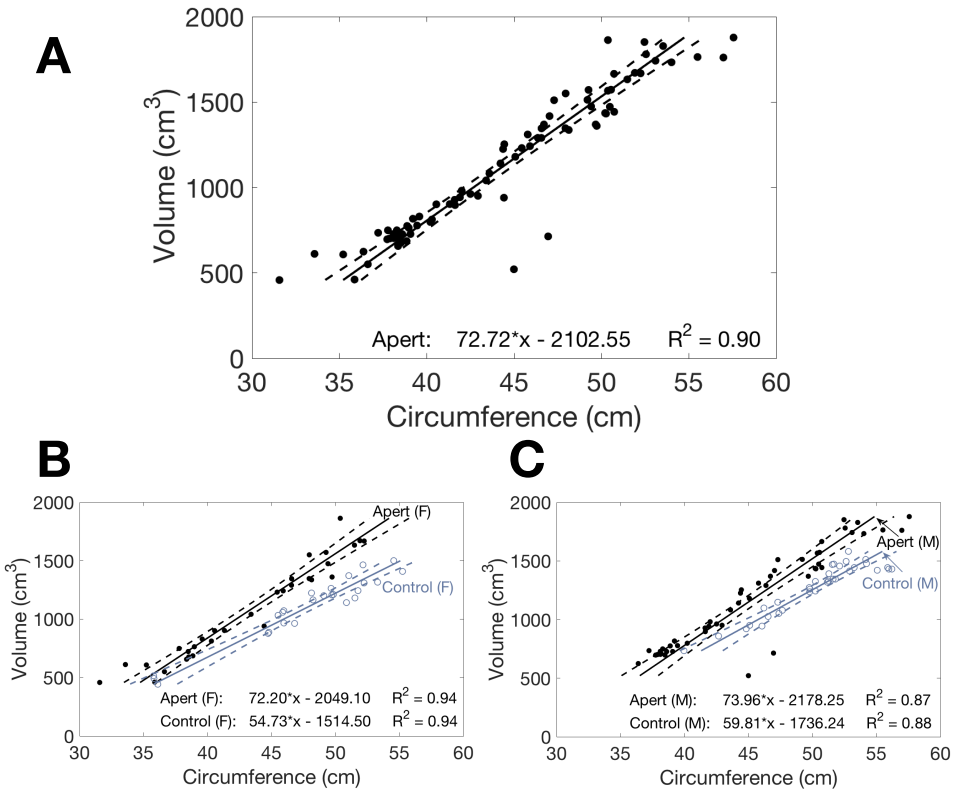

Figure 4.12 Apert ICV to OFC correlation. (**A**) All Apert OFC against ICV, (**B**) female Apert OFC against ICV, (**C**) male Apert OFC against ICV.

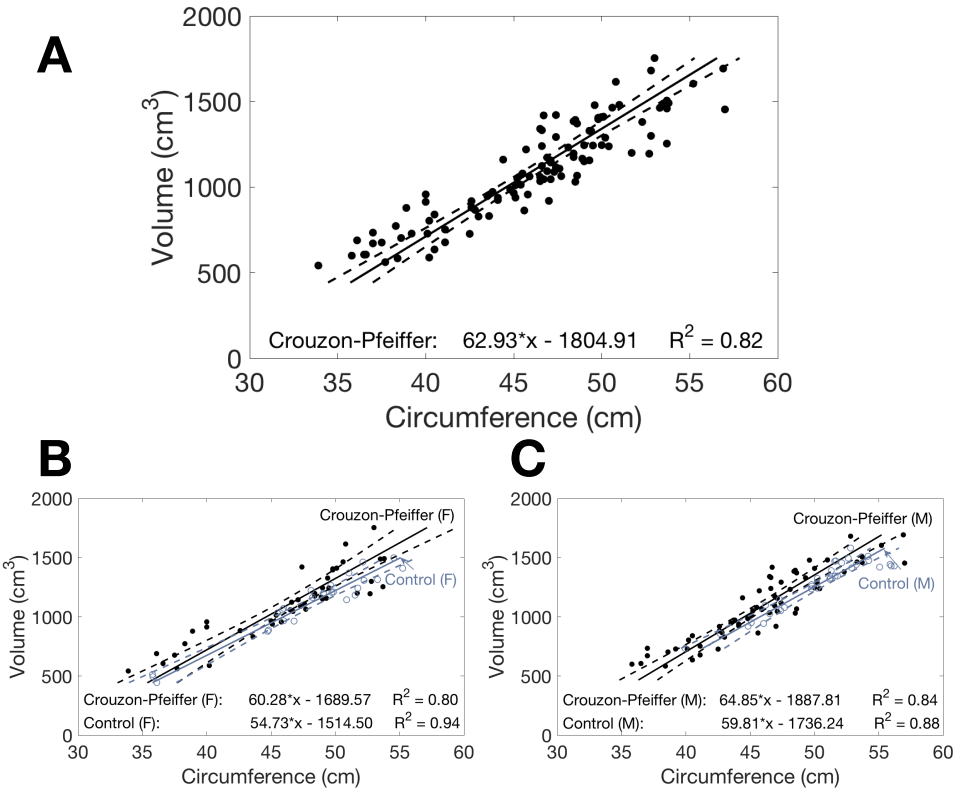

Figure 4.13 Crouzon-Pfeiffer ICV to OFC correlation (**A**) All Crouzon-Pfeiffer OFC against ICV, (**B**) female Crouzon-Pfeiffer OFC against ICV, (**C**) male Crouzon-Pfeiffer OFC against ICV.

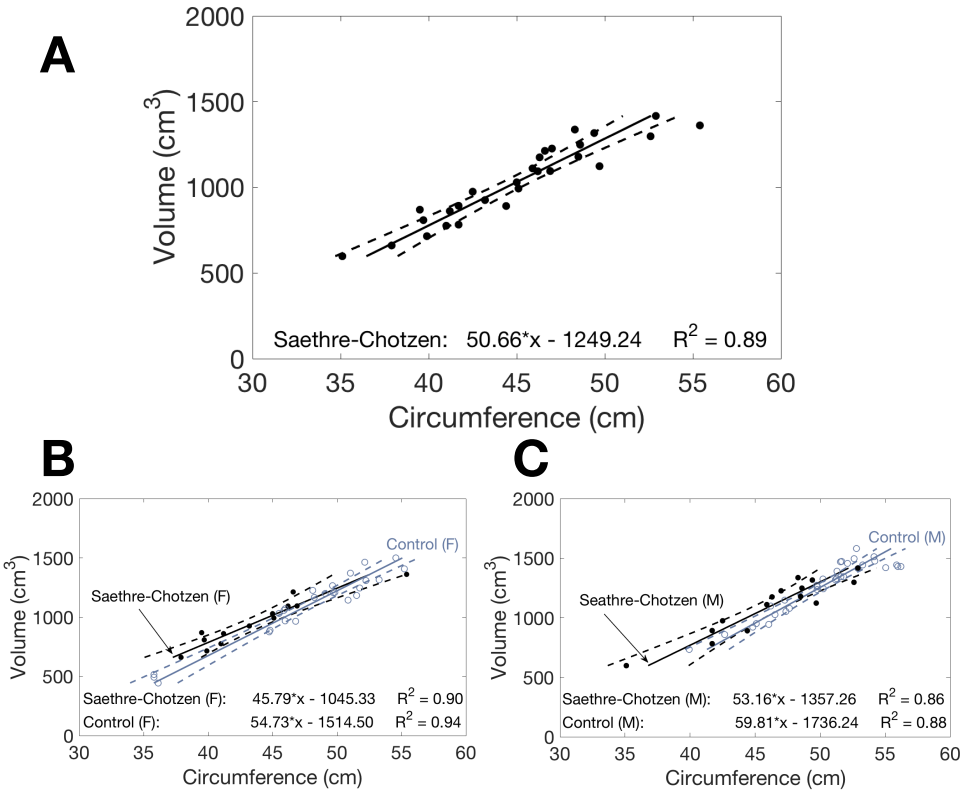

Figure 4.14 Saethre-Chotzen ICV to OFC correlation (**A**) All Saethre-Chotzen OFC against ICV, (**B**) female Saethre-Chotzen OFC against ICV, (**C**) male Saethre-Chotzen OFC against ICV.

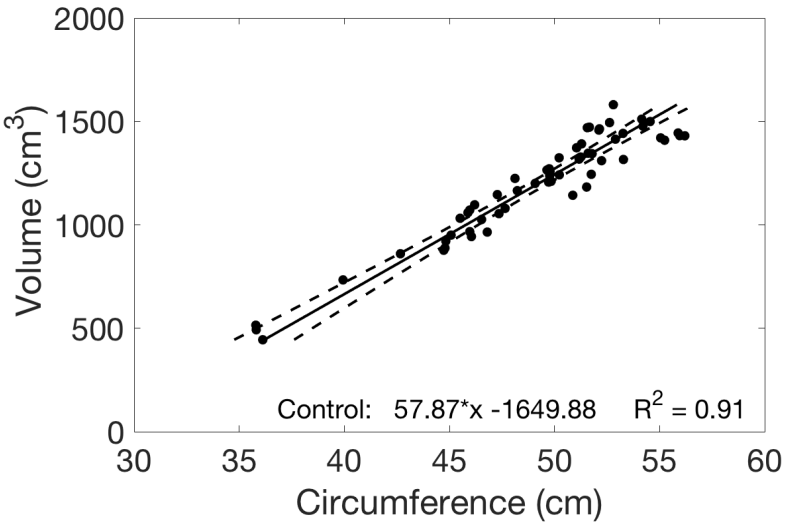

Figure 4.15 All control ICV to OFC correlation.

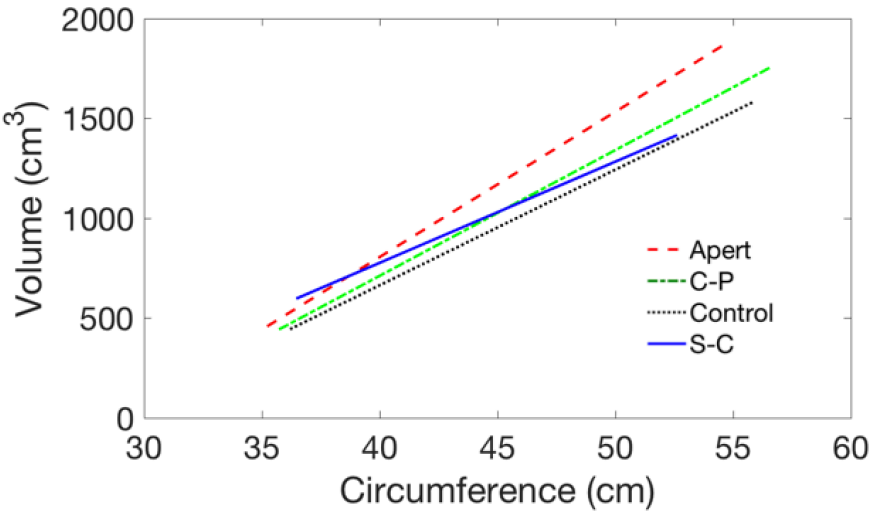

Figure 4.16 ICV to OFC summary for all groups.

Average head growth was overall similar for all syndromes and the control groups, apart from patients with Apert syndrome. Apert ICV began to diverge from the control group at day 63, becoming significantly different at day 206 (Figure 4.6). ICV

and OFC were highly correlated for all syndromes ($R^2 = 0.87$, male $R^2 = 0.85$, female $R^2 = 0.87$) and for the control group ($R^2 = 0.91$, male $R^2 = 0.88$, female $R^2 = 0.93$). ICV against OFC correlations for Apert, Crouzon-Pfeiffer, Saethre-Chotzen and control groups are shown in Figure 4.12 – 4.15. With the equations providing the ICV in cm^2 when given the OFC (x) in cm. Figure 4.6 shows the marked difference in Apert ICV as compared to the other groups, whereas Figure 4.11 shows overall similarity in OFC.

Mean ICV and OFC across all groups and subdivided age ranges are shown in Table 4.3. There was no significant ICV differences between Crouzon-Pfeiffer and control, or Saethre-Chotzen and control at any age group, nor with Apert and control in the 0-1year age group. From the 1-2year age group and upwards, there was a significant difference throughout (1-2 year $p = 0.03$, 2-4 year $p = 0.01$, 4-8 year $p = 0.02$, 8-12 year $p = <0.01$, 12-18 year $p = <0.01$).

Table 4.3 Mean ICV and OFC. Mean ICV and OFC across all age groups and syndromes.

Age	Apert		Crouzon-Pfeiffer		Saethre-Chotzen		Control	
	ICV (cm^3)	OFC (cm)	ICV (cm^3)	OFC (cm)	ICV (cm^3)	OFC (cm)	ICV (cm^3)	OFC (cm)
0-1 yr.	792.5	39.8	829.6	41.5	835.8	41.3	831.8	42.7
1-2 yr.	1363.9	46.8	1208.7	47.5	1097.8	46.4	1115.4	47.6
2-4 yr.	1450.6	49.4	1332.3	48.7	1281.9	48.3	1189.7	48.8
4-8yr	1625.8	50.3	1459.2	50.7	1309.0	50.7	1364.1	51.2
8-12 yr.	1691.5	52.0	1328.6	50.3			1439.1	53.4
12-18yr	1760.8	55.3	1360.6	53.2	1361.1	55.4	1318.0	53.1

4.4 Discussion

In this chapter, we have produced reference curves for a large series of children with Apert, Crouzon-Pfeiffer and Saethre-Chotzen syndromes and provided the necessary equations to transform OFC data into ICV estimates. Previous to this study, the literature lacked specific reference curves for ICV in patients with syndromic craniosynostosis. Having access to craniofacial growth curves offers clinicians the ability to directly compare clinical findings to published normal data. In the clinic, one can quickly assess whether a patient's growth curve is deflecting from the norm (an OFC not changing or showing growth of <0.5 SD within 2 years is a risk factor for developing papilloedema) (Francisca et al., 2015), and therefore when coupled with clinical data have a higher level of suspicion for raised intracranial pressure. When planning vault expansion surgery, the surgical team can use normal data to estimate a required percentage increase in intracranial volume. Post-operatively, by correcting for the underlying growth, change in volume can be assessed and indeed it was for this purpose that the study in this chapter was initially undertaken.

Children with Apert syndrome have a larger ICV when compared to the control group, in keeping with previous studies (Anderson et al., 2004; Gosain et al., 1995). The Apert group shows a similar ICV growth trajectory to the control group initially. After day 206, Apert ICV is significantly larger, shown by the 95% CI no longer overlapping (Figure 4.2 B). This divergence agrees with the significant difference between Apert ICV and Control ICV seen from the 1-2 year age group and onwards. This was not found in the Crouzon-Pfeiffer and Saethre-Chotzen groups, which is illustrated clearly by Figures 4.8 B and 4.9 B. ICV is highly correlated with OFC in Apert (R^2 = 0.9), and, when

compared to the control group, the line of best fit is shifted superiorly, indicating a larger ICV for a given OFC, in line with the phenotypical turricephalic head shape often seen in children with Apert syndrome. Male children with Apert syndrome have a larger ICV than female children with Apert syndrome, suggesting that sex specific growth curves should be used when referencing. In addition to this, there may exist a distinct ICV difference between the two predominant genetic mutations that lead to Apert syndrome; Ser252Trp (66%) or Pro253Arg (32%) (Johnson & Wilkie, 2011). Given that patients with Ser252Trp mutation present with more severe cranial defects and those with Pro253Arg present with a more severe degree of syndactyly, Ser252Trp patients may present with a more growth restricted skull. This was studied in 2004 by Anderson et al. their cohort of 16 patients with Ser252Trp mutation and 6 patients with Pro253Arg mutation showed no discernible difference in intracranial volume despite the phenotypical differences (Anderson et al., 2004). Total brain volume in children with Apert syndrome is also of interest. The larger Apert ICV may be matched by a larger total brain volume. Previously published studies have shown the relative severity of brain dysmorphology to vary widely in children with Apert syndrome (Renier et al., 1996). Neuroanatomical abnormalities reported include megalencephaly and ventriculomegaly among others (Cohen & Kreiborg, 1993, 1996). These abnormalities are often attributed to cranial vault or cranial base abnormalities. In a 2007 mouse model Aldridge et al. reported that FGFR2 mutations lead to a primary effect on the brain itself, as well as to the cranial vault. They found no evidence that suture fusion patterns were related to overall brain morphology, nor did they find any significant differences in brain morphology between those mice with Ser252Trp mutation and those with Pro253Arg mutation (Aldridge et al., 2010).

The Crouzon-Pfeiffer cohort ICV showed increased spread throughout the study timeframe (Figure 4.3). This was reflected in the R^2 being the lowest of all groups. ICV against OFC in this group remained strongly correlated. There were fewer patients with Saethre-Chotzen syndrome available for this study, leaving a cohort of 15 males and 13 females, but the trends were still clear, again with strong correlation for ICV against OFC.

In each syndrome cohort there were a number of outliers. We believe that this can be explained in part by the phenotypic variation seen in craniofacial syndromes, especially in Crouzon-Pfeiffer (Carinci et al., 2005). A further factor to consider in the Crouzon-Pfeiffer group is the Cohen classification of the Pfeiffer children who were either Type I or Type II / III, with 10/15 being type I. The older Pfeiffer children were all Type I (the oldest Type II / III child was 7 months old). This is likely to have contributed to the spread of results in the Crouzon-Pfeiffer group. Visible outlying data points in the Apert cohort can be seen lying superiorly to the line of best fit.

As discussed in chapter 2, raised ICP has been extensively reported in children with syndromic craniosynostosis with Tamburrini et al. (2005) documenting a 30-40% prevalence, and difficulty remains in determining the normal childhood ICP. This has led to a wide range of incidences reported in the literature (Fok et al., 1992). Thompson. Harkness et al. (1997) showed a 65% incidence of raised ICP in Crouzon Syndrome, 60% in Pfeiffer, 43% in Saethre-Chotzen and 38% in Apert Syndrome, whereas Marucci et al. (2008) found the incidence of raised ICP in Apert syndrome to be 83%. Both studies measured ICP transcranially and used mean pressures of greater than 15mmHg over 24 hours to indicate raised ICP.

In a further study, Renier and colleagues studied ICV and ICP in craniosynostosis and noted that volume measurement does not give a reliable indication of ICP, however

stating that in the presence of raised ICP, there will be restricted skull growth (Gault et al., 1992). Interestingly children with Apert syndrome are still at risk of raised ICP despite their significantly larger ICV. There appears to be little difference in ICV between the Crouzon-Pfeiffer, Saethre-Chotzen and control groups, indeed no group had a significantly lower ICV than the control which differs from the established ideas of craniosynostosis preventing skull and potentially brain growth. This would add further weight to the argument that raised ICP is not entirely caused by craniocerebral disproportion (Abu-Sittah, Jeelani, Dunaway, & Hayward, 2016; Anderson et al., 2004; Fok et al., 1992).

The strong correlation between ICV and OFC provides a useful proxy in the clinical setting or if the time-consuming measurement of ICV was not available. The OFC is easily obtained in clinic and reproducible, Sgouros, Hockley et al. (1999) described it as a crude technique, reflecting skull base growth rather than volume. This study found it to be closely related to ICV across the control group and all syndromic groups. Especially interesting was the strength of the correlation in Apert syndrome, where despite the turricephaly an R^2 of 0.9 was observed.

It should be noted that our control group is taken from a cohort of Great Ormond Street Hospital for Children patients, with normal head scans. Whilst this study benefits from both the syndromic patients and the control group being measured via the same technique, this may have introduced a bias in the control group. However, comparison of the control data with a study on the ICV in healthy children up to 72 months of age by Kamdar et al. (2009) has shown similar behaviour, with the 95% confidence interval overlapping with Kamdar's growth curve, thus implying our control group matches a normal control group.

Normative growth curves are at their most accurate when very large populations have been included in the data collection. As with all single centre studies on rare syndromes, our work is limited by low subject numbers. This is especially evident when further breaking down our data by syndrome, sex and age group; the rapid increase in ICV in the neonatal period is poorly accounted for here due to the limited number of data points in very young patients. We must acknowledge a limitation to the study here as there is potential for our data to be skewed by these low numbers.

4.5 Summary

In conclusion this chapter has provided reference ICV and OFC growth curves for unoperated children with syndromic craniosynostosis, as well as a control group. This allows craniofacial clinicians and researchers to adjust for syndrome specific underlying growth.

Previously when normalising a change in volume due to growth, growth curves for healthy children have been relied upon. The work in this chapter has shown that for patients with Crouzon-Pfeiffer and patients with Saethre-Chotzen syndrome this technique would suffice; however, it may overestimate the growth in a child with Apert syndrome . This work also provides further evidence to show that OFC can be used as a rapid clinical tool to estimate ICV in children who have not undergone cranial vault remodelling procedures. This would allow clinicians to assess whether a patient's growth curve is deflecting from the norm, and therefore indicating a potential source of raised ICP. This cohort has shown that children with Apert syndrome have larger ICVs than control children after the age of 6.7 months, whilst Crouzon-Pfeiffer and Saethre-Chotzen

ICVs remain similar to controls and that no group had significantly different OFC. The growth curves generated in this chapter are the first syndrome specific ICV and OFC growth curves to be published in the literature.

In chapter 5, these growth curves will be used to normalise volume changes in the entire GOSH spring assisted PVE cohort. This information is presented alongside and correlated to operative and clinical data to provide a detailed overview of the GOSH SAPVE experience.

Chapter 5 **SPRING ASSISTED POSTERIOR VAULT EXPANSION**

Part of the work described in this chapter was presented at The 20th Biennial Meeting of the European Society of Craniofacial Surgery, Athens, Greece, October 4-6th 2018 and the 47th Annual Meeting of the International Society for Paediatric Neurosurgery, Birmingham, UK, 20-24th October 2019.

Following the introduction of semi-automatic and fully automatic methods of ICV measurement in chapter 3, as well as growth curves to allow for normalisation of growth in chapter 4, this study utilises both in a retrospective analysis of all spring assisted posterior vault expansion (SAPVE) cases at GOSH since the introduction of this technique in 2008. Presented here is both the clinical experience of and a quantitative analysis of the ICV change due to SAPVE.

5.1 Introduction

Children with syndromic or multisuture craniosynostosis often present with turribrachycephaly or severe brachycephaly predisposing them to an underdeveloped, small posterior cranial fossa (Thomas et al., 2014). As discussed in Chapter 2, these patients are at risk of developing raised ICP, as well as hydrocephalus or a Chiari type 1 malformation (Cinalli et al., 2005).

Since 2008, the spring assisted technique has been the technique of choice for GOSH patients requiring PVE. This is due to the perceived advantages outlined in Chapter 2, namely, the guiding of expansion by springs rather than by rigid reorganisation of bony pieces, and a reduction in surgical time, blood loss, cost and in-patient stay. The springs are chosen over the distractors as they require no continuous break of the skin barrier and therefore reduce the risk of infection (Jeelani, 2019).

5.2 Methodology

5.2.1 Operative technique

The anaesthetised patient is placed in the prone position, with the neck in a neutral or slightly flexed position. Care is taken to ensure that the abdomen is freely suspended by placing gel pads below the pelvis and the chest, this avoids problems with venous return. A single 'Alice band' bicoronal incision is made down to the subgaleal plane. The skin flap is reflected posteriorly to a varying degree depending on severity of the case.

In children under the age of two, the flap is reflected back approximately 7cm, finishing anterior to the confluence of the lambdoid sutures. Separately, a pericranial flap is developed leaving the temporalis muscle in situ. A soft tissue tunnel is developed in the retromastoid area down to, but short of the foramen magnum. A curved or 'bucket handle' bicoronal osteotomy line is marked 5cm posterior to the skin incision and taken through the soft tissue tunnel towards the foramen magnum (Figure 5.1 A and B). When first performing this procedure, a linear coronal osteotomy was made, post-operatively however a prominent step between the anterior and the posterior bony segments was noted. The surgical technique was altered to include a curvi-linear osteotomy and off-set positioning of the spring footplate. This allowed for a more posterior-superior spring trajectory and has (anecdotally) reduced the post-operative bony step. A number of burr holes are made along the osteotomy line and into the retromastoid area, with the retromastoid burr holes being expanded into a small craniotomy allowing access to the transverse sinus and freeing of the dura towards the foramen magnum under direct vision. The osteotomies are completed, and the dura stripped from the inner table a few

centimetres anteriorly and posteriorly. The 'give' of the posterior bone flap is tested with the surgeon's thumbs and if felt sufficient the springs can be placed. Should the flap remain tight, the osteotomies can be extended further towards the foramen magnum, or the dural dissection can be widened until sufficient 'give' is felt. A small island of bone may be left in place over the confluence of the lambdoid sutures should the dura be stuck here, in doing so protecting the superior sagittal sinus.

In children over 2 years of age whose bones are less malleable, the posterior bone flap must be released entirely before being reattached to the calvarium using metal wires. The osteotomies can be completed above or below the torcula. Once sufficient give is achieved, two GOSH springs (further detailed below) are placed into prepared grooves ensuring the footplate of the spring is locked into position. Springs are placed facing each other, around 2 centimetres from either side of the midline (Figure 5.1 C and D). Spring strength is chosen by the operating surgeon; if two springs are felt to be insufficient, further springs can be placed along the osteotomy lines.

The pericranium is closed over the springs, providing stability to the construct and indicating how well the soft tissues will drape over the springs. Any spring protrusion or bony prominence can be overcome at this stage. The scalp is closed with absorbable sutures and the compressive help of an assistant, who ensures one hand is on the occiput and one on the forehead to avoid compression of the face and eyes. Once the skin is closed the springs will begin their expansion over the ensuing ten days.

Springs are aimed to be removed between six and twelve months after insertion, the team employ a reasonable degree of flexibility as to the interval between insertion and removal, this is due to logistics and geographical spread of GOSH patients. Spring removal is done on a day case basis, under general anaesthesia. The patient is positioned

as per the insertion and the original scar is reopened. The springs are uncovered using monopolar cautery. Generally, most of the bone gaps have ossified; however, care must be taken to avoid dural breach in any unossified areas. Once the springs are exposed, they are removed with a combination of Mitchel's trimmers, a Tessier periosteal elevator and a pair of heavy forceps. Care is taken when removing the footplate not to catch any dura in the tip. The wound is closed, and no drain or dressing is used (Figure 5.1 E).

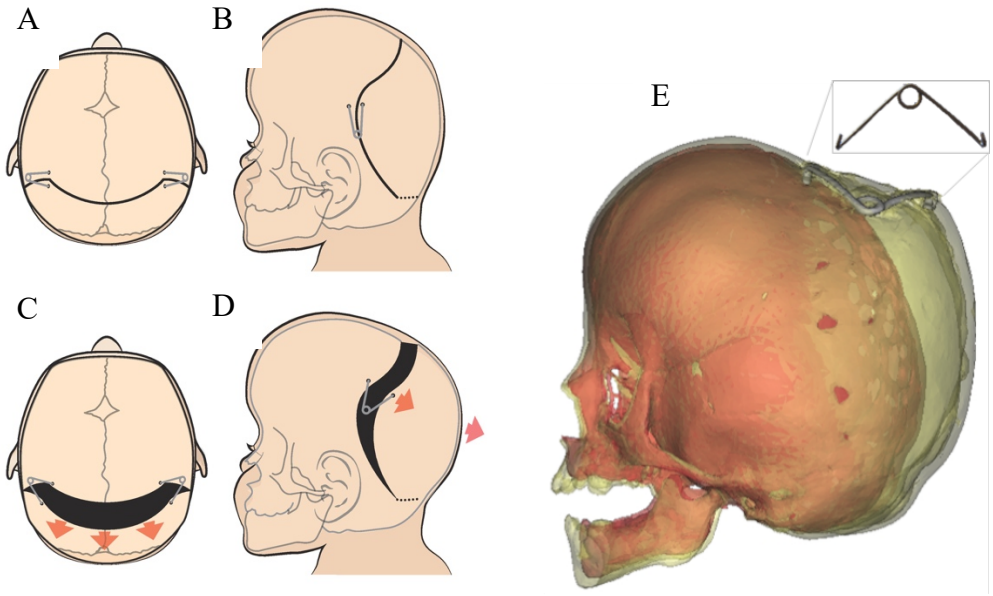

Figure 5.1 SAPVE operative technique. Operative technique demonstrating the curved bucket handle osteotomy in axial and sagittal views (**A** and **B**), and the osteotomies and spring placement with resulting vectors (**C** and **D**). **E** illustrates a 3D reconstruction showing the post-operative expansion (yellow) achieved by the now fully open spring overlaid to the pre-operative CT reconstruction (red).

5.2.2 Spring design

The GOSH springs, as touched upon in Chapter 2, are stainless steel wires fashioned to include a central helix and angled tips. The helix has a diameter of 10

millimetres and the tips have an opening distance at rest of 6 centimetres. The angled tips or footplates allow the springs to be securely lodged into small bony cuts and the springs display a gentle convexity to better fit the curvature of the calvarium. The wire diameter comes in three varieties of 1.0, 1.2 and 1.4 millimetres; with increasing thickness comes increasing loading and unloading stiffnesses. The springs are crimped closed at insertion where they display the highest load and as they gradually open over time the load reduces (Figure 5.2). Unpublished work by Dr Borghi and the craniofacial group at GOSH has shown the springs to reach a fully open position by day 80 post operation.

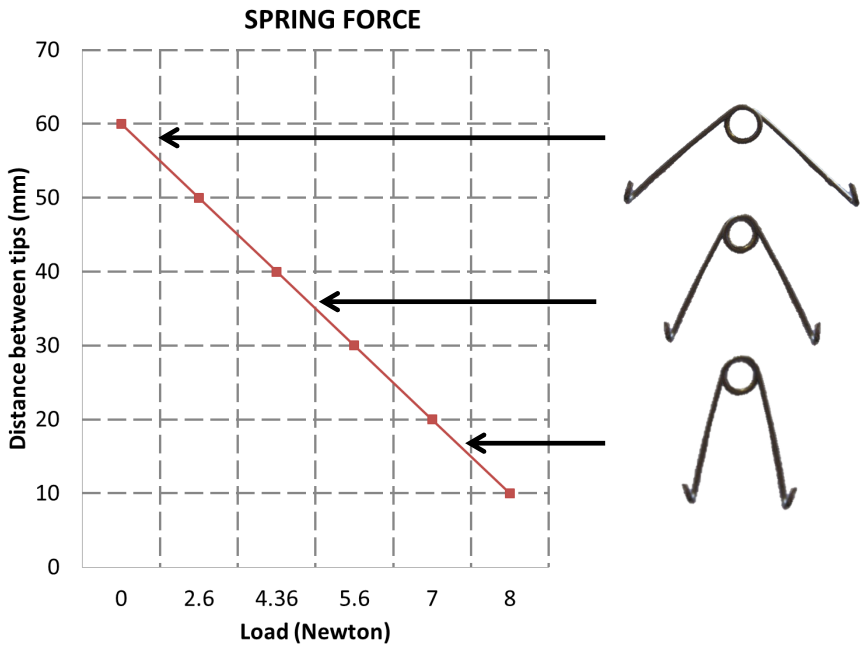

Figure 5.2 Crimping forces of a 1.0 millimetre GOSH spring. (Source: Rodgers et al., 2017)

5.2.3 Data analysis and statistics

SAPVE began to be performed at GOSH in 2008; as such, this study considered for inclusion all patients who had undergone SAPVE since 2008 and until August 2019.

Data were collected from hospital note review and included gender, genetic diagnosis, indication for PVE, age at spring insertion and at removal, previous surgeries and repeat PVE, operative time for insertion and removal, transfusion requirements and length of in patient stay for insertion and removal. Information was collected regarding ophthalmological outcomes, complications, and follow up surgical procedures.

Quantitative outcome was measured using ICV, which was calculated for those patients with available pre-operative and post-operative CT data. ICV measurement was done using the semi or fully automatic methods detailed in Chapter 3. Time between the pre-operative CT-scan and spring insertion varied between patients. In order to properly compare the ICV between patients, the pre-operative ICV were adjusted to the expected values for a patient of that age and syndrome on the day of surgery (ICV_{op}) using the growth curves of Chapter 4. As example, the equation for ICV calculation in Apert's patients is shown in Figure 4.2 and can be broken down as follows:

$$ICV = a * \log(x) - b ;$$

a = coefficient for the specific syndrome

x = age in days

b = base value for the specific syndrome

For recalculation, “b” was adjusted to the patient specific value, using the ICV and age at time of the pre-operative CT-scan:

$$b_{adjusted} = ICV_{CT} - a * \log(x)$$

Time between surgery and follow up CT-scan also varied highly between patients. Therefore, the change in ICV between time of post-operative CT scan and time of surgery was also adjusted for growth ($ICV_{post\text{-}op\text{-}adj}$). An assumption is made that the rate of skull growth following surgery remains on the same trajectory as an unoperated skull. This was done using the same diagnosis-specific curves as above, to assess the step ICV expansion due to the spring alone.

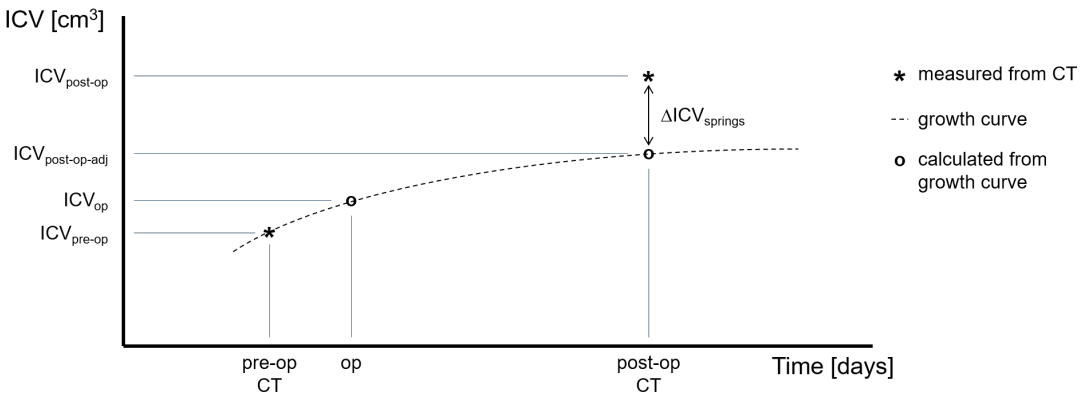

Figure 5.3 A stylised graph showing ICV adjustments to give ICV change due to springs alone

For the overall population, length of procedure was compared between insertion and removal using Student t-tests. The learning curve associated with spring insertion

was assessed by comparing the first and final ten spring length of insertion surgeries in the series.

Kaplan Meier survival analysis with Log Rank testing was used to assess freedom from reintervention (repeat PVE) for patients grouped by diagnosis and by age. Log rank tests were performed to determine any differences in survival distribution between the age groups or diagnoses.

For those patients with pre and post-operative ICV measurements, correlations between primary diagnosis, age at surgery, and ICV increases were investigated using paired Student t-tests to compare the ICV differences within groups and one-way ANOVA with post hoc testing (Hochberg GT2) or independent student t-tests to test between groups (different diagnosis, age groups, surgery type, and those patients scanned before and after the 100 day post operation time point). Where data was not normally distributed, non-parametric tests were used. These were all performed using IBM SPSS Version 25. The overall ICV study group was further delineated into groups determined by type and number of surgical procedures; patients who had SAPVE as a first and only procedure (Group 1), patients who had SAPVE as a first procedure and had FOA at spring removal (Group 2), and patients who had SAPVE as a first procedure and later required a repeat SAPVE (Group 3). ICV change following a repeat SAPVE was also assessed (Group 4). Where ICV was assessed, those patients had had no previous transcranial procedures.

5.3 Results

5.3.1 Demographics and indications

In total 172 patients (103 males, 60%) underwent SAPVE at GOSH between 2008 and 2019. At the time of writing, mean follow-up is 69.9 months (range 6.9 months to 11.8 years). The study population consisted of patients affected by non-syndromic (36%) or syndromic (64%) disorders. The latter included 44% with Crouzon-Pfeiffer, 27% with Apert syndrome, 10% with Muenke syndrome, 5% with TCF-12 related craniosynostosis, 4% with Saethre-Chotzen syndrome and 3% with ERF related craniosynostosis. In addition to this there was 1 Noonan syndrome patient, 1 Smith Lemil Opitz syndrome patient, 1 William syndrome patient, 1 Bartter syndrome patient, 1 Shprintzen-Goldberg patient and 1 patient with CHARGE syndrome. Genetic confirmation was available for 90 patients. Patients with diagnoses other than Crouzon-Pfeiffer and Apert were place in an 'other' cohort for further analysis. 36% of patients had non-syndromic multisuture synostosis (Table 5.1). Mean age at spring insertion for first PVE was 21.7 months (range 2.1 – 130.6), and at removal 33.5 months (range 2.9 – 144.4) with springs remaining in situ for a mean of 11 months (range 0.1 – 40.7) (Table 5.2). At the time of writing 20 patients have springs in situ. Examples of pre-operative and post-operative appearances of patients with Apert, Crouzon-Pfeiffer, Muenke and TCF-12 related craniosynostosis are shown in Figures 5.3 to 5.6.

Table 5.1 Overview of Study population on diagnosis, sex, age, and craniofacial surgical history.

Diagnosis	Total (n)	Sex (n)		Median age at SAPVE (months)	Age range (months)	Unoperated at time of SAPVE (n)*	Single SAPVE (n)**
		F	M				
Syndromic	110						
Crouzon	37	14	23	20.7	5.2-78.1	30	30
Apert	30	12	18	13.2	3.0-54.3	29	21
Pfeiffer	11	8	3	15.3	2.1-83.3	8	7
Muenke	11	6	5	14.4	5.8-58.7	10	11
TCF12	6	3	3	15.1	9.3-22.1	6	6
Saethre-Chotzen	5	2	3	17.5	8.8-25.5	5	5
ERF	3	1	2	53.1	29.1-59.0	3	3
Noonan	1	1	0	2.1	n/a	1	1
Smith Lemli Opitz	1	0	1	85.3	n/a	-	-
Williams	1	1	0	23.1	n/a	-	1
Bartter	1	0	1	47.6	n/a	1	1
Shprintzen-Goldberg	1	0	1	4.9	n/a	1	1
Craniofrontonasal Dysplasia	1	0	1	12.7	n/a	1	1
CHARGE syndrome	1	0	1	67.2	n/a	1	1
Non-syndromic	62						
Multi-Suture synostosis	51	12	39	15.7	4.0-130.6	45	45
Sagittal synostosis	1	0	1	23.9	n/a	-	1
Chiari 1 malformation	1	0	1	30.7	n/a	1	1
Cranial Dysraphism	2	1	1	12.8	7.7-17.9	2	2
Bicoronal synostosis	6	5	1	15.6	8.2-62.5	6	6
Lambdoid synostosis	1	0	1	13.6	n/a	1	1
Total	172	69	103	20.6	2.1-130.6	151	148

*no history of any type of craniofacial surgery; **these patients were sufficiently treated with one SAPVE insertion and removal of springs, no additional SAPVE was indicated; n = number of patients

A B C

Figure 5.4 Clinical photography of a female with Apert Syndrome before and after SAPVE. The photographs **A-C** were taken four months pre-operatively at an age of three months. Photographs **D-F** were taken seven months post-operatively at age 14 months. The post-operative images show a reduction in turricephaly, frontal bossing and increased anterior-posterior length compared to the pre-operative photographs (A-C vs. D-F).

A B C

Figure 5.5 Clinical photography of a male with Crouzon Syndrome before and after SAPVE. The photographs **A-C** were taken eight months pre-operatively at an age of 12 months. Photographs **D-F** were taken 12 months post-operatively at age 36 months. The post-operative images show increased anterior-posterior length compared to the pre-operative photographs (A-C vs. D-F).

D E F

Figure 5.6 Clinical photography of a female with Muenke Syndrome before and after SAPVE. The photographs **A-C** were taken five months pre-operatively at an age of four months. Photographs **D-F** were taken four months post-operatively at age 12 months. The post-operative images show increased anterior-posterior length compared to the pre-operative photographs (A-C vs. D-F).

A B C

D E F

Figure 5.7 Clinical photography of a male with TCF 12 Syndrome before and after SAPVE. The photographs **A-C** were taken four months pre-operative at an age of 18 months. Photographs **D-F** were taken four months post-operative at age 26 months. The

D E F

post-operative images show a reduction in turricephaly and increased anterior-posterior length compared to the pre-operative photographs (A-C vs. D-F).

Raised ICP was the stimulus for operation in 129 patients (75%). This was confirmed by deteriorating ophthalmological findings in 79 of these patients (61% of the patients with raised ICP), worsening clinical picture indicative of raised ICP in 6 patients (5%), radiographic finding in 3 patients (2%), intraparenchymal pressure monitoring in 31 patients (25%), or a combination of the above in 10 patients (8%). Of the patients who did not undergo SAPVE for raised ICP, nine (5% of the total) were performed to prevent raised ICP in the near future, this was based on literature and clinical experience for those patients felt to be more prone to develop RICP, and 34 (20%) were performed to improve head shape. Six (3%) of the 172 procedures were carried out on an emergency basis.

25 patients (30%) had previously undergone other transcranial procedures. These included: 5 anterior posterior shortening with biparietal expansions, 5 PCVR procedures, 3 FOA procedures, 2 FMD procedures, 2 spring assisted cranioplasties for scaphocephaly, 2 monobloc and RED frame procedures, and 1 sagittal suturectomy. Six patients had undergone multiple transcranial procedures pre SAPVE; one patient had a PCVR and an FMD, one had two FMD procedures, one had PCVR followed by monobloc and RED frame, followed by anterior posterior shortening with biparietal expansions and another PCVR, one had total calvarial remodelling and a PCVR, one had two PCVR procedures and one had anterior posterior shortening with biparietal expansions followed by FOA. One patient had FOA at the time of their SAPVE.

149 patients had a single SAPVE (87%) and 19 (11%) went on to have a repeat PVE; of these, 15 were SAPVE and 4 were traditional posterior cranial vault remodelling procedures (PCVR). Repeat surgery either SAPVE or PCVR was undertaken on average 19.8 months following the first SAPVE (range 9.5 to 43.3). Considering the repeat SAPVE only, 2 procedures were performed to improve head shape and the remaining 13 were necessitated by raised ICP. Overall, SAPVE was indicated for raised ICP in 75% of the cases, 5% for prevention of RICP and 19% for shape improvement (Table 5.3).

Table 5.2 Overview of first and redo SAPVE.

SAPVE	Mean age, months (range)	Mean time springs in situ, months (range)	Total (n)
First SAPVE	21.7 (2.1 – 130.6)	11 (3 days – 41 months)	172
Redo SAPVE	28.8 (16.9 - 49.9)	11.4 (1.8 – 33.6 months)	15
Total	20.6 (2.1 – 130.6)	10 (3 days – 51 months)	188

Table 5.3 Overview of indication for SAPVE.

SAPVE		PVE				Total
		First SAPVE		Second SAPVE		
		n	**% within subgroup**	**n**	**% within subgroup**	
ICP Concerns	**RICP**	***129****		***13***		***140****
	Clinical findings$^{\beta}$	6	4.7%	2	15..4%	14
	Ophthalmology$^{\chi}$	79	61.2%	10	76.9%	118
	BOLT-monitoring	31	24%	1	7.7%	32
	Radiology$^{\alpha}$	3	2.3%	0	0%	33
	Combination*	10	7.8			
			% of total		**% of total**	**% of total**
			75%		*86.7%*	74.9%
		n	**% within subgroup**	**n**	**% within subgroup**	
	Prevention of RICP	9	100	n/a	n/a	9
			% of total		**% of total**	**% of total**
			5.2%		*n/a*	4.8%
	Total ICP Concerns	*136*				
		n	**% within subgroup**	**n**	**% within subgroup**	
Shape	**Correction**	34	100	2	100	36
			% of total		**% of total**	**% of total**
			19.8%		*13.3*	19.3%
Total number of SAPVE		**172**			**15**	**187**

$^{\beta}$Concerns were solely based on clinical findings, such as headaches; $^{\chi}$; $^{\alpha}$ radiology findings, such as copper beaten skull; * combination of above factors

5.3.2 Surgery

The mean operative time (recorded as knife to skin to final dressings) for insertion of springs with no additional procedures was 2 hours 20 minutes (range 1 hour to 5 hours 35 minutes) and removal (with no additional procedures) was significantly shorter at 1 hour 27 minutes (range 32 minutes to 4 hours 10 minutes p = <0.001). Mean total

operating time was 3 hours 47 minutes. 43 patients (25%) had additional procedures at the time of removal (FOA n=32, additional PCVR n=6, monobloc and RED frame n=2, FOA, Le Fort III and RED frame n=1, vertex remodelling n=1 and foramen magnum decompression n=1). When removal of springs was combined with FOA, mean operative time was significantly longer at 3 hours 11 minutes (range 2 hour 2 minutes to 4 hours 45 minutes, $p = <0.001$) than the time for removal surgery without additional procedures. Spring removal combined with FOA was undertaken in patients with a wide range of diagnoses (Table 5.4) and occurred in significantly younger patients than spring removal alone (15 months vs. 25.1 months respectively, $p = 0.005$).

Of 128 patients who underwent simple SAPVE and removal without further procedures, 87 received a mean of 204.4ml of allogenic blood, with the remainder receiving no blood intraoperatively. For spring removal 16 patients received a mean of 63.3ml. In the 43 cases where spring removal was combined with an additional procedure; at insertion, 28 of these patients required a mean transfusion of 171.2ml and at removal 32 required a mean transfusion of 425.4ml.

Table 5.4 Overview SAPVE with fronto-orbital advancement at time of removal of springs.

	SAPVE + FOA at time removal springs		
Diagnosis	**n**	**% within diagnosis**	**Total SAPVE**
Multi-sutural synostosis	10	22.7%	44
Muenke	6	54.5%	11
TCF12	5	83.3%	6
Saethre-Chotzen	3	60.0%	5
Bicoronal synostosis	3	50.0%	6
Apert	1	3.3%	30
Crouzon-Pfeiffer	1	2.1%	48
Bartter	1	100.0%	1
Shprintzen-Goldberg	1	100.0%	1
Craniofrontonasal dysplasia	1	100.0%	1
Total	32	20.1%	153

In the cases where removal of springs was combined with another procedure, springs remained in situ for a mean of 12.1 months (range 0.9 - 40.6); there was no significant difference between this length of time and when springs were removed with no additional procedures (10.2 months, range 0.1 to 33, $p = 0.137$). There is a wide range in the length of time that springs remain in situ, this is owing to a number of reasons; GOSH patients are geographically very spread out, and many of those with syndromic diagnoses will have to undergo multiple elective procedures under multiple surgical specialties. In order to reduce travel burden and exposure to general anaesthetic, the team attempt to combine spring removal with another elective admission. Operative time for insertion of springs reduced with experience. The first ten consecutive spring insertions took an average of 3 hours whereas the final ten in the series took an average of 2 hours ($p = 0.03$).

5.3.3 Hospital stay

Mean inpatient hospital stay for SAPVE insertion alone was 5 nights (range 0 to 34). Mean stay for removal alone was 2 nights (range zero to 22). When removal of springs was combined with another procedure, mean stay was 3 nights (range 1 to 22). These differences were not statistically significant.

5.3.4 Clinical outcomes and complications

Considering the 129 patients who underwent first SAPVE for raised ICP, ophthalmological data was available for 93 patients. An overall post-operative improvement was seen in either visual acuity or papilloedema in 90 patients (97%). Of the three patients that showed no improvement one had stable visual acuity that showed no worsening and two had worsening acuity and no improvement in papilloedema.

Complications were assessed for all patients using the Oxford craniofacial complication scale, the scale used to compile complication data for the UK Craniofacial National Audit (Paganini et al., 2019). This scale consists of six Grades; with Grade 0 being no complications, Grade 1 being no delay in discharge, reoperation or long-term sequelae, Grade 2 being delay in discharge, but no further operation required, Grade 3 being reoperation, but no long-term sequelae, Grade 4 being unexpected long-term deficit or neurological impairment (permanent disability), and Grade 5 being mortality (Table 5.5).

Table 5.5 Complications at spring insertion and removal.

Grade	Complication description	Number of Complications			
		1st insertion	1st removal	2nd insertion	2nd removal
0	No complications	148	169	17	19
1	No delay in discharge, reoperation or long-term sequelae	1			
2	Delay in discharge but no further operation required	3	2	1	
3	Reoperation but no long-term sequelae	21		1	
4	Unexpected long-term deficit or neurological impairment (permanent disability)				
5	Mortality	1			

At first SAPVE, 26 complications were seen in 23 patients. Grade one complications were as follows: one patient with secondary alopecia due to scalp flap compromise which later resolved. This patient was initially treated elsewhere and presented with an unusually located scar from a prior bicoronal incision, at GOSH a standard bicoronal incision was performed, which caused scalp flap compromise. Grade two complications were as follows: one patient required intravenous antibiotics following a post-operative chest infection and one patient sustained a sinus tear intraoperatively which required a post-operative transfusion, the same patient required a course of oral antibiotics for a post-operative wound infection. Grade three complications occurred in 19 patients with 21 events. These included; one subgaleal collection requiring washout, two retained drains that required removal under general anaesthetic, nine eroding or outwardly dislodged springs that required early removal and nine post-operative surgical site infections requiring removal of springs and washout (Table 5.6). There were no grade 4 complications. There was one grade 5 complication: this patient had cranial dysraphism,

pansynostosis and a history of an encephalocele repair aged seven weeks. There was significant intraoperative and post-operative blood loss leading to post-operative supratentorial ischaemia. A bifrontal decompression was performed, however ICP continued to rise, was unable to be controlled and along with the family's wishes ongoing care was withdrawn.

There were two grade two complications at removal of springs; one patient had a minor post-operative bleed which was observed and managed conservatively, and one patient required intravenous antibiotics for a wound infection.

Two complications were seen at repeat SAPVE: one grade two complication, where a patient with known central and obstructive sleep apnoea had a respiratory arrest on the ward but made a full recovery and one grade 3 complication where a patient returned to theatre for washout for a post-operative haematoma. There were no complications at removal following repeat SAPVE.

Table 5.6 Overview early removal of springs.

Reason for early removal of springs	No of cases
Skin infection	10
Exposure of springs	8
Outwards dislodged springs	1

5.3.5 Follow up

Mean length of follow up at time of submission is 69.9 months (range 6.9 months to 11.8 years). One patient has been lost to follow up. 19 patients required repeat SAPVE or PCVR, this was undertaken at an average of 19.8 months and is further discussed

below. 16 patients (11% of those whose first transcranial procedure was SAPVE) have not had this length of follow up.

Excluding those patients that had extra procedures at spring removal, 14 patients went on to have at least one further craniomaxillofacial procedure. Eight out of 38 patients with Crouzon-Pfeiffer syndrome proceeded to monobloc plus RED frame, an average of 11 months post SAPVE. One Crouzon-Pfeiffer patient underwent two monobloc plus RED frames procedures three years apart. Two patients with Apert syndrome later required monobloc plus RED frame, one at 9.8 months and one at five years following SAPVE. One additional Apert patient underwent monobloc and RED Frame at time of spring removal.

Three patients had anterior 2/3 remodelling an average of 10 months (range 6.4 – 16.3). One of these patients had monobloc advancement with RED frame 4 years after their anterior 2/3 remodelling. Two patients underwent Le Fort III osteotomies with RED frame distraction, of which one was 16 months, and one was 7.7 years after first SAPVE. The latter patient required two further FOA. Following repeat SAPVE two patients had FMD, this was undertaken at 10.3 and 18.3 months post-operatively (Table 5.7).

Table 5.7 Overview additional craniomaxillofacial procedures following SAPVE.

	Number of Follow up Procedures by Diagnosis		
	Apert	**Crouzon-Pfeiffer**	**Multisuture**
Monobloc + RED Frame	2	9	
Le Fort III + RED Frame		1	1
Anterior 2/3 remodelling		1	2
FMD		3	
FOA		2	
Total procedures	2	16	3

Following SAPVE as a first vault expanding procedure, 19 patients had a repeat PVE (15 SAPVE, four PCVR). One of the patients undergoing PCVR had their initial SAPVE to alter head shape, all other initial SAPVE were carried out to ameliorate raised ICP. Patients that required repeat SAPVE had their initial SAPVE at a significantly younger age than those who did not; 24.6 months compared to 10.6 months ($p = < 0.001$). Patients diagnoses included; nine Apert syndrome, eight Crouzon-Pfeiffer, and two non-syndromic multisuture synostosis. One repeat procedure (PCVR) was performed due to a post-operative infection following the first SAPVE demanding early spring removal. Two procedures were performed to improve head shape, the remaining 16 were necessitated by raised ICP, including the patient whose initial procedure was to alter head shape.

Indication for surgery was determined by ophthalmological findings alone in 10 patients, a combination of ophthalmological and intraparenchymal pressure monitoring findings in two patients, deteriorating clinical picture in two patients, and a combination of ophthalmological findings, radiological findings and worsening clinical picture in 2 patients.

Mean age at spring insertion was 28.8 months (range 16.9 to 49.9); springs remained in situ for a mean of 11.4 months (range 1.8 to 33.6). Repeat surgery, either SAPVE or PCVR, was undertaken on average 19.8 months following the first SAPVE (range 9.5 to 43.3). The mean operative time for insertion of springs was three hours and three minutes (range two hours and five minutes to four hours and 24 minutes) and removal was one hour 29 minutes (range 58 minutes to two hours 55 minutes). One patient had an FOA at the time of spring removal, operative time for this procedure was three hours and 40 minutes.

Regarding repeat SAPVE mean inpatient hospital stay for SAPVE insertion alone was six nights (range three to 19), . Mean stay for removal alone was 3 nights (range 1 to four). The removal of springs plus FOA case required a four-night stay.

Pre and post-operative ophthalmology data were available for 15 of the 16 repeat PVE patients who underwent their repeat due to raised ICP. Within the group of 15 patients, 12 had SAPVE and three had rigid PCVR. An overall improvement was seen in 12 of the 15 patients. All three rigid PCVR patients showed an improvement in both their visual acuity and papilloedema. Nine of the 12 SAPVE patients showed an improvement in either visual acuity or papilloedema with 2 showing an improvement in both. Of the three who showed no improvement; one maintained a stable baseline and two had missing pre-operative baseline visual acuity studies.

In the Kaplan Meier survival analysis, patients aged 0-1-year-old showed a significantly increase incidence for a repeat SAPVE (Log rank test, $p = 0.01$, Figure 5.7). Repeat SAPVE was performed at similar time points for the included diagnoses. There was a significant difference in the requirement for repeat SAPVE between diagnostic groups (Log rank tests, $p = <0.001$, Figure 5.8). Patients with Apert syndrome, followed by patients with Crouzon-Pfeiffer syndrome required a repeat SAPVE more frequently as compared to the rest of the diagnostic groups. Patients with Apert syndrome or Crouzon-Pfeiffer syndrome required repeat PVE at similar ages and at a time point closer to their initial SAPVE than multi sutural synostosis and ‘other’ diagnosis patients

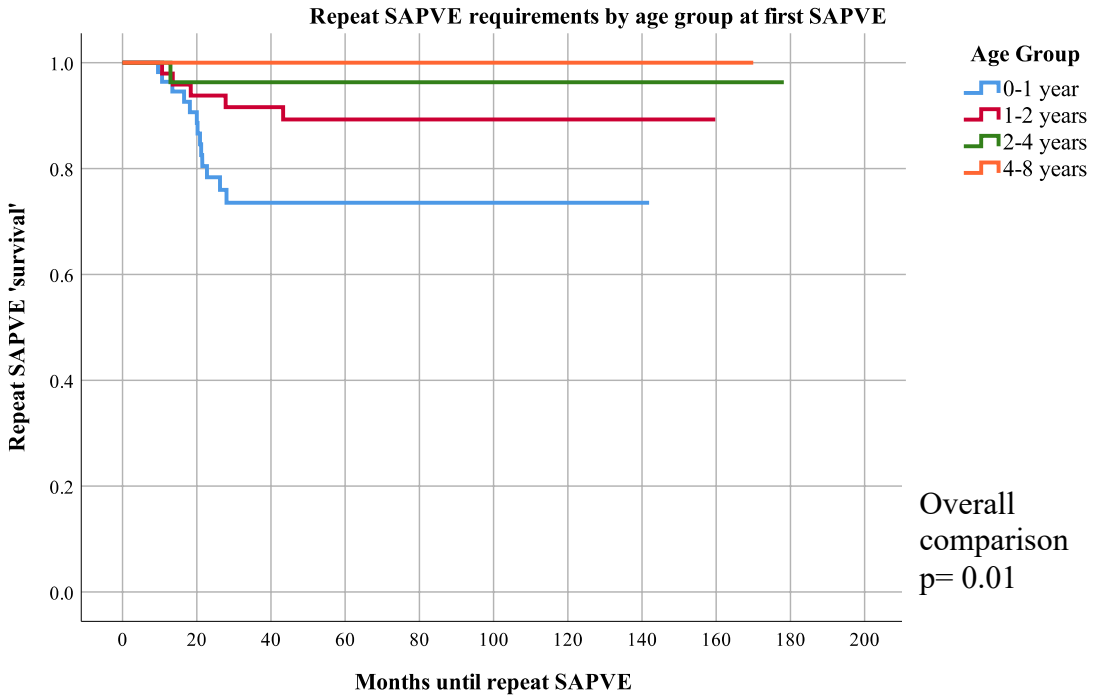

Figure 5.8 Kaplan – Meier survival analysis, showing time until repeat PVE by age group at first SAPVE. Patients in the zero – one age group were more likely to require a repeat PVE.

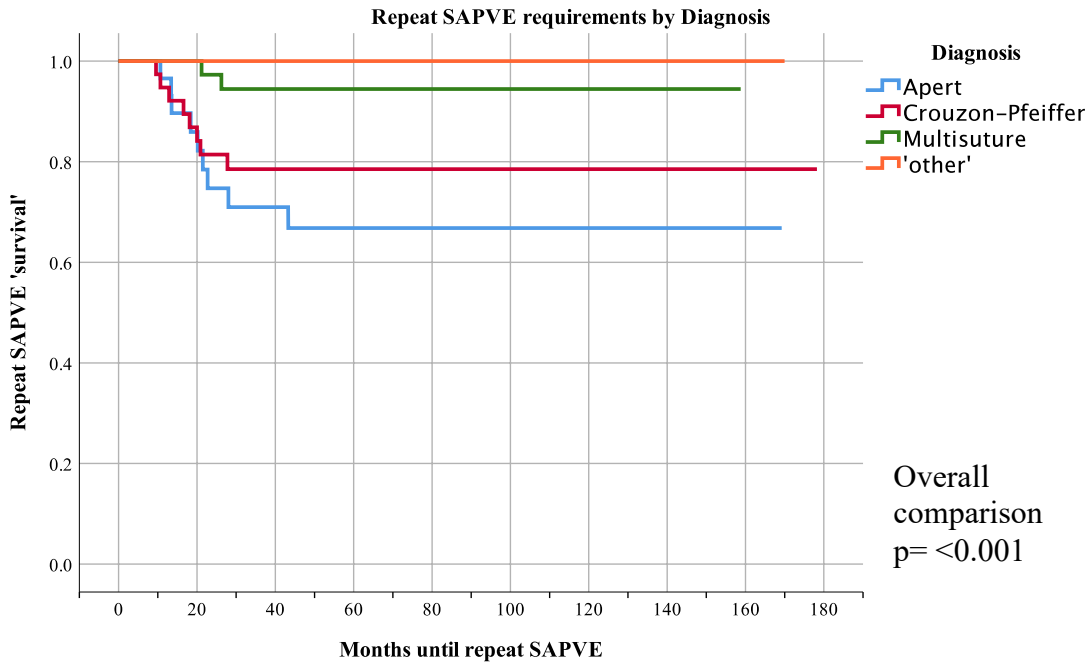

Figure 5.9 Kaplan – Meier survival analysis, showing time until repeat PVE by diagnosis. Repeat PVE was required at similar time points regardless of diagnosis, likelihood of repeat PVE requirement decreased through Apert > Crouzon-Pfeiffer > multisuture > other diagnoses.

5.3.6 ICV measurements

Pre and post-operative ICV measurements were available for 74 patients (45 male, 61%). Diagnoses included: Apert (n=16), Crouzon (n=18), Pfeiffer (n=4), multisuture (n=24) and 'other' (n=12, including 4 Muenke, 3 TCF-12, 2 Saethre-Chotzen, 1 cranial dysraphism, 1 ERF and 1 Noonan). Average age at SAPVE was 20.1 months (range 2.1 – 67.2). Pre-operative CT scan was performed at a mean age of 17.4 months (range 1.4 – 65.2), post-operative CT scan was performed at a mean age of 30.7 months (range 4 – 86.9). The mean time between pre-operative CT scan and SAPVE was 2.7 months (range 0 days to 19.7 months). Mean time between SAPVE and post-operative scan was 10.6 months (range 6 days – 72.3 months). The mean time between pre and post-operative CT scans was 16.5 months (range 7 days – 73.5 months) (Table 5.8).

Mean measured pre-operative ICV was 1065.9cm^3 (539.5 – 1632.4cm^3); mean measured post-operative ICV was 1418.6cm^3 (965 – 1864cm^3). Mean $ICV_{at\text{-}op}$ was 1127.6cm^3 (603 – 1633cm^3); mean $ICV_{post\text{-}op\text{-}adj}$ was 1219.1cm^3 (703 – 1688cm^3). There was a significant increase in ICV due to springs; mean adjusted ICV change was 201.1 cm^3 (8 – 537cm^3) ($p = <0.001$). Mean adjusted percentage ICV change was 19.1% (1 - 64).

Table 5.8 Overview of ICV study population at first SAPVE.

Diagnosis	Total (n)	Sex		Mean age at SAPVE (months)	Mean time between pre-op CT scan and SAPVE (months)	Mean time between SAPVE and post op CT-scan (months)	Mean time between pre and post-op CT-scan (months)
		F	M				
Crouzon- Pfeiffer (combined)	22	10	12	20.1 (2.1 – 45.1)	0.7	11.1	12
Multi-suture synostosis	24	8	16	25.7 (3.6 – 49.4)	2.8	15.3	18.1
Apert	16	4	12	12.4 (3.6 – 49.4)	3.5	11.4	14.8
Other*	12	7	5	19 (2.1 – 53.1)	4.9	19.5	24.2
Total	74	29	45	20.1	2.7	13.4	16.5
*= 4 Muenke, 3 TCF-12, 2 Saethre-Chotzen, 1 cranial dysraphism, 1 ERF, and 1 Noonan;							

5.3.6.1 Diagnostic subgrouping

Patients were subdivided by diagnosis. A significant increase in ICV was seen across all syndromes (Table 5.9). No significant differences were found between the Crouzon and the Pfeiffer groups; they were therefore combined as in Chapter 4 (Rutland et al., 1995). The 'other' group contained too disparate a collection of diagnoses and was therefore excluded from further ICV analysis. Comparison between groups showed no significant difference in pre-operative ICV, post-operative ICV, $ICV_{at\text{-}op}$, $ICV_{post\text{-}op\text{-}adj}$, adjusted ICV change or adjusted percentage ICV change (Figure 5.9).

Table 5.9 ICV change by diagnosis. pre-op = preoperative; post-op = postoperative; ICV*at-op* = volume adjusted to the expected values for a patient of that age and syndrome on the day of surgery; ICV*post-op-adj* = volume adjusted to the expected values for a patient of that age and syndrome on the day of surgery and adjusted for growth in between time of post-operative CT scan and time of surgery. Mean adjusted change is Post-op ICV minus $ICV_{post\text{-}op\text{-}adj}$

Diagnosis	Pre-op ICV cm^3 (range)	Post-op ICV cm^3 (range)	$ICV_{at\text{-}op}$ cm^3 (range)	$ICV_{post\text{-}op\text{-}adj}$ cm^3 (range)	Mean adjusted ICV change		
					cm^3 (range)	% (range)	p-Value
Apert (n=16)	1011.9 (702-1632)	1499.4 (1129–1863)	1132.4 (746–1633)	1271.6 (904–1688)	227.8 (87-452)	21.3 (8-48)	**<0.001**
Crouzon-Pfeiffer (n=22)	1118.3 (562-1620)	1363.7 (965-1864)	1130 (603-1620)	1203 (703-1653)	163.1 (57-296)	16 (5-44)	**<0.001**
Multi-suture (n=24)	1089 (662-1469)	1431.2 (1204-1763)	1140 (833-1470)	1231 (992-1485)	200.2 (8-537)	18.6 (1-64)	**<0.001**
Other (n=12)	993.7 (539.5-1331)	1386.9 (1093-1717)	1090.4 (793-1416)	1153.8 (9322-1445)	233.1 (96-499)	22.6 (10-49)	**<0.001**

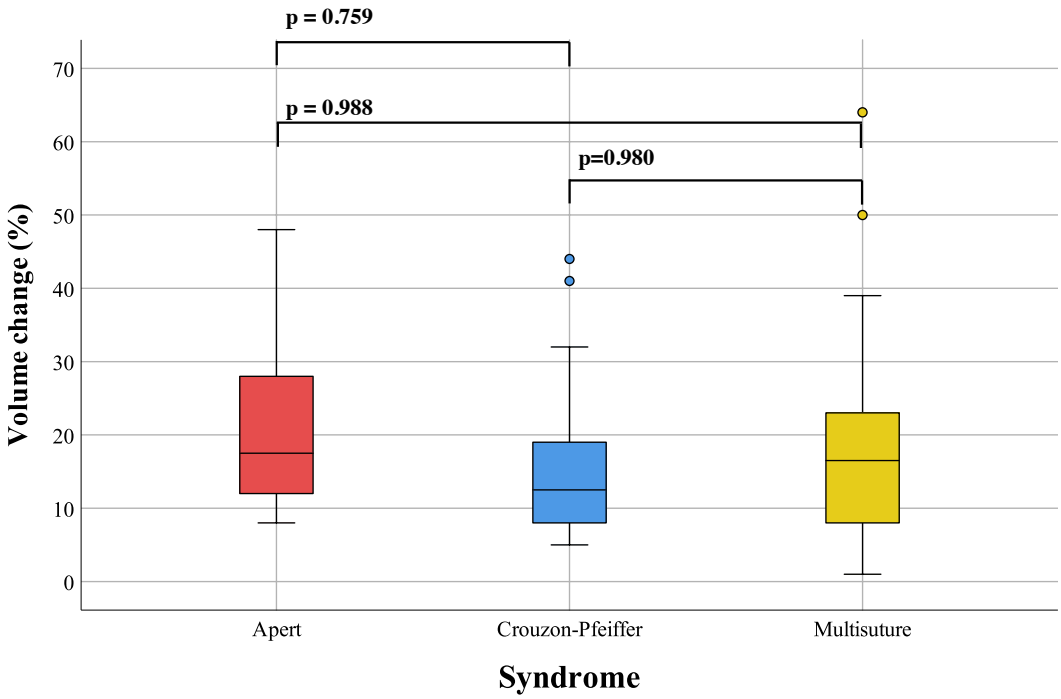

Figure 5.10 Boxplot comparison of percentage ICV change by diagnosis. Solid line within boxes shows median, boxes represent the interquartile range, whiskers indicate 1.5 times away from inter-quartile range. Statistical significance between groups indicated above boxplot. Dots shows outliers.

5.3.6.2 Age subgrouping

Patients were then divided into age groups at first SAPVE. The same age grouping was used as in Chapter 4. All age groups showed a significant step increase in ICV following SAPVE (Table 5.10). The zero-to-one-year old group had a significantly smaller pre-operative ICV, and $ICV_{at\text{-}op}$ than all other groups (p = <0.001). They showed a significantly smaller $ICV_{post\text{-}op\text{-}adj}$ than the one-to-two and four-to-eight years old groups (p = 0.022 and 0.004 respectively). They showed a significantly larger adjusted ICV increase than the two-to-four-year old group (p = 0.037) and they showed a significantly

larger adjusted percentage ICV increase than all other groups (Figure 5.10). No significant difference was seen in post-operative volumes, and there was no significant difference across any domain in the other age groups.

Table 5.10 ICV change by age group at first SAPVE.

Age (years)	Patients (n)	Additional vault remodelling at removal of springs (n)	Pre-op ICV cm^3 (range)	Post-op ICV cm^3 (range)	$ICV_{at\text{-}op}$ cm^3 (range)	$ICV_{post\text{-}op\text{-}adj}$ cm^3 (range)	ICV change		
							cm^3 (range)	% (range)	p-Value
0-1	27	6	877.3 (539-1339)	1354.5 (967-1763)	966.7 (603-1378)	1110.2 (703-1411)	244.3 (19-537)	26.3 (2-64)	**<0.001**
1-2	29	12	1114.5 (711-1620)	1441.6 (965-1864)	1171.5 (857-1620)	1252.6 (908-1654)	189 (8-499)	17.1 (1-49)	**<0.001**
2-4	10	1	1232.4 (1103-1512)	1403.1 (1210-1818)	1236.8 (1108-1521)	1272.8 (1130-1688)	130.3 (51-213)	10.6 (4-19)	**<0.001**
4-8	8	0	1338.6 (1119-1632)	1535.1 (1367-1863)	1344 (1125-1633)	1364.4 (1130-1688)	170.7 (50-237)	13 (4-21)	**<0.001**

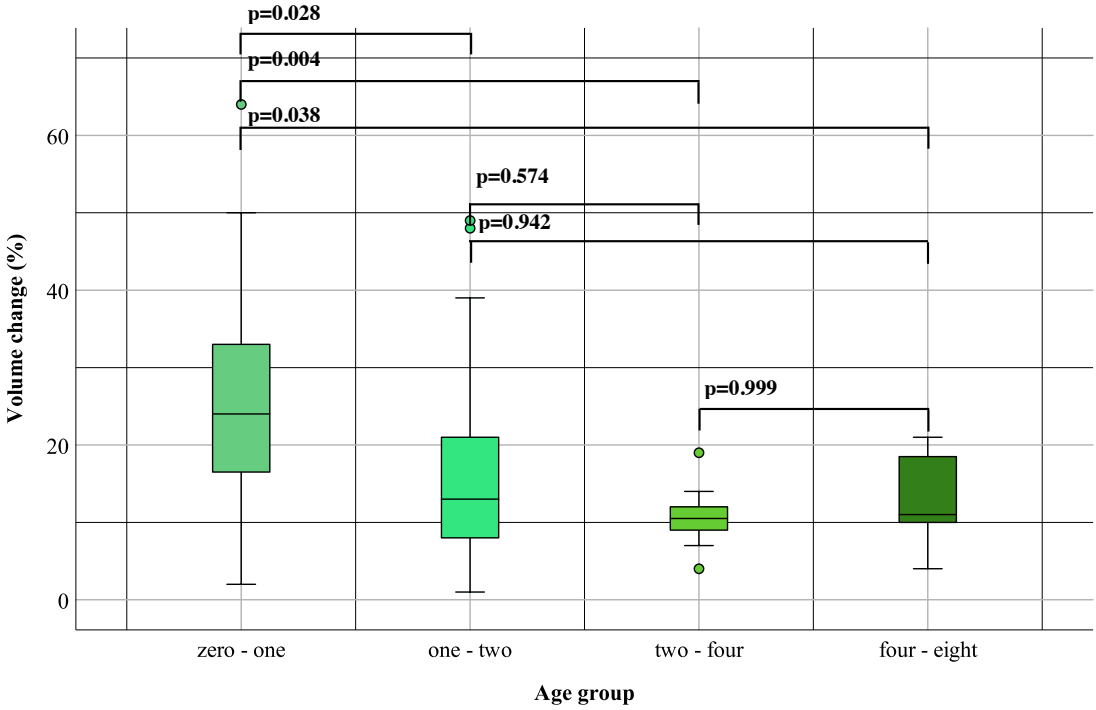

Figure 5.11 Boxplot comparison of percentage volume change by age group.

5.3.6.3 Diagnosis plus age subgrouping

The same age groups were then used to further analyse ICV change in each diagnostic group (Table 5.11). The Apert group was split into a zero-to-one-year group (n=10) and a one-to-two-year group (n=5), the remaining patient with Apert syndrome was not included. Both year groups showed a significant step increase in ICV following SAPVE (p = <0.001 and 0.004 respectively). No significant difference in percentage ICV increase following SAPVE was found between the two groups (Figure 5.11).

The Crouzon-Pfeiffer group was split into a zero-to-one-year group (n=6), a one-to-two-year group (n=10) and a two-to-four-year group (n=6). All year groups showed significant step increase in ICV following SAPVE (p = 0.002, 0.007 and 0.002

respectively). A significantly larger percentage ICV increase was seen between the zero-to-one-year group and both the one-to-two-year group and the two-to-four-year groups (p = 0.003 and 0.03 respectively). No significant difference was seen between the one-to-two-year group and the two-to-four-year groups (Figure 5.12).

The multisuture group was split into a zero-to-one-year group (n=9), a one-to-two-year group (n=7) a two-to-four-year group (n=3) and a four-to-eight-year group (n=5). The two-to-four-year group did not show a significant step increase in ICV, although it did trend towards significance (p = 0.058). All other year groups did show a significant step increase in ICV following SAPVE. No significant difference was seen in percentage ICV change follow in SAPVE between age groups (Figure 5.13).

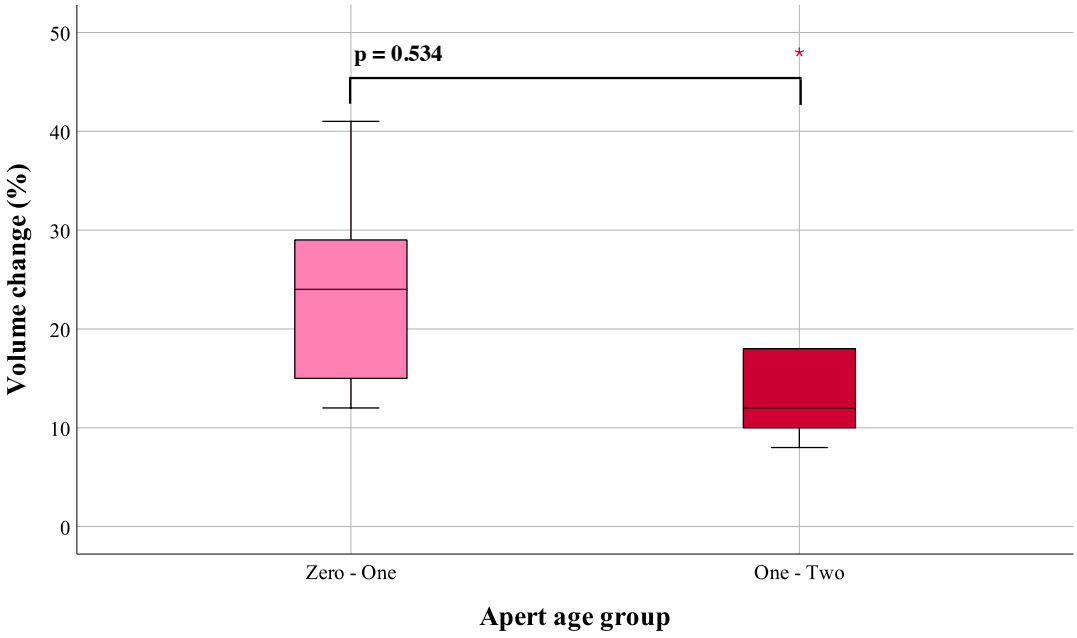

Figure 5.12 Boxplot comparison of percentage ICV change by age group in Apert cohort.

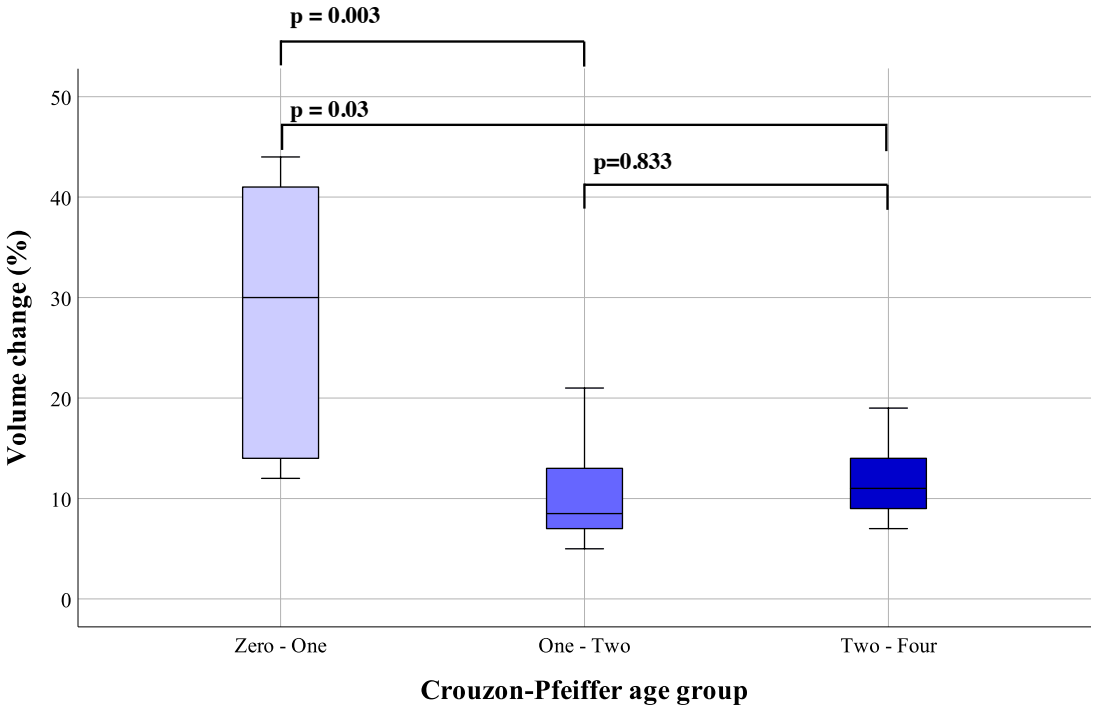

Figure 5.13 Boxplot comparison of percentage ICV change by age group in Crouzon-Pfeiffer cohort.

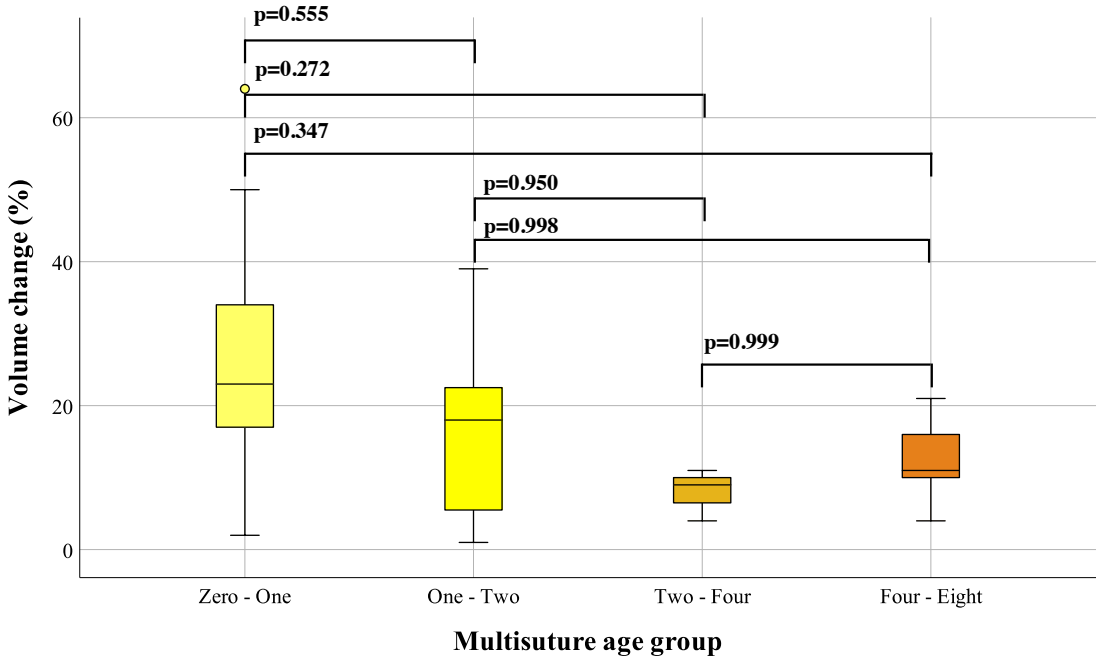

Figure 5.14 Boxplot comparison of percentage ICV change by age group in the multisuture cohort.

Fifteen patients had their post-operative scan less that 100 days post operation. The springs may not have been full opened and therefore the calvarium fully expanded. Comparison between this group of patients and those scanned more than 100 days post operation showed no significant differences in any ICV metric tested.

5.3.6.4 Operative subgrouping

An overview of this subgrouping is shown in Table 5.11, with further information per group show in Tables 5.12 to 5.15.

Table 5.11 Overview of subgroups within the study population.

	Patients (n)	Description
Group 1	37	Single SAPVE
Group 2	19	Single SAPVE and FOA at time of springs removal
Group 3	9	Two SAPVE, ICV change relates only to first SAPVE
Group 4	9	Two SAPVE, ICV change relates only to repeat SAPVE
Total	74	

Table 5.12 Overview of Group 1 (single SAPVE) study population.

Diagnosis	Total (n)	Sex		Mean age at SAPVE (months)	Mean time between pre-op CT scan and SAPVE (months)	Mean time between SAPVE and post op CT-scan (months)	Mean time between pre and post-op CT-scan (months)	Indication for SAPVE	
		F	M					ICP	Shape
Crouzon-Pfeiffer	15	8	7	28.7 (4.3-67.2)	0.9 (0-2.7)	11.2 (0.1-61.8)	12.1 (0.2-61.8)	14	1
Multi-suture synostosis	10	4	6	28.9 (5-67.1)	2.4 (0.2-7.7)	18.5 (2.2-71.2)	20.9 (3.2-72)	8	2
Apert	7	2	5	9.2 (5.9-13.5)	3.8 (0.1-8.5)	5.9 (1-13.1)	9.7 (2-21.7)	5	2
'Other'*	5	4	1	40.1 (2.1–67.2)	1 (0.2-2.4)	3 (0.1-7)	4 (1-7.9)	5	0
Total	37	18	19	25.1	1.8	11.7	13.5	32	5

*= 1 bicoronal synostosis, 1 CHARGE syndrome, 1 cranial dysraphism, 1 ERF, and 1 Noonan

Table 5.13 Overview of Group 2 (SAPVE plus FOA at spring removal) study population.

Diagnosis	Total (n)	Sex		Mean age at SAPVE (months)	Mean time between pre-op CT scan and SAPVE (months)	Mean time between SAPVE and post op CT-scan (months)	Mean time between pre and post-op CT-scan (months)	Indication for SAPVE	
		F	M					ICP	Shape
Crouzon-Pfeiffer	1	0	1	11.4	0	5.2	5.2	1	0
Multi-suture synostosis	8	2	6	11.7 (4.2–23.1)	3.5 (0.1-10.8)	9.8 (4.7-20.3)	13.3 (4.8-22.5)	7	1
Apert	1	0	1	23.9	19.7	3.7	23.4	1	0
'Other"*	9	4	5	17.2 (11.4-25.5)	6.3 (0.1-12.6)	9.1 (3.7-26.8)	15.4 (5.6-28.2)	4	5
Total	19	6	13	15	5.5	8.9	14.4	13	6

*= 4 Muenke, 3 TCF-12, 2 Saethre-Chotzen

Table 5.14 Overview of Group 3 (required repeat SAPVE, 1st SAPVE) study population.

Diagnosis	Total (n)	Sex		Mean age at SAPVE (months)	Mean time between pre-op CT scan and SAPVE (months)	Mean time between SAPVE and post op CT-scan (months)	Mean time between pre and post-op CT-scan (months)	Indication for SAPVE	
		F	M					ICP	Shape
Crouzon-Pfeiffer	4	2	2	10.5 (6.6-15.4)	0.8 (0.3-1.3)	12.4 (2.4-27.6)	13.1 (3.1-28.4)	4	0
Multi-suture synostosis	1	1	0	6.7	1.8	12.2	14	1	0
Apert	4	1	3	8.5 (5-16.1)	1.6 (0.2-4.9)	13.5 (1.8-26)	15.1 (3-26.3)	4	0
Total	9	4	5	9.4	1.3	12.8	14.1	9	0

Table 5.15 Overview of Group 4 (repeat SAPVE, 2nd SAPVE) study population.

Diagnosis	Total (n)	Sex		Mean age at repeat SAPVE (months)	Mean time between pre-op CT scan and SAPVE (months)	Mean time between SAPVE and post op CT-scan (months)	Mean time between pre and post-op CT-scan (months)	Indication for repeat SAPVE	
		F	M					ICP	Shape
Crouzon-Pfeiffer	4	2	2	27.2 (12.1–43)	1.8 (0-6.6)	4 (0.5-7.6)	5.8 (2.3-7.8)	4	0
Multi-suture synostosis	1	1	0	20.7	9	2.3	11.3	1	0
Apert	4	1	3	26.5 (15.8–32.7)	1.3 (0.2-2)	23.2 (2.3-50.6)	24.5 (4.1-52.6)	4	0
Total	9	4	5	28.5	2.3	12.4	14.7	9	0

A significant step increase in ICV following SAPVE was seen in groups 1, 2, 3 and 4 (Table 5.16). There was a significant difference in age at first SAPVE between group 1 (those patients only requiring a single SAPVE) and groups 2 and 3 (those patients undergoing FOA at the time of spring removal and those patients requiring repeat SAPVE respectively), with group 1 undergoing SAPVE at a significantly older age ($p = 0.005$ and 0.028 respectively). There was no significant difference between the age that group 2 and group 3 underwent SAPVE ($p = 0.916$).

Table 5.16 ICV change by pre-determined group.

Group	Pre-op ICV cm^3 (range)	Post-op ICV, cm^3 (range)	ICV_{at-op} cm^3 (range)	$ICV_{post-op-adj}$ cm^3 (range)	ICV change		
					cm^3 (range)	% (range)	p-Value
Group 1 (n=37)	1126 (562-1620)	1428.9 (965-1864)	1170.5 (715-1620)	1251.8 (876-1653)	177.1 (19-452)	15.9 (2-48)	<0.001
Group 2 (n=9)	980.4 (539-1331)	1432 (1136-1717)	1097 (833-1416)	1178.8 (932-1445)	253.2 (8-529)	24.8 (1-64)	<0.001
Group 3 (n=9)	928.6 (737-1083)	1280.6 (1142-1420)	956.7 (748-1169)	1111.2 (945-1338)	169.4 (87-290)	18.4 (8-32)	<0.001
Group 4 (n=9)	1339.9 (1141.9-1420.4)	1522.5 (1320-1766)	1359.4 (1211-1456)	1427.7 (1215-1606)	94.8 (12-323)	7.3 (1-26)	0.014
Total (n=74)	1090.6 (539-1620)	1423 (965-1865)	1148.8 (715-1620)	1237.4 (876-1653)	185.6 (8-529)	17.5 (1-64)	

Groups 1, 2 and 3 were further compared (Figures 5.14 and 5.15):

- When comparing groups 1 and 2; Group 1 had a significantly smaller step increase in ICV following SAPVE ($p = 0.02$), and a significantly smaller percentage ICV gain due to SAPVE ($p = 0.015$).
- When comparing groups 1 and 3; group 1 had significantly larger adjusted ICV_{at-op} ($p = 0.006$). There were no significant differences in IVC change or percentage ICV change due to the springs ($p = 0.858$ and 0.522 respectively). Group 1 underwent first SAPVE at a significantly older age, 25.1 months compared to Group 3 at 9.4 months ($p = 0.028$).
- When comparing groups 2 and 3; group 2 had a significantly larger adjusted ICV_{at-op} ($p = 0.028$). There were no significant differences in IVC change or percentage ICV change due to the springs ($p = 0.085$ and 0.256 respectively).

- Group 3 and Group 4 were the patients that underwent 2 SAPVEs; group 3 related to their first SAPVE and group 4 their second. When comparing these, group 4 showed a significantly smaller percentage ICV following SAPVE (p = 0.009) (Figure 5.15).

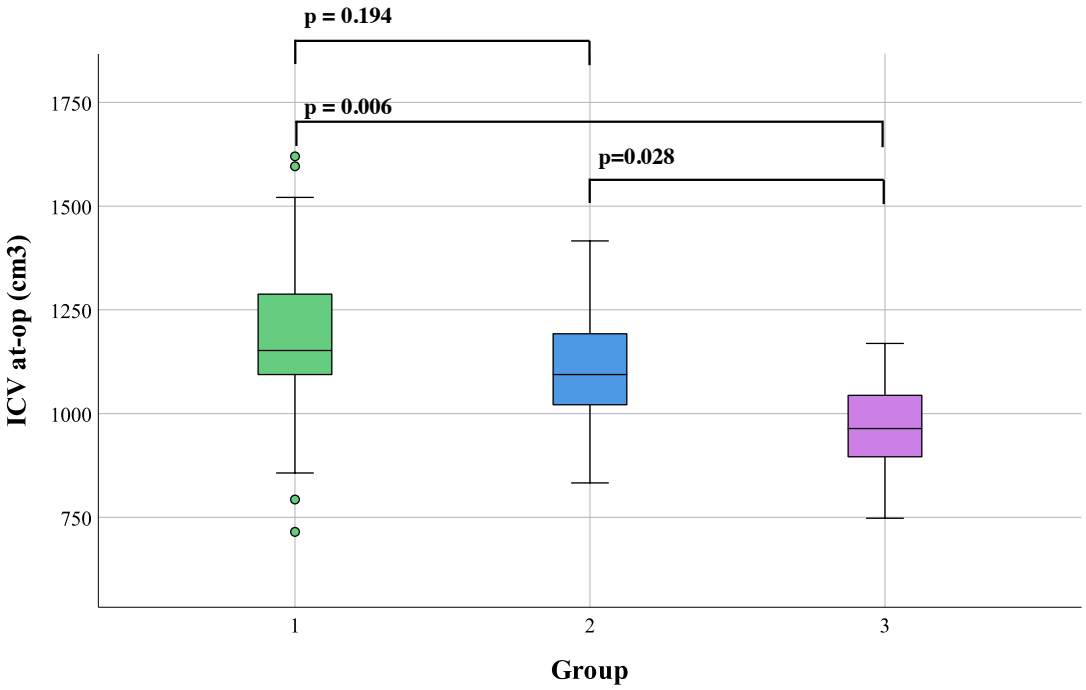

Figure 5.15 Boxplot comparison of $ICV_{at\text{-}op}$ by group.

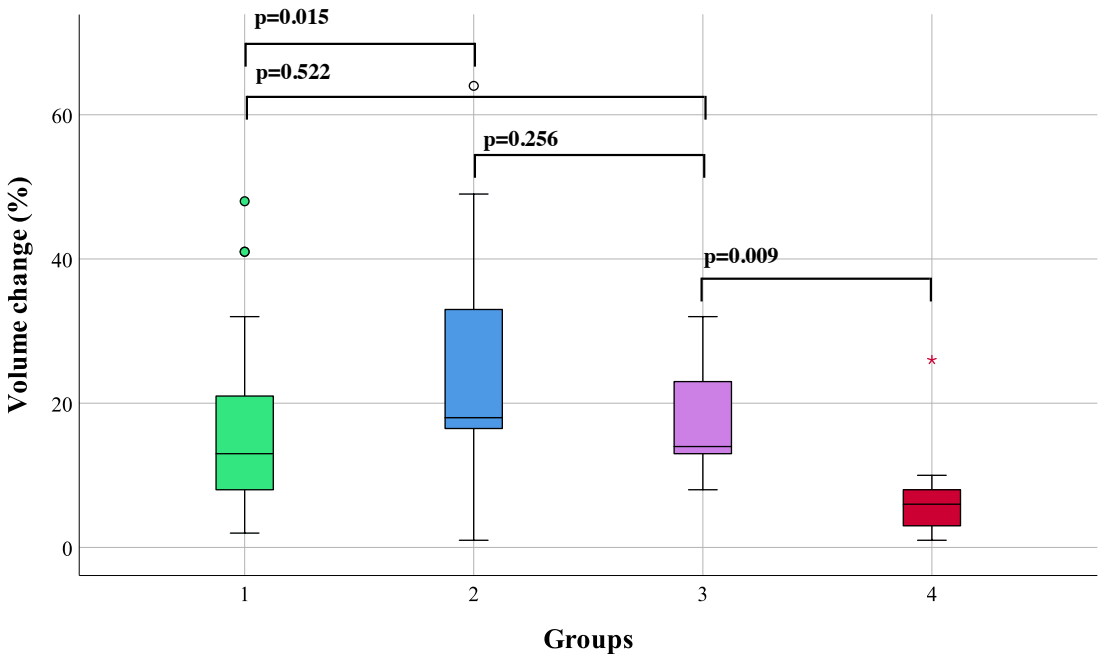

Figure 5.16 Boxplot comparison of percentage ICV change by group.

5.4 Discussion

5.4.1 Clinical metrics

The purpose of this study was to perform a comprehensive review of the SAPVE procedures undertaken at GOSH since their introduction in 2008. The posterior route for calvarial expansion has been favoured over the anterior route since 1996. It has continued to evolve ever since with innovative spring-assisted or distractor based techniques. The amount of advancement feasible using traditional PCVR is limited due to scalp closure and there is potential for relapse if the patient adopts a supine position postoperatively, especially as the newly created space by the expansion has not yet been filled with brain. Methods which provide gradual expansion, such as SAPVE or distraction have shown to

omit these issues by allowing for gradual expansion, with secondary ossification. The springs were chosen over the distractors at GOSH as they require no continuous break of the skin barrier and were therefore presumed to reduce the risk of infection (Jeelani, 2019).

This review included both baseline and procedural factors, such as transfusion requirements and procedural duration, as well as an analysis of ICV changes across a number of different patient cohorts / groupings. To date, most SAPVE studies in the literature have been technical notes, case reports or small series including fewer than 20 patients (Arnaud, Marchac, Jeblaoui, Renier, & Di Rocco, 2012; Costa et al., 2015; De Jong et al., 2013). This consecutive series of 172 patients, with a mean follow up of 6.75 years, is the most comprehensive series managed by a single unit.

Despite the comprehensive study numbers, there are many variables within the cohort, making conclusions difficult to draw in some subgroups. A cohort where all patients had the same diagnosis, were operated on at the same age and had matched pre and post-operative imaging would be ideal; however, syndromic and multisuture synostosis are both rare and heterogenous. As such, analysis was carried out on the whole cohort and in an attempt to standardise results, smaller subsets were created where patients were matched by diagnosis and age at first surgery. 26 patients underwent transcranial procedures before or at the time of their first SAPVE. These 26 patients included patients referred from other institutions having already been operated upon, or patients requiring anterior or posterior vault expanding procedures before the introduction of springs at GOSH. These patients were excluded from the volumetric studies to remove the effect of their previous surgery on the analysis.

Raised ICP was the predominant driver for SAPVE in our cohort. The majority of these procedures were performed on an elective basis, with six being required as an emergency. As per GOSH protocol, the majority of raised ICP was diagnosed on ophthalmological findings. These included delay in visual evoked potentials, worsening visual acuity and the finding of papilloedema (Liasis et al., 2006). Although this study showed a 97% improvement of papilledema as a result of the SAPVE, two patients' ophthalmological findings worsened, with one, a patient with Apert syndrome, going on to have a repeat SAPVE 13.5 months later. Interestingly this patient had a below average percentage volume increase at first SAPVE (10%). The second patient, a patient with Crouzon syndrome did not require a repeat PVE, but also showed a 10% volume increase following first SAPVE. Ophthalmological testing in the young child can be problematic and one must be cognisant of these limitations. Further work could include a cohort study on all patients undergoing SAPVE who had invasive ICP monitoring and compare them retrospectively with their ophthalmological findings. This may provide insight in the translation of measured ICP values to ophthalmological test results in patients with craniosynostosis, further enhancing our understanding of non-invasive ICP assessment.

First SAPVE was undertaken at an average age of 21.7 months (range 2.1 – 130.6). The extreme range is due to referral of one patient at 10 years of age. Excluding this patient gave an average age at first SAPVE as 16 months. The springs remained in situ for an average of 11 months. Where possible, this was combined with other planned general anaesthetic procedures. In the UK craniofacial surgical provision for patients with syndromic craniosynostosis is supra-regionally funded, this generates a wide geographical spread of patients coming to GOSH, in addition to this many GOSH craniofacial patients come from overseas (the Middle East in particular), logistically this

means that planning the removal of springs can be challenging. Ideally the springs are removed around six months post operatively, as by this time they have fully expanded, the bony gap has had time to ossify and the patient has had time to recover from their previous surgery. At the time of spring removal 43 patients had additional transcranial procedures. This included 32 FOAs. The patients who undergo FOA (Table 5.4) at the time of spring removal tend to present with a brachycephalic head shape, one which before posterior expansion became the primary procedure of choice would have first had an FOA and then gone on to have secondary vault expanding procedure if required. It is felt by the Craniofacial team at GOSH that this cohort of patients are likely to still require the FOA in early life and therefore this is combined with removal of springs. None of the SAPVE plus FOA group went onto require repeat PVE.

For simple SAPVE with no additional procedures at spring removal, median total operative time was three hours 27 minutes. Published data shows traditional PCVR taking between two hours 44 minutes and four hours 5 minutes, PVDO taking two hours 49 minutes and SAPVE taking three hours 35 minutes (De Jong et al., 2013; Steinbacher et al., 2011). These findings are comparable with the SAPVE findings at GOSH. Operative time for insertion of springs reduced with experience.

Median length of stay for SAPVE insertion was three nights (removal with no additional procedures was one night, increasing to four nights when combined with another procedure), these findings also compare equally with the published data from De Jong et al. (2013) for SAPVE and Steinbacher et al. (2011) for PVDO with total hospital stays of 4 and 3.25 days respectively. 70% of patients who underwent SAPVE as a first transcranial procedure required a mean transfusion of 204ml of allogenic blood. At removal, 13% required a mean of 63ml transfusion, when an additional procedure was

combined with spring removal 74% of patients required a mean of 425ml. Thomas et al. study of 31 PVDO procedures showed an 80% transfusion rate at an average of 270ml, a similar requirement to SAPVE with no additional procedures (Thomas et al., 2014).

In our series there were 26 unplanned post-operative events in 23 patients following their first SAPVE. This included 21 (12%) return to theatre episodes requiring a general anaesthetic (Table 5.5), again similar to the 16% described in PVDO by the Oxford Team (Thomas et al., 2014). Surgical site infection and dislodged springs were the most common complications occurring in 18 patients (nine and nine respectively). The 12% return to theatre rate for post-operative infection is of interest to note, given that one of the assumed benefits of SAPVE over PVDO is the protection of skin barrier. To fully assess this, a direct comparison of the two techniques, ideally within the same unit, using the same operative protocols is required.

Infections settled once springs had been removed, apart from two cases of osteomyelitis: one required debridement followed by long term antibiotics, the other long-term antibiotics alone. There was one mortality in a patient with a complex medical history and a diagnosis of cranial dysraphism. During elective SAPVE there was significant intraoperative blood loss. Post-operative seizures and apnoeic episodes necessitated intubation. ICP continued to rise post-operatively. The patient returned to theatre for removal of springs and remained stable for 24 hours before deteriorating. A further CT showed supratentorial ischaemia and reduced ventricular volume. Bifrontal decompression was performed; however, this failed to improve the patient's condition and supportive care was later withdrawn.

In addition to those patients who underwent FOA at the time of spring removal, 14 patients continued on to further transcranial procedures (Table 5.7), but there are a

small number of patients who have not had sufficient follow up to confidently rule out further procedures. Repeat PVE was undertaken at an average of 19.8 months post-operatively, and there are 16 patients in the cohort where follow up falls short of this time period.

To address midface retrusion in patients with Apert syndrome, a bipartition distraction procedure or Le Fort II/III plus zygomatic repositioning also with distraction is often carried out (Hopper, Kapadia, & Morton, 2013). At GOSH this is done at between eight to ten years of age (O'Hara et al., 2019). The mean length of follow up for patients with Apert syndrome in this study was 7 years, with the maximum being 11.75 years. Interestingly none of the patients studied had undergone either bipartition distraction or Le Fort II/III plus zygomatic repositioning at time of writing.

In patients with Crouzon-Pfeiffer syndrome, the secondary surgery of choice at GOSH is a monobloc with or without distraction. The aim again is for this to be carried out at around eight to ten years of age, however in this cohort the average age for a Crouzon-Pfeiffer patient to undergo a monobloc plus RED frame procedure was 5.6 years. Crouzon-Pfeiffer made up the majority of patients who went on to have further procedures within the study period, with eight going on to have monobloc plus RED frame procedures. Mean length of follow up for patients with Crouzon-Pfeiffer syndrome was 6.6 years. Given the length of follow up, further SAPVE and midface or fronto-facial procedures are likely to be required in the future. Therefore, reported numbers, especially for repeat SAPVE may fall short of the final number.

Following SAPVE 19 patients (13%) underwent a repeat PVE, 15 of these were SAPVE and 4 PCVR. Insertion of springs at repeat SAPVE took an hour longer than at first SAPVE, this additional time is accounted for by the scar tissue and more difficult

dural dissection encountered at repeat surgery. Removal of springs took the same amount of time. Inpatient stay was longer for both insertion and removal, again accounted for by the increased complexity of redo surgery.

Kaplan Meier survival analysis curves were employed to indicate which groups of patients were more likely to need a repeat PVE. A significantly higher number of repeat SAPVE procedures were required in those patients who underwent their SAPVE at a younger age. This might be due to the phenotypic severity of the patients that require expansion at a young age, i.e., more phenotypically severe patients require PVE at a younger age and might require relatively larger expansion. This expansion may not be possible given the preoperative ICV of the less developed cranium. Patients with Apert syndrome required more repeat SAPVE as compared to Crouzon-Pfeiffer, multisuture and 'other' diagnosis patients. Patients with Apert or Crouzon-Pfeiffer syndrome required repeat PVE at similar ages and at a time point closer to their initial SAPVE than multisuture and 'other' diagnosis patients.

5.4.2 ICV metrics

As shown in Chapter 4, if patients with Apert syndrome are excluded, the majority of patients with craniosynostosis display normal ICV when compared to a control population. In order to quantitatively analyse ICV changes due to SAPVE, pre and post-operative ICV were assessed and adjusted to give absolute and percentage values of ICV increase attributable to the SAPVE. As in most craniofacial institutions, at GOSH, exposure to ionising radiation is kept to a minimum. CT scans are taken preoperatively to aid surgical assessment and planning, but in the follow-up period CT scans are not normally taken unless complications arise, which could include raised ICP and the need

for further expansion. This unfortunately meant the exclusion of a number of patients who had not had follow up CT scans. This invariably adds a degree of bias to the data presented, as those patients who achieved a larger post-operative ICV may have avoided further surgical procedures (and therefore further CT scans). This could potentially reduce the number of follow up fronto-facial procedures as well as repeat PVE (Ter Maaten et al., 2018). Despite being unable to include over half the cohort, this assessment of ICV change in a single cohort remains the largest reported, as compared to current published literature, at time of submission.

The cohort of 74 patients achieved a significant step increase in ICV following SAPVE (Table 5.9) independent of initial diagnosis. There were no significant differences in absolute ICV change or percentage ICV change.

Additionally, SAPVE achieved a significant increase in ICV in each analysed age group. The youngest patients at first SAPVE, the zero-to-one-year cohort, gained a significantly larger percentage increase in ICV than all other age groups (Figure 5.10).

In order to further scrutinise where ICV change is most apparent, patients were subdivided by both diagnosis and age group at first SAPVE. Patients with Apert syndrome fell into either the zero-to-one-year or one-to-two-years age group; both groups showed a significant increase in ICV pre to post-operatively. No significant difference in percentage ICV change was found between the two groups (Figure 5.11). Patients with Crouzon-Pfeiffer syndrome fell into the zero-to-one-year, one-to-two-years or two-to-four-years age groups. The zero-to-one-year group showed a significantly larger percentage increase (Figure 5.12). Again, the zero-to-one-year group had significantly smaller pre-operative ICV. There were sufficient multisuture patients to study all four age

groups, with all showing a significant ICV increase following SAPVE. There was no significant difference in percentage ICV change (Figure 5.13).

When assessing percentage ICV change by diagnosis and age, the younger patients (zero-to-one-year group) had a larger (but not significant) percentage ICV increase than those in the older age groups. Given that these children begin with a smaller ICV this is not wholly unexpected, as technically is should be easier to gain more expansion from a more malleable skull. That this did not reach significance may be testament to the ability of SAPVE to significantly increase ICV across a range of ages. Interestingly, in the Crouzon-Pfeiffer cohort there was a significantly larger increase in the zero-to-one-year group than the older groups. With the small number of subjects per group it is difficult to draw conclusions, however when cross-checked against the Apert zero-to-one-year group there was no significant difference.

Patients were then grouped by type and number of procedures, this included; those patients who had SAPVE as a first, and as of yet only procedure and those patients having SAPVE as a first and only procedure with an FOA at spring removal. The final two groups consisted those patients who required a repeat SAPVE, with group 3 analysing their initial SAPVE and group 4 analysing their second SAPVE.

A significant volume increase was seen in each group (Table 5.16). Closer analysis of the SAPVE (Group 1) and SAPVE plus FOA at spring removal (Group 2) cohorts showed the latter to have a significantly larger step increase in absolute and percentage ICV. The frontal ICV increase provided by the FOA helps to explain the greater absolute and percentage ICV increase achieved in the plus FOA group.

Group 1 underwent their SAPVE at a significantly older age than groups 2 and 3, and a significantly larger $ICV_{at\text{-}op}$. There were no significant differences in absolute or

percentage ICV expansion achieved. In the younger patient with a smaller starting ICV, it may be technically more difficult to achieve a post-operative ICV necessary to avoid the need for a repeat vault expanding procedure. Therefore, despite group 3 receiving a reasonable percentage and absolute ICV increase, the starting ICV may be such that a single SAPVE alone cannot produce a large enough post-operative ICV.

The patients who had FOA at the time of spring removal (group 2) underwent their initial SAPVE at a significantly older age than those patients that required a repeat SAPVE (group 3). Their $ICV_{at\text{-}op}$ were significantly different, with group 2 having a larger $ICV_{at\text{-}op}$, however despite the additional FOA, their percentage ICV change (whilst larger) was not significantly different (24.7% compared to 18.4%). None of the patients who underwent first SAPVE and had FOA at time of spring removal required repeat vault expansion, this may suggest that, if technically possible, and felt to be of benefit to the frontal cranial morphology, an FOA could be performed at time of spring removal in patients requiring SAPVE at a young age.

In the cohort that required repeat SAPVE (Group 3), operative ICV change was compared for first and repeat SAPVE. There was a significant ICV increase at both procedures. Repeat SAPVE increased by a significantly smaller percentage ICV (7.3% compared to 18.4%) than initial SAPVE. This may be explained by the increased internal push from the rapidly expanding brain in the younger patient at first procedure as compared to second procedure.

5.5 Summary

In conclusion, 172 patients who underwent SAPVE were analysed. This is the largest group studied in the literature by a factor of 11. The operative technique and spring design used by the craniofacial team at GOSH were detailed and explained. Results showed that the majority of patients required SAPVE to treat raised ICP, and that this was done successfully. Clinical parameters such as transfusion requirement, length of hospital stay, and complication profile was comparable with those for PVDO and PCVR. Significant increases in ICV can be achieved by SAPVE when undertaken at any age and in any diagnosis. Larger step percentage volume increases were achieved when SAPVE was undertaken at an earlier age however, younger patients and those with Apert or Crouzon-Pfeiffer syndrome were significantly more likely to require a repeat PVE. This knowledge is useful for both patient and parent counselling and surgical planning. Parents of children with Apert or Crouzon-Pfeiffer syndrome who require SAPVE before one year of age can be warned that this evidence suggests their children are likely to require a further vault expansion in the future. Parents considering SAPVE to alter head shape may be counselled that performing the surgery at a later date will reduce the potential need for a repeat procedure. Comparison of patients requiring a single or two SAPVE showed no difference in percentage ICV increase. This would suggest that age at first procedure and syndromic diagnosis are more important factors in deciding which patients will require a repeat procedure. This chapter also compared SAPVE to published data on PVDO and PCVR and has shown it to be as safe. Examination of ophthalmological data indicated that SAPVE can successfully manage raised ICP.

Chapter 6 now investigates whether optic nerve sheath diameter can be used as a proxy for ICP, and therefore when SAPVE is being undertaken to manage raised ICP, be used to measure operative success.

Chapter 6 **OPTIC NERVE SHEATH DIAMETER: RELATIONSHIP TO ICV AND POTENTIAL USE AS A NON-INVASIVE MEASURE OF INTRACRANIAL PRESSURE**

Part of the work described in this chapter was presented at The 20th Biennial Meeting of the European Society of Craniofacial Surgery, Athens, Greece, October 4-6th 2018

As discussed in Chapter 2, raised intracranial pressure has been extensively reported in children with syndromic craniosynostosis (Abu-Sittah et al., 2016; Marucci et al., 2008; Tamburrini et al., 2005). Direct and indirect methods of ICP measurement have advantages and disadvantages (Xu et al., 2016). Chapter 5 described the clinical outcomes of the GOSH PVE cohort, using ophthalmological changes as a marker for whether or not SAPVE reduced ICP. As ophthalmological examinations can be challenging in infants (McGraw, Winn, Gray, & Elliott, 2000), this chapter aims to investigate whether changes in optic nerve sheath diameter (ONSD) can be used as a non-invasive measure of ICP changes following cranial vault expansion.

6.1 Introduction

In syndromic craniosynostosis, multiple factors exist which can contribute to raised ICP, as described in chapter 2. Unlike in situations such as traumatic brain injury or epidural haematoma, the onset and rise of ICP in syndromic craniosynostosis can be insidious, occurring over a long time period (Xu et al., 2016). The study of raised ICP in syndromic craniosynostosis is problematic. First of all, there is an incomplete understanding of what constitutes a 'normal' childhood ICP. As discussed in Chapter 2, Renier et al. defined a normal childhood ICP as below 10mmHg, abnormal above 15mmHg and borderline when in between (Renier et al., 1982). This definition remains widely used but has been challenged in the literature with some authors suggesting 20mmHg as an upper limit (Hayward et al., 2016). When assessing patients for raised ICP at GOSH, non-invasive methods are preferred. Pattern evoked visual potentials are used in conjunction with visual acuity measurement and fundoscopy. A small number of

patients will undergo invasive ICP monitoring via ICP bolt if ophthalmological testing has proved difficult or inconclusive. Craniosynostotic patients who present with changes in these parameters and are felt to be at risk of raised ICP will then have a head CT before undergoing SAPVE.

Given that ONSD and ICV can be measured on these same CT scans, the aim of this chapter is to investigate the optic nerve sheath diameters of the GOSH SAPVE cohort pre and post-operatively and relate these findings to ICV changes and published thresholds for ONSD to indicate raised ICP.

6.2 Methodology

A retrospective review of all SAPVE cases undertaken at GOSH between 2008 and 2018 was performed. Inclusion criteria included all patients with usable pre and post-operative head CT scans i.e., those scans that included the entire cranial vault, contained no artefact, and were of sufficient quality to measure ONSD and ICV. In addition to ONSD and ICV measurements, demographic data, craniosynostotic diagnosis, and indications for surgery were also collected.

Left and right ONSD were measured at the point at which the ophthalmic artery crossed the optic nerve and from the slice which showed the largest diameter at this point. This point is usually located 8 to 12mm posterior to the globe and is not affected by tremor, gaze deviation or involuntary movement of the eyes (Bekerman, Sigal, Kimiagar, Ben Ely, & Vaiman, 2016). All ONSD measurements were made by the primary author using the calliper tool within the free, open source medical image viewer Horos (Nimble

Co LLC d/b/a Purview, Annapolis, MD USA). Windowing parameters were WW 360, WL 60 (Figure 6.1). Mean ONSD between left and right was used for subsequent analysis.

Published thresholds for detecting ICP over 15mmHg and used for comparison here are 4.97mm and 5.49mm, in the under and over ones respectively. These thresholds are for cohorts above and below one year of age at the time of their imaging, and, therefore, where the following results are stratified by age, this is based on age at scan rather than age at operation (Padayachy et al., 2016).

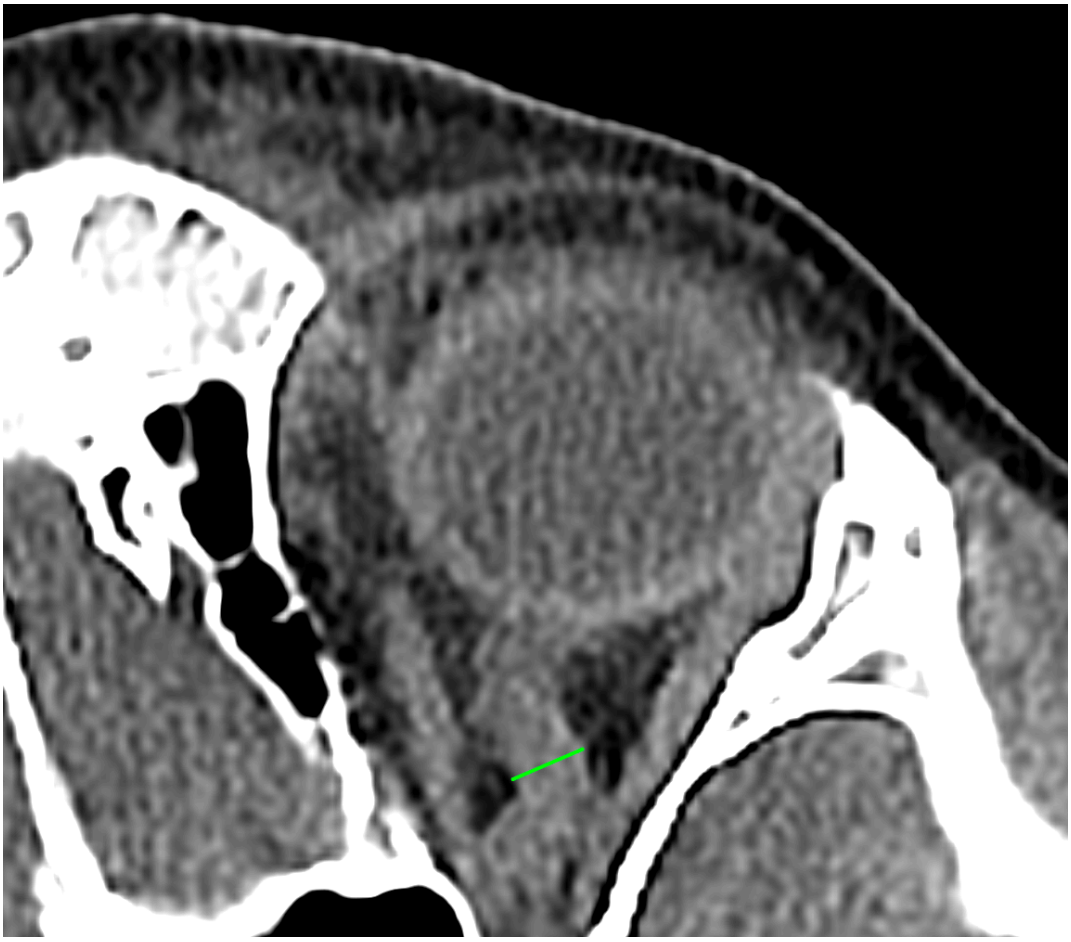

Figure 6.1 Left ONSD measuring 4.34mm, 9.8mm posterior to the globe.

ICV was measured using the semi or fully automatic method detailed in Chapter 3. In an attempt to correlate the spring related ICV change to the ONSD changes ICV was adjusted for growth as per the techniques in Chapter 5. Unlike ICV, the ONSD was not adjusted for growth. This adjustment would have required ONSD growth curves generated from large cohorts of unoperated children with syndromic craniosynostosis. This is not available in the published literature. It was felt that the value of these adjustments would have been minimal and therefore these curves were not created.

ICP assessment was undertaken using ophthalmological techniques or in a small number of patients by invasive ICP bolt monitoring. Ophthalmological techniques included assessment of visual acuity, papilloedema and visual evoked potentials. These assessments were done by specialist paediatric ophthalmologists and optometrists. When diagnosed on invasive monitoring, raised ICP was defined as > 15mmHG.

Statistical analysis was performed using IBM SPSS Version 25 (IBM SPSS Statistics for Macintosh, Version 25.0). Paired student t-tests were used to compare ONSD difference between each eye, and pre and post-operatively. Independent student t-tests were used to compare ONSD and ICV, as well as to compare the results between children aged less than or more than one year of age and to compare the results between those operated on for raised ICP or for shape change. Coefficient of determination (R^2) was used to correlate ONSD and ICV. *P* Values of < 0.05 were considered significant.

6.3 Results

There were 172 SAPVE undertaken at GOSH between 2008 and May 2019, and of these 74 (43%) had usable pre and post-operative CT scans. All patients had syndromic

(n=51, 69%) or non-syndromic multisuture synostosis (n=23, 31%). Syndromic diagnoses included Crouzon n=18 (35%), Apert n=16 (33%), Pfeiffer n=4 (8%), Muenke n=4 (8%), TCF-12 n=3 (6%), Saethre-Chotzen n=2 (4%), ERF n=1 (2%), Noonan n=1 (2%), cranial dysraphism n=1 (2%), CHARGE n=1 (2%). 60 patients (81%) underwent SAPVE to relieve raised ICP.

Where raised ICP was the indication for surgery, it was suspected based on deteriorating ophthalmological findings in 38 patients (52%), a combination of ophthalmological and radiological findings in 15 patients (20%), clinical findings in 4 patients (5%), radiological findings alone in 2 patients (3%) and a combination of ophthalmological and clinical findings in one patient (1%). The remaining 14 patients (19%) were operated on for alteration of head shape and / or prophylactically to prevent raised ICP. Age, ONSD and ICV results for the raised ICP and aesthetic / prevention group are shown in Table 6.1.

Table 6.1 Age, ONSD and ICV results.

	Raised ICP (n=60)						Aesthetic/preventive (n=14)					
	Mean	**Range**					**Mean**	**Range**				***p* =**
Age (months)												
at op	21.5	2.1-67.2					13.7	5-35.9				**0.012**
at pre-op scan	19.6	1.4-65.2					8.2	1.7-32.8				**0.001**
at post-op scan	33	4-87					20.7	12.1-43.9				**0.001**
<1yr age group (n=39)	6 (n=28)	1.4-11.4					4.9 (n=11)	1.7-7.7				0.337
>1yr age group (n=35)	31.7 (n=32)	12.76-65.2					20.4 (n=3)	13.2-33				0.262
			Adjusted ICV change pre -post						**Adjusted ICV change pre -post**			
			Mean (*p* =)	**Range**	**% (mean)**	**% (range)**			**Mean (*p* =)**	**Range**	**% (mean)**	**% (range)**
ONSD (mm)												
<1yr group pre-op	4.16	2.57-5.63	-0.14 (0.153)	-0.73-1.46	2.1	-18.9-27.2	3.80	2.5-5	-0.10 (0.508)	-0.51-1.37	1.30	-15.1-27.5
<1yr group post-op	4.02	2.85-5.25					3.82	2.8-4.6				
>1yr group pre-op	5.42	3.30-6.90	-0.59 **(<0.001)**	-0.62-2.10	10.1	-5.2-31.1	4.28	3.6-5.3	-0.29 (0.451)	-0.90-0.92	7.70	-1.7-23.3
>1yr group post-op	4.84	3.18-6.47					3.99	3-5.4				
ICV (cm^3)												
<1yr group pre-op	902	562-1333	234 **(<0.001)**	19-520	28.5	2-79	920	540-1339	320 (<0.001)	145-560	35	15.7-65.6
<1yr group post-op	1364	967-1727					1467	1181-1763				
>1yr group pre-op	1231	855-1632	147 **(<0.001**)	10-240	12	1-22	1371	1151-1620	79 (0.041)	53-123	6	3.9-7.6
>1yr group post-op	1441	965-1864					1511	1347-1746				

For the 60 patients operated for raised ICP, 20 patients (33%) were less than one year of age at the time of their SAPVE, and 49 (80%) had syndromic diagnoses. Of the 14 patients operated for shape and / or prevention of raised ICP, seven patients (50%) were less than one year of age at the time of their SAPVE, and seven (50%) had syndromic diagnoses. No patients had intervening shunt insertion between scans.

Patients in the ICP, over one-year group showed a significant decrease in their ONSD post-operatively, whereas the remaining groups did not. When comparing whole cohort results between those patients under or over one year of age, there were significant differences in pre-operative ONSD ($p = <0.001$), post-operative ONSD ($p = <0.001$), absolute ONSD change ($p = 0.003$), percentage ONSD change ($p = 0.005$), and pre-operative ICV ($p = <0.001$), post-operative ICV ($p = 0.098$), absolute ICV change ($p = 0.001$), and percentage ICV change ($p = <0.001$).

Within the under one cohort operated on to ameliorate raised ICP, six out of 28 patients (21%) had a preoperative ONSD over the Padayachy et al. threshold of 4.97mm. In the over one, 17 of the 33 patients (52%) had preoperative ONSD over the Padayachy et al. threshold of 5.49mm.

All six under ones who pre-operatively were above the 4.97mm threshold and 11 of the 17 over ones who pre-operatively were above the 5.49mm threshold fell to within the age appropriate normal range for ONSD following SAPVE.

No patients in the under one group who began below the 4.97mm raised ICP threshold had increased to above the threshold following SAPVE. One of the 16 patients in the over one-year cohort who were below the 5.49mm threshold pre-operatively had an ONSD that increased above the raised ICP threshold when scanned 6.7 months following SAPVE.

11 patients (15%) had invasive ICP bolt procedures within 71 days (median 29) of an available CT scan. Nine of the 11 patients (12%) had invasive ICP monitoring indicating raised ICP. All were over one year of age at the time of their ICP measurement (range 1.3 – 12.8 years) and at the time of their CT scan. They had a mean ONSD of 4.93mm (range 3.17 – 6.03), six ONSD measurements were below the 5.49mm threshold. One of the eleven patients was shown to have normal ICP (ONSD = 4.13mm) and one a low – normal ICP (ONSD = 3.95mm).

One patient in the below one year of age shape / preventative cohort began above the 4.97mm Padayachy et al. threshold and fell to below the threshold following SAPVE. All patients in the over one shape / preventative cohort began below the 5.49mm threshold and remained below it.

As per the Heredy et al. paper, regression analysis was performed on the pre-operative images which showed a very weak correlation between age and ONSD in the ICP ($r^2 = 0.198$) (Figure 6.2).

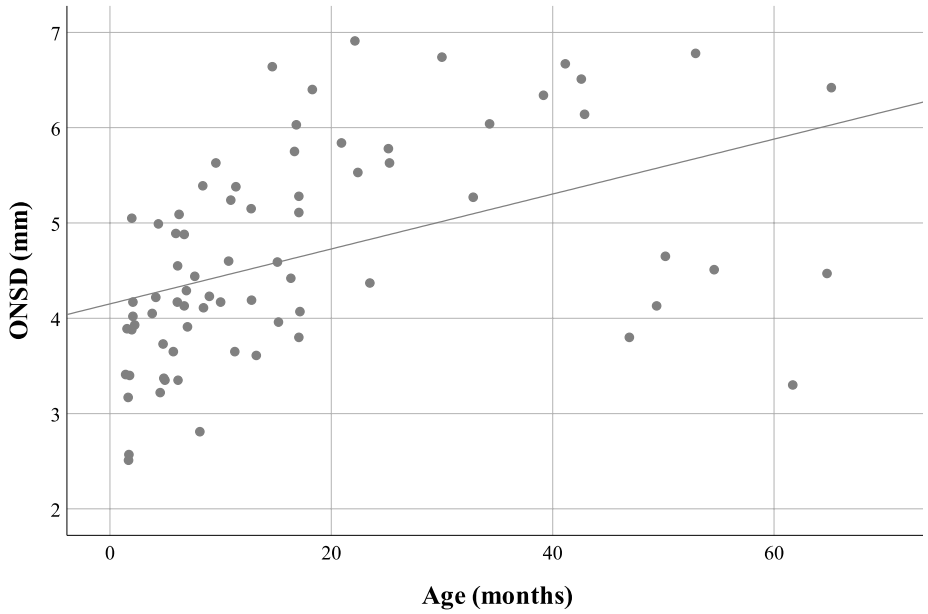

Figure 6.2 Scatter plot to show very weak correlation between ONSD and Age (r^2 = 0.198).

There were no significant differences found between patients operated on for raised ICP and those for shape change and / or prophylactically to reduce the risk of raised ICP in pre-operative ONSD, post-operative ONSD, pre-operative ICV and post-operative ICV (p = >0.05).

Patients were further divided into cohorts by diagnosis. These were Apert, Crouzon-Pfeiffer and non-syndromic multi-suture, the remaining diagnoses were placed in an 'other' cohort. They included Saethre-Chotzen, Muenke, TCF-12, ERF, Noonan, cranial dysraphism, and CHARGE. In the patients treated for raised ICP, cohort numbers were as follows: Crouzon-Pfeiffer (n=21), Apert syndrome (n=14), Multi-suture non-syndromic (n=15), 'other' (n=10). There was no significant difference between any cohort in: age at pre-operative CT scan, pre-operative ICV, post-operative ICV, and absolute or percentage ICV change. The Crouzon-Pfeiffer cohort had a significantly

higher pre and post-operative ONSD than both the Apert and the non-syndromic multi-suture cohorts, p = >0.001 and p = 0.001 respectively. There was no significant difference in absolute or percentage ONSD change between any cohorts. Results are shown in Tables 6.2 and 6.3.

Table 6.2 ONSD and ICV results per diagnostic cohort in the ICP group.

Cohort	Age at pre-operative scan (months)	Pre-operative ONSD (mm)	Post-operative ONSD (mm)	ONSD change (mm)	ONSD change (%)	Pre-operative ICV (cm^3)	Post-operative ICV (cm^3)	Adjusted ICV change (cm^3)	Adjusted ICV change (%)
Apert (n=15)	11.5 (1.97–49.39)	4.2 (3.22–5.09)	4 (3.26–5.07)	0.2 (-0.32–1.08)	4.3 (-9.68–21.14)	1073 (710.59–1688.5)	1519.3 (1129–1862.8)	216.9 (82.6–454.9)	22.8 (7.6–54.7)
Crouzon-Pfeiffer (n=21)	19.6 (1.64–42.88)	5.6 (3.17–6.91)	5 (3.28–6.29)	0.6 (-0.35–2.1)	9.8 (-10.10–31.12)	1094.5 (562.16–1590.36)	1345.4 (964.58–1863.95)	167.6 (59.41–291.48)	17.2 (5.89–47.18)
Multi-suture (n=15)	24.9 (1.41–65.18)	4.4 (2.81–6.42)	4.2 (2.9–6.18)	0.2 (-0.62–1.46)	3.1c (-15.15–27.15)	1089 (661.60–1469.2)	1410.1 (1203.9–1687.1)	177 (9.59–520.07)	19.2 (0.8–78.6)
'Other' (n=9)	26.3 (1.71–64.78)	4.8 (2.57–6.78)	4.4 (2.83–6.47)	0.4 (-0.73–1.88)	6 (-18.9–29.71)	1089 (735.3–1331.1)	1401 (1093.4–1717.1)	199.1 (77.99–493.2)	20.2 (8–67.1)

Table 6.3 ONSD and ICV results per diagnostic cohort in the shape / prophylactic group.

Cohort	Age at pre-operative scan (months)	Pre-operative ONSD (mm)	Post-operative ONSD (mm)	ONSD change (mm)	ONSD change (%)	Pre-operative ICV (cm^3)	Post-operative ICV (cm^3)	Adjusted ICV change (cm^3)	Adjusted ICV change (%)
Apert (n=2)	3.7 (1.68-5.72)	3.1 (2.51–3.65)	3.2 (2.83–3.62)	-0.1 (-0.03–0.35)	-6 (-12.7–0.77)	891.4 (702.7–1080.1)	1523.4 (1487.6–1559.2)	273.6 (188.4–358.7)	34.2 (17.4–51)
Crouzon-Pfeiffer (n=1)	15.2	4	3	0.92	23.3	1620.11	1745.73	123.39	7.62
Multi-suture (n=7)	10.3 (2.24-32.82)	4.4 (3.37–5.27)	4.2 (3.56–5.36)	0.1 (-0.51–1.37)	2.3 (-15.06–27.48)	1071.2 (852.6–1343)	1492.2 (1298.7–1762.5)	253.5 (52.52–507.78)	26.2 (3.9–65.6)
'Other' (n=4)	5.1 (1.78–7)	3.8 (3.4–4.29)	3.7 (3.32–4.54)	0.1 (-0.24–0.58)	2.5 (-5.69–8.63)	834.1 (539.5–1002.4)	1357.2 (1180.7–1541.4)	279.1 (195.68–369.06)	35 (20–46)

In the patients treated for shape alteration and / or prophylactically to prevent raised ICP the cohort numbers were as follows: multi-suture non-syndromic (n=7), 'other' (n=4), Apert (n=2), Crouzon-Pfeiffer (n=1). Given the low numbers within the cohorts' one-way ANOVA with post hoc testing was not possible. A t-test between the multi-suture and 'other' cohort showed no significant differences in the same variables as tested for the ICP cohort.

Percentage and absolute ICV change and percentage and absolute ONSD change following SAPVE did not show any significant correlation in any age group or cohort (Figures 6.3 & 6.4).

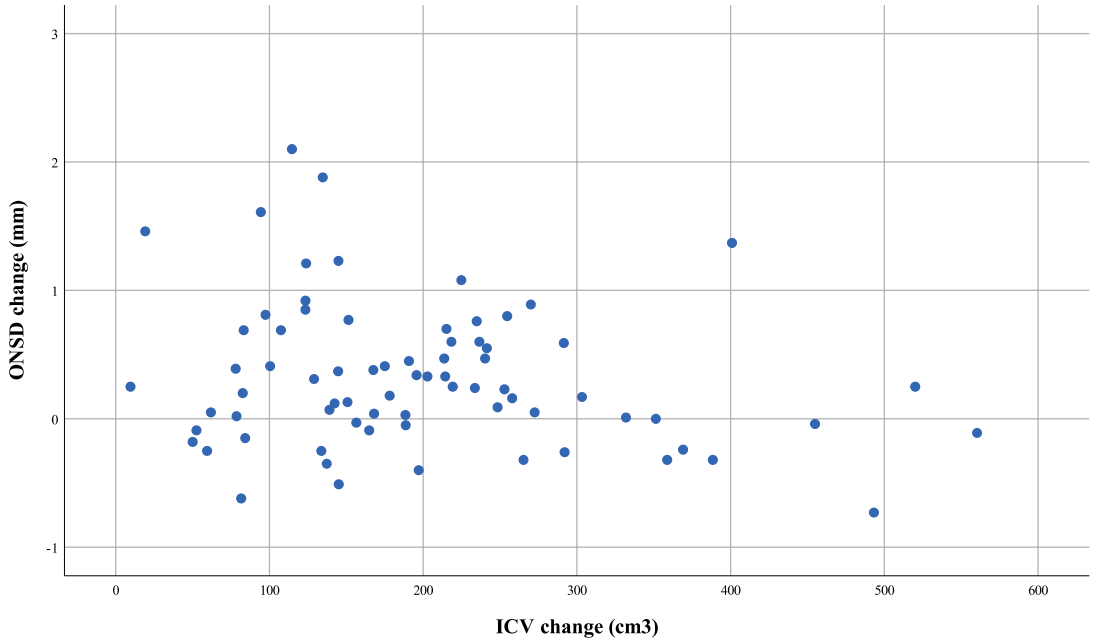

Figure 6.3 Scatter plot of absolute ONSD changes showing non-linear relationship with ICV change ($R^2 = 0.05$).

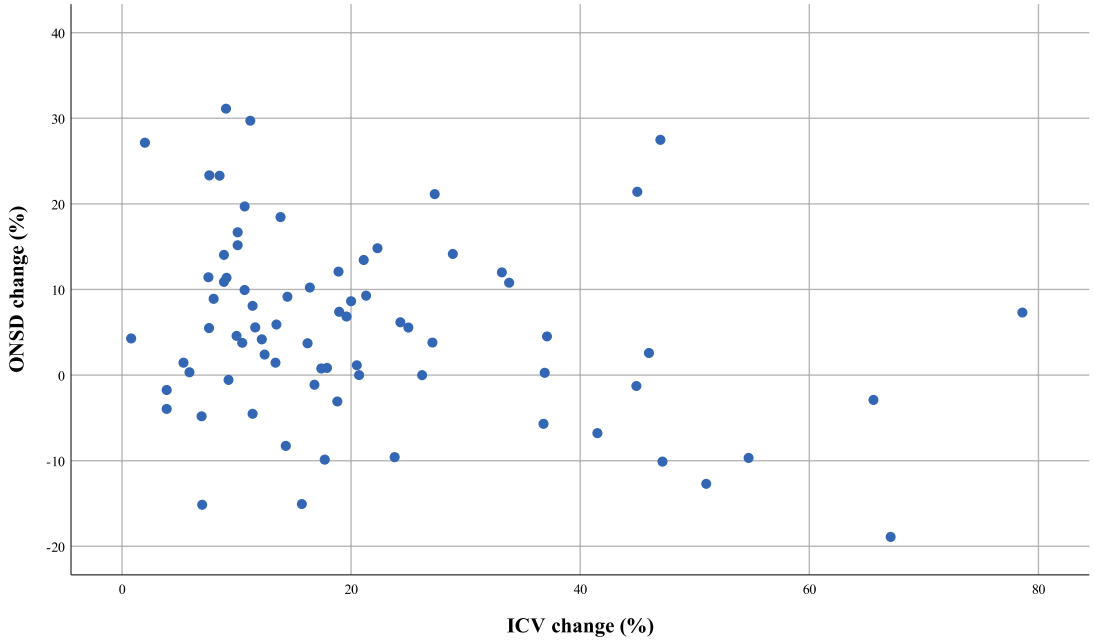

Figure 6.4 Scatter plot of percentage ONSD changes showing non-linear relationship with ICV change ($R^2 = 0.065$).

6.4 Discussion

The gold standard, invasive, ICP measurement techniques require a surgical procedure and an inpatient hospital stay. To find a non-invasive alternative could reduce both surgical trauma and cost to the provider. The optic nerve sheath has been investigated as a potential conduit to the brain and its measurement used as a proxy to assess raised ICP within the cranium. Different methods have been used to measure ONSD, with published studies using trans-orbital ultrasound, MRI or CT (Driessen et al., 2011; Geeraerts et al., 2008). Studies have shown good agreement between measurements made using USS and CT as well as between MRI and CT (Driessen et al., 2011; Haredy et al., 2018). No published studies have compared changes in ICV with changes in ONSD and

given that ICV would be measured on CT, it was felt reasonable to perform CT ONSD measurements.

74 patients were included in this study, 81% of whom were operated on to ameliorate raised ICP. The remaining were operated on to alter head shape or to prophylactically reduce the chance of the patient having raised ICP in the future. When considering those patients shown clinically to have raised ICP and therefore operated on to reduce their ICP, mean pre-operative ONSD was 4.16mm in the under ones and 5.42mm in the over ones. This is lower than the Padayachy et al. thresholds of 4.97mm and 5.49mm for under and over one years of age respectively as well as the Haredy et al. threshold of 6mm for patients over one (Haredy et al., 2018; Padayachy et al., 2016). As Haredy et al. point out, there is considerable variation in the literature around the cut off levels for raised ICP. Historically ONSD thresholds of 4mm for patients over one year of age, 4.5mm for one to four years of age and 5mm for patients over four have been used (Ballantyne et al., 1999), and this study would be in closer agreement to these levels.

Within the under one cohort, six out of 28 patients had an ONSD above the Padayachy et al. threshold of 4.97mm for an ICP of >15mmHg. Whereas if the Ballantyne et al. threshold of 4mm is used this number increases to 20 out of the 28.

In the over one group, 17 out of 33 patients had ONSD above the 5.49mm Padayachy et al. threshold. Once again, if using the Ballantyne et al. threshold, now of 4.5mm for children aged one to four or over 5mm for children over the age of four, this number increases to 22 out of 33.

SAPVE reduced the ONSD of all six patients in the under one-year old group who began above the Padayachy et al. threshold of 4.97mm, to below it, as well as reducing 11 out of 17 patient's ONSD in the over one-year old group. Of the remaining 8 patients that did not reduce into the normal level, all but one showed an improvement in their papilloedema post operatively and none required a further SAPVE at a later date.

When considering the Ballantyne et al. thresholds, 11 out of 20 patients in the under one-year group had their ONSD reduced into the normal range by SAPVE and six out of the 22 in the over one-year cohort.

Eleven patients had invasive ICP pressure monitoring within 71 days of a CT scan on which ONSD could be measured. All were over one year of age at the time of their scan. If taking the Padayachy et al. thresholds for raised ICP of 5.59mm for over ones, three patients shown to have raised ICP by invasive monitoring would have ONSD in agreement. If using the Ballantyne et al. thresholds of over 4mm for those patients under one year, over 4.5mm for one to four-year-old patients and over 5mm for patients over four years of age, all patients but one patient had ONSD measurements in agreement with their invasive ICP monitoring result.

Following SAPVE there was a significant decrease in the ONSD in those patients who were over one at the time of their scan and operated on for raised ICP. There was a decrease, but this did not reach significance in ONSD in the under ones operated on for ICP and both age group cohorts operated on for shape change. ICV increased significantly in all groups.

As would be expected with normal growth, previous studies have found a positive correlation between age and ONSD (Ballantyne et al., 1999; Haredy et al., 2018). The results published here were only able to show a very weak correlation between ONSD

and age. The weak correlation found between age and ONSD, as well as the disparity in the clinically raised ICP patients and their ONSD measurements as compared the Padayachy et al. thresholds perhaps highlights the difficulty in using reference ranges created for control children when studying children with craniosynostosis. Given these findings, and the discrepancies in published normal values, it is difficult at present to recommend the use of ONSD as a marker for ICP change in children with craniosynostosis. Validation of ONSD as a marker for ICP would require a prospective study where invasive ICP monitoring is undertaken concurrently with CT scanning in the same admission. To ethically approve this would be difficult and finding a reasonable sized cohort of children who coincidently have had both investigations proved difficult. Should this be overcome the results would add to the literature, may validate the technique and allow its use, however until that time it remains difficult to recommend. These children may have altered baseline ONSDs following prolonged periods of sub clinically raised ICP leading to optic atrophy and a degree of optic nerve sheath scarring, or as Khan, Britto, Evans, & Nischal (2005) postulated after finding a positive expression of FGFR-2 in the optic nerve sheath, there may be abnormal deposition of fibrous tissue here in those patients with FGFR-2 related craniosynostosis.

When ONSD findings were further subdivided by diagnosis, significant differences were seen in mean pre and post-operative ONSD between the Apert and Crouzon-Pfeiffer cohorts and between the Crouzon-Pfeiffer and non-syndromic multi-suture cohorts. The Crouzon-Pfeiffer pre-operative CT scans were taken at a median age of 17.1 months, with Apert and non-syndromic multi-suture groups taken at 6.1 and 12.8

months respectively, which may explain this finding. There was no significant difference in absolute or percentage ONSD change between any cohorts.

This study did not show a significant correlation between the relative or absolute volume increase following PVE and the relative or absolute change in ONSD.

6.5 Summary

In paediatric craniosynostotic patients undergoing SAPVE for raised ICP, preoperative ONSD was found to be smaller than previously reported. Where ONSD was compared with invasive ICP monitoring acquired 2 months before/after the CT scan, it did not correlate to the most recently published thresholds; however it did correlate with those thresholds published by Ballantyne et al. in 1999 (Ballantyne et al., 1999). A statistically significant reduction in OSND was seen post-operatively in patients operated on after one year of age for raised ICP. This finding is interesting when considered in conjunction with the findings from chapter 5, that patients requiring repeat PVE underwent their first PVE at a significantly younger age of 10.6 months as opposed to 24.6 months in those patients that did not. This study did not show a significant correlation between the relative or absolute volume increase following PVE and the relative or absolute change in ONSD. Using ONSD as a marker for ICP in children with craniosynostosis should be done with care and this study would suggest following the thresholds published by Ballantyne et al.

In Chapter 7, a direct comparison of SAPVE, PVDO and PCVR focusing mainly on ICV outcomes is performed by combining data from two Craniofacial Centres; Great Ormand Street Hospital and Seattle Children's Hospital.

Chapter 7 A TWO CENTRE COMPARISON OF THREE TECHNIQUES FOR POSTERIOR VAULT EXPANSION IN SYNDROMIC CRANIOSYNOSTOSIS

This work was made possible by the generous financial assistance of; The University College London Bogue Fellowship Committee and The Alex Simpson Smith Memorial Fund.

Part of this work has been presented at the 18th Biennial Meeting of the International Society of Craniofacial Surgery, Paris, France, September 16th-19th 2019 and the Winter Scientific Meeting of the British Association of Plastic, Aesthetic and Reconstructive Surgeons, Monte Carlo, Monaco, 4th-6th December 2019.

In chapter 5, an in-depth analysis of SAPVE procedures performed at GOSH was undertaken and described. Within that chapter a comparison of SAPVE, PVDO and PCVR was realised through analysis of the published literature. In order to more closely examine the differences in clinical and volumetric outcomes achieve by these techniques a direct evaluation was necessary. Since 2008 SAPVE has been the mainstay PVE technique at GOSH and therefore to attain the necessary PVDO and PCRV data, a two centre comparison was required. This was made possible through a collaborative project with the Seattle Children's Hospital (SCH) Craniofacial centre, where the surgical approach to PVE is via PVDO or PCVR. During data collection it became apparent that the majority of PVDO procedures at SCH were carried out on patients with Apert or Crouzon syndrome and before the age of two years. In order therefore to more closely align the two centres, only those children with Apert or Crouzon syndrome, who were operated before the age of two years were investigated. Chapter 7 describes this collaborative project and outlines the comparative results obtained.

7.1 Introduction

Children with Apert and Crouzon syndrome commonly require cranial vault expansion in order to manage potential, impending or diagnosed raised ICP. Published incidences of raised ICP in Apert syndrome range from 45% - 83% (Marucci et al., 2008; Renier et al., 1996) and in Crouzon 61% - 63% (Abu-Sittah et al., 2016; Gault et al., 1992). Craniofacial centres worldwide have differing protocols as to when and how cranial vault expansion should be undertaken. The majority advocate a prophylactic, posterior approach, undertaken before the age of one year in an attempt to prevent the

development of raised ICP. At GOSH the practice differs in that an expectant approach is taken, with cranial vault expansion being undertaken as and when raised ICP occurs (Forrest & Hopper, 2013; Marucci et al., 2008; Spruijt, Joosten, et al., 2015). The purpose of this chapter is not to compare these protocols but rather to compare the techniques used to achieve a posterior expansion. As discussed in Chapter 3 and 6, PVE can be accomplished by traditional PCVR, PVDO or SAPVE. PCVR is a static procedure, whereas both PVDO and SAPVE are dynamic. PVDO was first introduced by the Birmingham group in 2008 and has been broadly adopted by craniofacial centres worldwide (White et al., 2009). Spring assisted expansion was introduced by Lauritzen, Sugawara, Kocabalkan, and Olsson in 1998 and has been used for a number of indications since (Arnaud et al., 2012; Lauritzen et al., 1998; Lauritzen et al., 2008). SAPVE has been used by GOSH for the majority the posterior vault expansions since 2008.

The two dynamic techniques allow for reduced tension scalp closure and cause a gradual post-operative adaptation of the soft tissues over the period of distraction / consolidation, rather than an immediate stretching of the tissues over a fixed, static construct. From a morphological standpoint, they convey benefits to the anterior aspect of the calvarium and, given that scalp closure is not a limiting factor, they potentially provide a greater volume expansion. In addition to these advantages, the reduced surgical trauma is reported to cause less overall blood loss, shorter operative times and reduced intensive care unit stay (Steinbacher et al., 2011; Taylor et al., 2012; Ter Maaten et al., 2018). Disadvantages of the dynamic techniques include the requirement for two operative procedures, as both insertion and removal require a general anaesthetic, device

related complications, and, in PVDO, patient compliance and parental involvement in the distraction protocol (Thomas et al., 2014).

The purpose of this study therefore is to demonstrate how the dynamic methods compare and how they both compare to the traditional static technique of PCVR from both a clinical and a volumetric perspective.

7.2 Methodology

7.2.1 Patient selection

All patients under the age of two years with Apert or Crouzon syndrome that underwent either PCVR or PVDO at SCH or SAPVE at GOSH and had complete records including pre and post treatment CT scans were considered for the study. This was a retrospective study over a ten-year period between 2008 and 2018.

7.2.2 Operative technique

PCVR, PVDO and SAPVE are carried out in the prone position. The SAPVE technique has been outlined comprehensively in Chapter 5 (Figure 7.1 A-C).

PCVR was performed through a coronal scalp incision with a sub-galeal dissection from just posterior to where the coronal sutures would lie and continuing inferiorly to the skull base. The parietal and occipital bones were dissected from the dura and removed, then orthotopically replaced in an expanded position with resorbable fixation. Blood products are administered from the beginning of the case with the volume determined by estimated blood loss, with a goal not to let the haematocrit drop below 20%.

For PVDO a standard bicoronal approach is also used. A proposed posterior craniotomy is marked onto the calvarium from vertex to torcula. Burr holes are created and a limited dural dissection is carried out below the planned osteotomies. One distraction device is placed into each temporal bone, parallel to the Frankfort horizontal plane. The devices are placed to give uniform parallel vectors to avoid device stress caused by diverging or converging vectors. Standard mandibular devices are used (KLS Martin, Tuttlingen, Germany); these measure 1.5mm with a 25mm – 35mm barrel. Final device choice is based on skull morphology and required distraction distance. The device is fixed using five screws at a 4mm depth per footplate with the distractor arms exiting the anterior scalp flap. The devices are then activated to ensure correct function before being returned to the neutral position. A flat Blake's drain is placed under the scalp and the bicoronal wound closed.

Distraction begins after a latency period of one – two days. A distraction distance of 20 to 35mm is aimed for, and this is achieved by 1 - 2mm per day distraction, for around two to three weeks. After a consolidation period of six to eight weeks, the devices were removed through direct parallel incisions over the distractor under general anaesthetic. The blood transfusion protocol is the same as for PCVR.

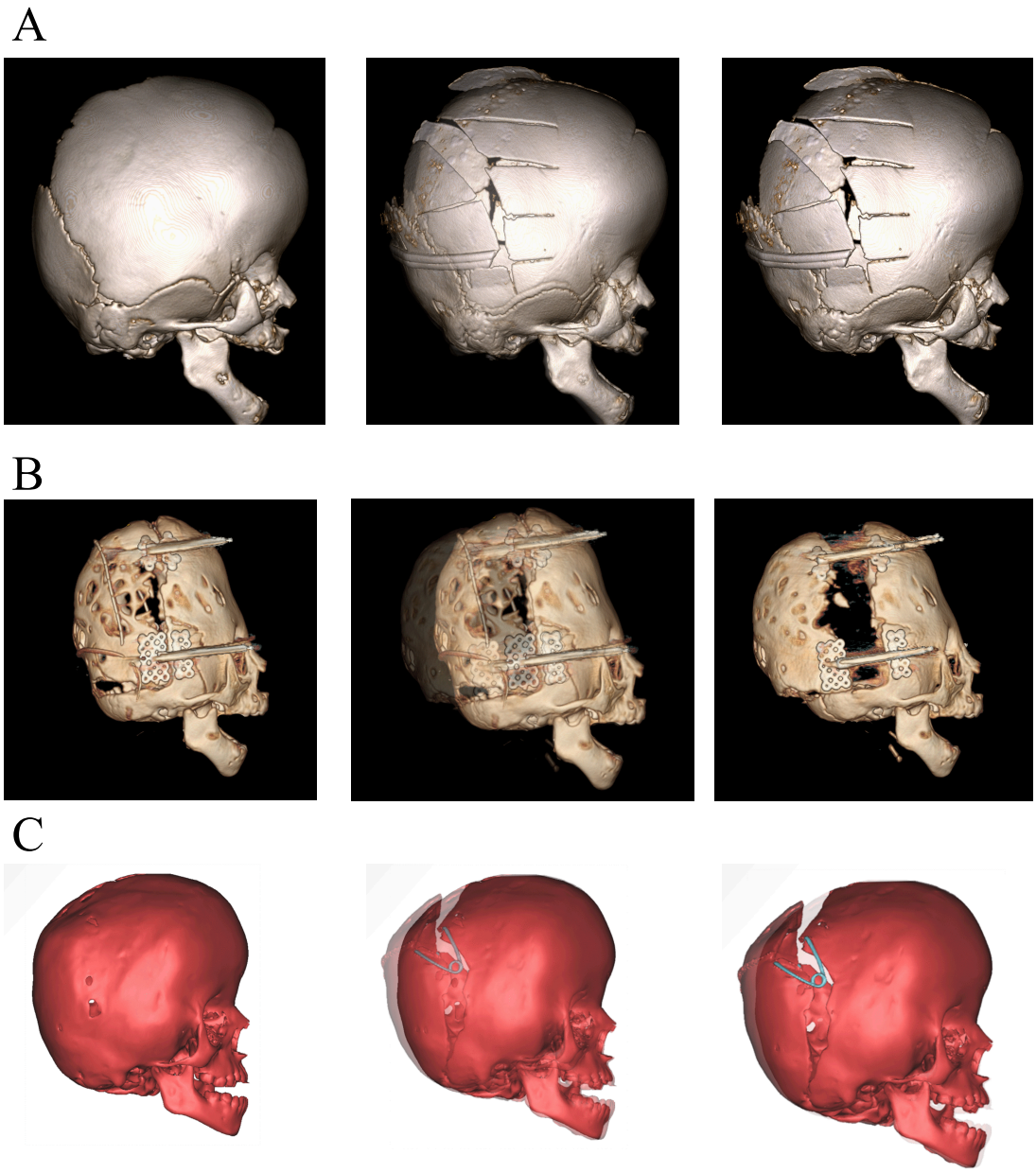

Figure 7.1 Operative Techniques: **A** – PCVR showing barrel staving, **B** – PVDO showing distractors and **C** – SAPVE showing springs.

7.2.3 Data analysis and statistics

The same data were collected from hospital chart review at GOSH and SCH. These included demographic data as well as genetic diagnosis, type of vault expanding procedure, age at first procedure, and at device removal if undergoing PVDO or SAPVE, time taken for each procedure as well as length of hospital stay. Further data collection included transfusion requirements and complications, as well as whether any follow-on surgical procedures were required. Complications were graded using the same Oxford complication scale as used in the chapter 5 (Paganini et al., 2019). ICV was measured (by the primary author) pre and post-operatively using the fully automatic method described in Chapter 3 and normalised for growth as described in Chapter 5, using the equations presented in chapter 4. One Crouzon PCVR patient who had their pre-operative CT scan aged 12 days of age was excluded from ICV analysis. This patient, with a severe phenotype, presented at day 5 with bicoronal, bilambdoid and sagittal synostosis and went on to have PCVR aged 5.2 months. The extremely young age at scan and the steep growth curve in the very young patient was found to render the normalisation process less reliable. ICV difference per technique was analysed with paired Student t-tests. One-way ANOVA with post-hoc testing (Hochberg GT2) was used for intra-group analysis.

7.3 Results

After excluding those patients who had undergone previous transcranial procedures, had additional procedures at the time of device removal or did not have pre and post-operative imaging, there were 33 patients to be included in this study. Patient

demographics and operative data statistics are reported in Table 7.1, and further detailed by diagnosis in Tables 7.2 and 7.3. Patients underwent SAPVE at a significantly older age and were on average 2.5 months older than those undergoing PVDO, who in turn were one month older than those in the PCVR group.

Table 7.1 Summary of demographic and operative data (mean ± std dev) by procedure type.

	PCVR	**PVDO**	**SAPVE**
Number of Cases (males)	7 (5M)	12 (5M)	14 (9M)
Apert	3 (1M)	7 (2M)	7 (2M)
Crouzon	4 (4M)	5 (3M)	7 (3M)
Patient Age (months)	7.9 ± 5.5	9.1 ± 2.5	11.6 ± 5.8*
Total Operative Time[χ]	3:24 ± 0:55	3:52 ± 0:36	3:49 ± 0:48
(Device Insertion)	-	(2:45 ± 0:35)	(2:21 ± 0:33)
(Device Removal)	-	(1:07 ± 0:18)	(1:28 ± 0:28)
Transfusion Volume (ml)	646 ± 326	561 ± 319	197 ± 13**
Length of Stay (days)	6 ± 3.8	8.8 ± 6.4	5.3 ± 2
(Device Insertion)	-	(7.8 ± 5.9)	(4.1 ± 1.2)
(Device Removal)	-	(1.0 ± 1)	(1.2 ± 1)
Device in situ (months)	-	2.9 ± 0.6	9 ± 6.6***

*statistically significant at p = 0.034 and 0.047 against PCVR and PVDO respectively

**statistically significant at p = 0.002 and 0.003 against PCVR and PVDO respectively

***statistically significant at p = 0.004 and 0.010 against PVDO

[χ] Recorded as knife to skin to final dressings

Table 7.2 Patients with Apert syndrome only - Summary of demographic and operative data (mean ± std dev) by procedure type.

	PCVR	**PVDO**	**SAPVE**
Number of Cases	3 (1M, 2F)	7 (2M, 5F)	7 (5M, 2F)
Patient Age (months)	9.8 ± 7.5	9 ± 3	9.3 ± 3
Total Operative Time[χ]	3:48 ± 1:02	4:04 ± 0:38	3:49 ± 0:49
Device Insertion	-	3:00 ± 0:37	2:17 ± 0:30
Device Removal	-	1:04 ± 0:15	1:34 ± 0:31
Transfusion Volume (ml)	811.3 ± 384.5	609.3 ± 412.1	230 ± 154.4*
Length of Stay (days)	4.2 ± 2.3	11.9 ± 6.9	5.9 ± 2.5
Device Insertion	-	10.6 ± 6.4	4.3 ± 2.3**
Device Removal	-	1.3 ± 1.3	1.6 ± 1
Device in situ (months)	-	3 ± 0.6	7 ± 5.1

*statistically significant at p = 0.017 and 0.013 against PCVR and PVDO respectively

**statistically significant at p = 0.042 and 0.010 against PVDO

[χ] Recorded as knife to skin to final dressings

Table 7.3 Patients with Crouzon syndrome only - Summary of demographic and operative data (mean ± std dev) by procedure type.

	PCVR	PVDO	SAPVE
Number of Cases	4 (4M, 0F)	5 (3M, 2F)	7 (4M, 3F)
Patient Age (months)	6.6 ± 4	9.2 ± 2.1	18.4 ± 3.4*
Total Operative Time$^{\chi}$	3:01 ± 0:46	3:36 ± 0:22	3:50 ± 0:50
Device Insertion	-	2:24 ± 0:17	2:26 ± 0:38
Device Removal	-	1:12 ± 0:22	1:33 ± 0:36
Transfusion Volume (ml)	522.5 ± 256.3	495.2 ± 125.6	163.4 ± 103.4**
Length of Stay (days)	7.3 ± 4.6	4.4 ± 1.1	4.7 ± 1.3
Device Insertion	-	3.8 ± 1.1	3.9 ± 1.1
Device Removal	-	0.6 ± 0.5	0.8 ± 0.5
Device in situ (months)	-	2.8 ± 0.7	11 ± 7.6***

* statistically significant at p = <0.001 and 0.001 against PCVR and PVDO respectively

**statistically significant at p = 0.009 and 0.010 against PCVR and PVDO respectively

***statistically significant at p = 0.029 and 0.010 against PVDO

$^{\chi}$ Recorded as knife to skin to final dressings

7.3.1 Operative parameters

Total operative time was shortest for the single stage PCVR, however the total operative time for the two stage PVDO and SAPVE was similar and the difference not statistically significant (Figure 7.2). The insertion and removal of distractors in PVDO and springs in SAPVE took a similar amount of time, again with no significant difference. Distractors remained in situ a significantly shorter length of time as compared to the springs. There were no significant differences in length of stay across the three procedures (Figure 7.3).

SAPVE required a significantly lower amount of allogenic blood to be transfused than both PCVR and PVDO. There was no statistically significant difference between

PCVR and PVDO. PCVR had the highest transfusion requirement, requiring an average of 85ml more than PVDO. PVDO patients received an average of 365ml more allogenic blood than those undergoing SAPVE (Figure 7.4).

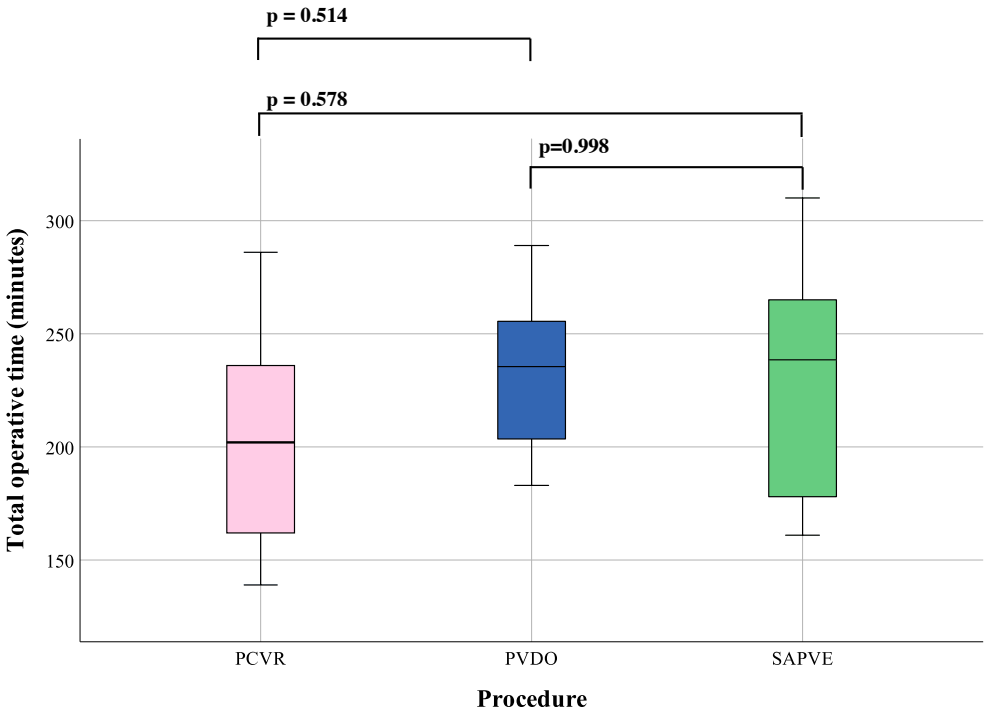

Figure 7.2 Boxplot comparison of total operative time by procedure type.

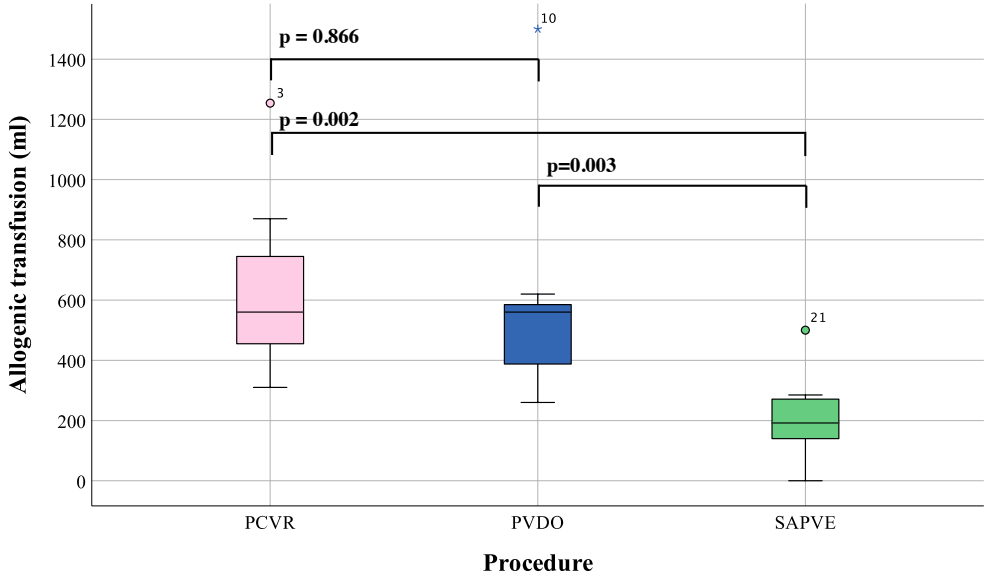

Figure 7.3 Boxplot comparison of blood transfusion requirements by procedure type (includes both insertion and removal for PVDO and SAPVE).

When further comparing by syndrome within the individual procedure cohorts, Apert and Crouzon in PCVR showed no significant differences in age at procedure, procedure time, transfusion rates or length of stay.

Following insertion of distractors, Apert PVDO patients had a significantly longer post-operative stay, with an average stay of 11 nights (range 3 - 19 nights) as compared to an average stay of 4 nights for patients with Crouzon syndrome (range 3 - 6 nights) ($p = 0.031$). There were no significant differences in age at procedure, procedure time, transfusion rates or device in situ time.

Patients with Apert syndrome underwent SAPVE at a significantly younger age, with a mean age at first procedure of 9.3 months as compared to 18.4 months for Crouzon ($p = <0.001$). There were no significant differences in procedure time, transfusion rates, device in situ time or length of stay.

7.3.2 Complications

Complications were recorded in one of the seven PCVR cases, four of the 12 PVDO cases and one of the 14 SAPVE cases. Complication grades are detailed in Table 7.4. There was one Grade 1 complication post PCVR, a superficial skin infection below a post-operative moulding helmet which required antibiotic treatment. This was the only patient who received a helmet. Post PVDO complications included one Grade 1 – a device related superficial skin infection which resolved with antibiotics – and three Grade 3 complications – one mechanistic failure of distractor device requiring removal, one CSF leak during distractor device activation which required a dural repair and insertion of a lumbar drain, and one migration of the activation arm of the device below the skin requiring an operation to re-expose it. There was one Grade 1 complication in the SAPVE cohort: a retained drain which required a return to theatre to remove.

Table 7.4 Complications by procedure type.

Type	Complication description	No. of Complications		
		PCVR	PVDO	SAPVE
0	No complications	6	8	13
1	No delay in discharge, reoperation or long-term sequelae	1	1	
2	Delay in discharge but no further operation required			
3	Reoperation but no long-term sequelae		3	1
4	Unexpected long-term deficit or neurological impairment (permanent disability)			
5	Mortality			

7.3.3 Further procedures

All patients undergoing PCVR went on to have fronto-orbital advancement (FOA) procedures at around 17 months of age. One patient in the PCVR cohort required a repeat PCVR at age of 12 months, five months after initial PCVR. Six patients (50%) in the PVDO cohort went on to have FOA at an average age of 20 months. Significantly fewer PVDO patients went on to have FOA when compared to PCVR ($p = 0.016$).

In the SAPVE cohort, one patient had a PCVR twenty-one months after their SAPVE. One patient had a monobloc and RED frame distractor procedure 8 years after their SAPVE and one patient went on to have a Le Fort III followed by two FOA procedures, also 8 years following their SAPVE. A further procedure rate of 21%.

7.3.4 ICV measurements

Intracranial volume changes (normalised for growth as per chapter 5) are shown in Tables 7.5 – 7.7

Table 7.5 ICV changes in the whole cohort.

Group	Pre-op ICV cm^3 (range)	Post-op ICV, cm^3 (range)	$ICV_{at\text{-}op}$ cm^3 (range)	$ICV_{post\text{-}op\text{-}adj}$ cm^3 (range)	ICV change		
					cm^3 (range)	% (range)	p-Value
PCVR (n=6)	887.5 (665-1331)	1218.3 (996-1518)	1016.3 (726-1339)	1034.8 (835-1752)	183.5 (93-330)	19.2 (7-33)	**0.003**
PVDO (n=12)	1125.8 (722-1618)	1432.2 (978-2010)	1170.8 (726-1622)	1259.2 (807-1752)	173 (10-455)	15.2 (1-39)	**<0.001**
SAPVE (n=14)	1067.2 (703-1590)	1470.4 (965-1864)	1152 (857-1596)	1249.6 (904-1653)	220.8 (57-452)	20 (5-48)	**<0.001**

Table 7.6 ICV changes for Apert cohort.

Group	Pre-op ICV cm^3 (range)	Post-op ICV, cm^3 (range)	ICV_{at-op} cm^3 (range)	$ICV_{post-op-adj}$ cm^3 (range)	ICV change		
					cm^3 (range)	% (range)	p-Value
PCVR (n=3)	904.7 (682-1331)	1315.3 (996-1518)	1120.7 (835-1339)	1120.7 (835-1339)	194.6 (93-330)	18 (7-28)	0.110
PVDO (n=7)	1170.5 (861-1618)	1503.6 (1108-2009)	1218.6 (933-1622)	1339.3 (1031-1752)	164.3 (76-257)	13 (8-16)	**<0.001**
SAPVE (n=7)	955.9 (703-1458)	1538.6 (1129-1727)	1119.3 (877-1460)	1234.7 (904-1493)	303.9 (178-452)	28.6 (12-48)	**<0.001**

Table 7.7 ICV changes for Crouzon cohort.

Group	Pre-op ICV cm^3 (range)	Post-op ICV, cm^3 (range)	ICV_{at-op} cm^3 (range)	$ICV_{post-op-adj}$ cm^3 (range)	ICV change		
					cm^3 (range)	% (range)	p-Value
PCVR (n=3)	870.4 (665-1090)	1121.4 (1033-1254)	912 (726-1101)	949 (837-1101)	172.4 (125-239)	20.3 (14-33)	**0.037**
PVDO (n=5)	1063 (721-1400)	1332.2 (977-1639)	1104 (726-1500)	1146.8 (807-1562)	185.4 (10-455)	18.2 (1-39)	0.065
SAPVE (n=7)	1178.6 (855-1590)	1402.1 (965-1864)	1184.7 (857-1596)	1264.4 (908-1653)	137.7 (57-239)	11.4 (5-21)	**0.003**

When comparing as a whole cohort or comparing just the patients with Crouzon syndrome, there was no significant difference in measured pre-operative ICV, measured post-operative ICV, ICV_{at-op}, $ICV_{post-op-adj}$, absolute step ICV change and percentage step ICV change between PCVR, PVDO and SAPVE (Figures 7.5 and 7.6).

When comparing PCVR, PVDO and SAPVE outcomes for patients with Apert syndrome alone, there were no significant differences in measured pre-operative ICV, measured post-operative ICV, ICV_{at-op}, or $ICV_{post-op-adj}$. SAPVE showed a significantly larger absolute step ICV change and percentage step ICV change than PVDO ($p = 0.045$

and 0.025 respectively). There were no significant differences in these parameters between SAPVE and PCVR (Figure 7.6).

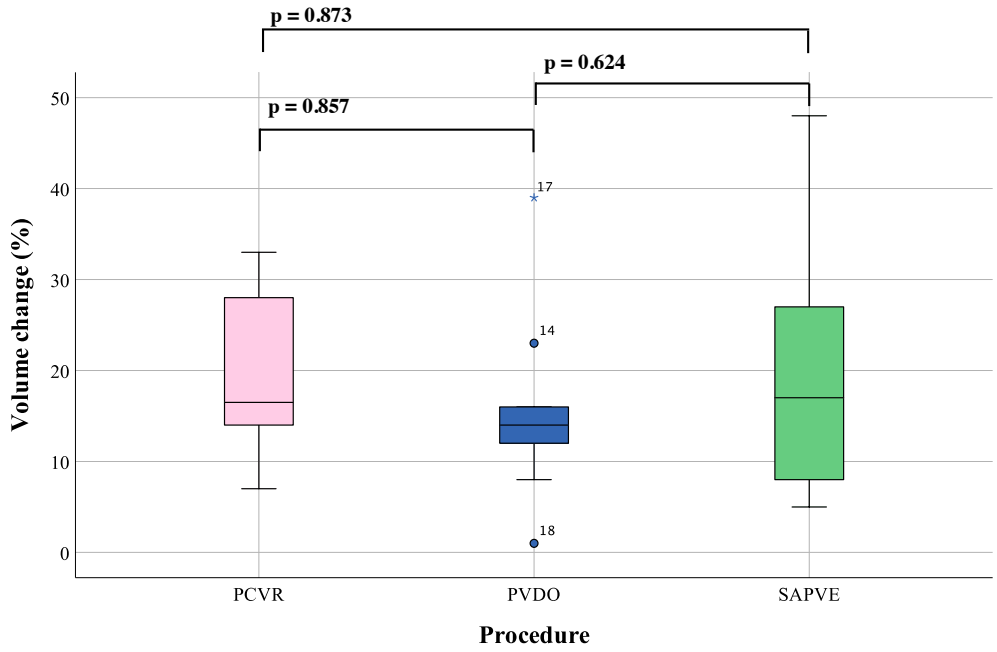

Figure 7.4 Boxplot comparison of percentage volume change by procedure type.

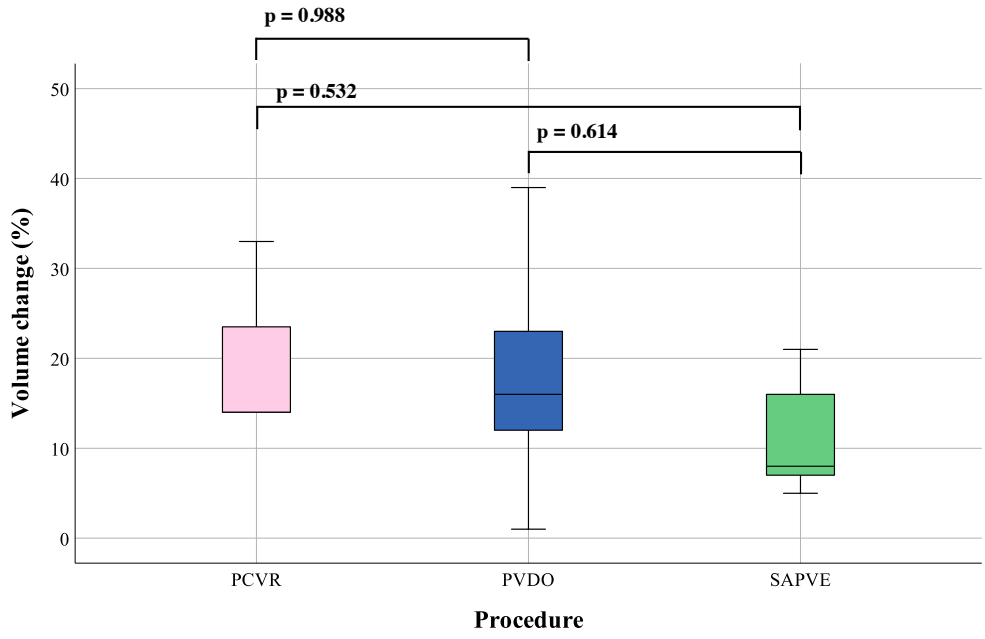

Figure 7.5 Boxplot comparison of percentage volume change by procedure type in patients with Crouzon syndrome.

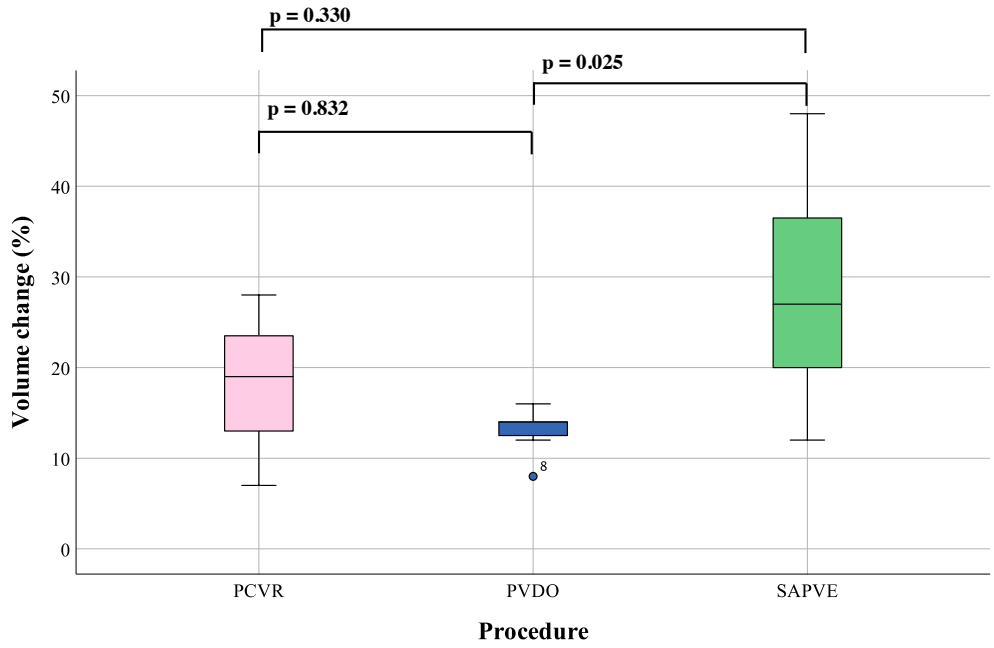

Figure 7.6 Boxplot comparison of percentage volume change by procedure type in patients with Apert syndrome.

When comparing patients with Apert or Crouzon syndrome undergoing PCVR or PVDO there were no significant differences in ICV metrics. In SAPVE, percentage ICV gain attributable to the procedure was significantly greater in patients with Apert syndrome as compared to patients with Crouzon syndrome (28.6% and 11.4% respectively, $p = 0.013$). There were no other significant differences in ICV metrics.

7.4 Discussion

Undertaking this study at two different institutions allowed for data to be collected on the three most commonly used techniques for posterior cranial vault expansion. There exists a degree of complexity in cross border collaboration. Data collection is more convoluted as both institutions are governed by strict ethical, data sharing and confidentiality rules. No identifiable data was shared, and all measurements were

completed on anonymised data. In comparing the two sites, it must be acknowledged that these centres exist in two very different healthcare systems, each with different referral pathways, funding streams and governance objectives. Despite that, this study assumes patient care and safety are the primary concern in both centres and the two teams have acted accordingly. This study has indicated that there are a number of differences in age at surgery, clinical and volumetric outcomes for PCVR, PVDO and SAPVE, when undertaken at two different institutions. When examining age at surgery, all patients underwent PCVR and PVDO at a similar age. Overall SAPVE was undertaken at a significantly older age and this was driven by a significantly older Crouzon cohort, with Apert SAPVE being undertaken at a similar age to PCVR and PVDO. The age difference between SAPVE and PCVR / PVDO in the Crouzon cohort makes drawing firm conclusions about this and the whole cohort difficult. As detailed in the methodology, the normalisation process appears less robust in those patients undergoing their pre-operative CT scan at a very young age and in addition to this, calvarial morphology and bone properties differ with age. A cohort study with a greater number and age matched subjects would be difficult to obtain but would be preferable. The discussion and interpretation of results that follows is cognisant of these limitations.

Each technique had similar total procedure times and inpatient admissions, with no significant differences found between the techniques despite the two procedures required for PVDO and SAPVE. This is in both agreement and disagreement with the published literature comparing PCVR and PVDO, where in 2012 Taylor et al. (2012) reported no significant difference in all perioperative parameters including operative time and length of stay, however Steinbacher et al. in 2011 showed no significant difference

in operative time but a significantly reduced inpatient stay, which was purportedly due to the more limited dissection required for PVDO.

The Steinbacher paper reported a significantly reduced estimated blood loss as a percentage of total blood volume in PVDO. The proxy outcome for estimated blood loss used in this study was transfusion requirement, which showed that SAPVE required significantly less allogenic blood to be transfused than both PCVR and PVDO. This was found in both the Apert and Crouzon cohorts. PVDO had a lower transfusion requirement than PCVR in both Apert and Crouzon cohorts, however this did not reach statistical significance. The difficulties in making direct comparisons between two centres are illustrated neatly by the transfusion requirement findings. Both centres use different transfusion protocols. At SCH, blood products are administered from the beginning of the case with the volume determined by estimated blood loss, with the goal not to let the haematocrit drop below 20%. At GOSH, the team aim to have the patients' pre-operative haemoglobin above 100g/L, prescribing pre-operative iron if necessary. Haemoglobin levels are only measured intra-operatively and are not done routinely in the post-operative period on the ward unless clinically indicated. These discrepancies could be overcome with a direct comparison of pre and post-operative haemoglobin (having removed intra-operative blood product volumes).

The distractors remained in situ for a significantly shorter amount of time than the springs. The break in the skin barrier required by the distractors may encourage earlier removal than the 'closed' system of the springs.

Technical limitations of all three techniques have been previously described. These include difficulty of skin closure over the PCVR leading to limitations in expansion volume and device related problems such as footplate loosening, device failure or device

extrusion in the PVDO and SAPVE techniques (Greives et al., 2015; Lauritzen et al., 2008; Thomas et al., 2014). Difficult closure of PCVR incisions was experienced by the operating surgeons and reported verbally although there are no objective measures of that represented here. Similar complication profiles were seen across PVDO and SAPVE. Despite the distractor break in the skin barrier, there was only one post-operative infections reported, with complications instead relating to the distractor device itself. Complications in both the PVDO and SAPVE group, whilst requiring returns to theatre were minor rather than major and caused no long term sequalae.

When examining the cohort as a whole, the adjusted $ICV_{at\text{-}op}$, was lower but not significantly so in PCVR patients, likely due to their younger age at surgery (7.9 months for PCVR as compared to 9.1 and 11.6 months for PVDO and SAPVE respectively). All techniques obtained a significant absolute ICV increase and a similar percentage ICV increase. PCVR and PVDO obtained similar percentage ICV increases when used in patients with Apert or Crouzon syndrome. SAPVE gained a significantly larger percentage ICV increase than PCVR and PVDO in patients with Apert syndrome, and a smaller, but not significantly different ICV increase in patients with Crouzon syndrome. It is difficult to compare the volume measurements made in this study to those previously published, as most studies have few participants and contain cohorts with a heterogeneous collection of syndromic diagnoses. An interesting observation is that PVDO seems to achieve a more consistent ICV increase, (Figures 7.4, 7.5, 7.6), perhaps due to the increased control of the expansion as afforded by the distractor device. SAPVE was undertaken at a significantly older age in patients with Crouzon syndrome and predictably achieved a smaller (but not significantly so) percentage ICV increase. This is in

agreement with the findings in chapter five, where older children gained a smaller percentage ICV increase. In patients with Apert syndrome, SAPVE achieved a significantly larger percentage ICV increase, and was performed at a younger age. This could indicate that in the younger patient with a more malleable calvarium, the springs can perform well, and in the older patient, with a more developed calvarium the springs are unable achieve their full potential, and the direct control and force of the distractors is preferable. When comparing the Crouzon and Apert cohorts undergoing SAPVE, the patients with Crouzon syndrome were operated on at an older age and required a shorter in patients stay. They may have had less complicated procedures or indeed the team may have been happy to discharge a slightly older, more robust patient back to their home environment earlier. This however is merely a supposition and would require further work to justify.

One of the more recently suggested advantages of PVDO is its ability to delay or remove the need for later FOA due to the anterior benefits it provides such as reduction in frontal bossing as well as a decrease in supraorbital retrusion (Ter Maaten et al., 2018). In addition to this, delaying frontal advancement (albeit in unicoronal synostosis), has been shown to minimise relapse rates and the need for readvancement surgery, therefore reducing overall surgical burden (Selber et al., 2008). This study showed a 50% reduction in the need for FOA following PVDO as compared to PCVR; the reasons for this are difficult to ascertain. It may be due to the gradual expansion of the posterior fossa allowing for a gradual expansion of the anterior fossa. This is in line with ter Maaten et al. who used Newton's Third Law of Motion, where every action has an equal and opposite reaction as the explanation (Ter Maaten et al., 2018). Equally the follow up period is shorter for the PVDO patients, as PVDO is a more recently adopted procedure

and, therefore, these patients may go on to have FOA, but have not come to that point yet. When a further vault expanding procedure was required in the SAPVE cohort the posterior route was favoured again, with one requiring a further PCVR. Two SAPVE patients underwent later fronto-facial procedures.

7.5 Summary

This chapter presented a two centre study which compared PCVR, PVDO and SAPVE in 33 patients with either Apert or Crouzon syndrome. This is the first direct comparison of these three techniques in the literature. Both clinical and volumetric data have been reported and were similar across the three techniques. SAPVE was undertaken at an older age and required less blood to be transfused. All techniques achieved a similar percentage ICV increase. Fewer PVDO and SAPVE patients went on to require FOA at a later date. PVDO and SAPVE may cause less overall surgical trauma as evidenced by the reduced blood transfusion requirement and the reduced need for later FOA.

Whilst providing novel data, this study is not without its limitations. It is challenging to compare techniques between centers and within a center over time since the surgeries are not done in isolation but as part of protocolised care. Protocolised care which in this study differs between institutions. Although exclusion criteria were used to minimise confounding from age or diagnosis, this study has a number of limitations that prevent direct comparison. It falls foul of the low subject numbers available when studying rare diseases and is hindered by the markedly different healthcare systems of the two institutions. To minimise confounding, patient cohorts were limited to less than two years of age at time of surgery and growth curves were used to control for early skull

growth. However, these corrected values are only valid if the patients in our cohorts follow the same growth as the unoperated cases used to create the curve. SAPVE use following an expectant approach to the treatment of ICP, whereas PVDO and PCVR were part of a prophylactic approach. PCVR vs PVDO use was not randomised, so there may have been a selection bias for each technique. These variabilities prevent reliable, direct comparison between the three techniques in terms of quantitative skull changes and need for secondary surgeries.

Overall, this study demonstrates that safe and effective treatment of intracranial volume and pressure in young syndromic patients can be achieved following either an expectant or prophylactic approach using one of the three studied posterior vault expansion techniques.

Chapter 8 **CONCLUSIONS**

The main themes, findings, and outcomes from the thesis are summarised in this chapter. The previous chapters are drawn upon to describe how the application of novel volume measurement techniques, collation of normative data and international collaborative work has contributed towards our understanding of cranial vault expansion. Further to this, the limitations of the study are also discussed, as well as suggestions for future research and final comments.

8.1 Overview

The aim of this thesis was to combine 3D volumetric measurement techniques with clinical data, thereby improving the understanding of how craniosynostosis affects intracranial pressure, and how cranial vault expansion can best be used to overcome this dangerous clinical situation. This work has shown that it is possible to automate ICV measurement, saving time and reducing bias. Utilising these techniques allowed for the creation of syndrome specific ICV and OFC growth curves which can be used to normalise for growth when assessing volumetric changes of the cranial vault in craniofacial surgery. Cranial vault expansion by a number of different techniques has been shown to be a safe and effective way to increase ICV and reduce ICP. It is hoped that this research will bolster clinical decision making, improve surgical outcomes and ultimately have a positive impact on patients' quality of life.

The first objective was to determine the optimal method of measuring intracranial volume and assess what data was needed to provide accurate measurements. Establishing objective one would give the tools necessary to achieve objective two: the generation of ICV growth curves for control patients and patients with craniofacial syndromes. This

was done using the depository of imaging for unaffected children and craniofacial patients yet to undergo surgery at GOSH. The third and final objective was to understand the most advantageous ICV increase and the most appropriate surgical means to achieve it.

8.2 Detailed outcomes

8.2.1 Chapter 3 – Intracranial volume measurement

Three different ICV measurement techniques were assessed including manual, semi-automatic and fully-automatic methods. When measuring ICV in the setting of craniosynostosis, each technique was shown to give similar results. Manual and semi-automatic techniques provide varying degrees of user control whilst a fully automatic technique performs ICV calculation through command line instructions alone. The fully automatic method has the advantage of being faster to use and runs to a strict pipeline, both advantageous factors when analysing large datasets. In the setting of rare disease such as the craniosynostosis syndromes, large data sets are difficult to acquire. Multi-unit collaboration could be an answer to this; however as seen when analysing imaging from peripheral hospitals some data sets contain suboptimal numbers of slices per scan. The comparison of CT scans with full, half, quarter and an eighth number of slices showed that the linear relationship between full and an eighth of the number of slices remains high, but that the limits of agreement increase with a decreasing number of slices. To summarise:

1. Similar results can be obtained using manual, semi-automatic or automatic techniques with decreasing amount of time taken to perform each method

2. Images acquired at different units can be used to form large datasets; however, one must be aware that limits of agreement increase with a decreasing number of slices

8.2.2 Chapter 4 – Intracranial volume and head circumference

In chapter 4, reference ICV and OFC growth curves for unoperated children with syndromic craniosynostosis, as well as a control group were created. The growth curves, whilst interesting in their own right for confirming children with Apert syndrome to have larger intracranial volumes, also provide syndrome specific equations to allow researchers to adjust for growth between two timepoints, such as pre and post-operative CT scans. This chapter also provided further evidence to show that OFC can be used as a rapid clinical tool to estimate ICV. Allowing clinicians to assess whether a patient's growth curve is deflecting from the norm, and, therefore, indicating a potential source of raised ICP.

8.2.3 Chapter 5 – Spring assisted posterior vault expansion

In chapter 5, the syndrome specific growth curves created in the previous chapter were used to normalise volumetric data as part of a larger, detailed, retrospective clinical analysis of all SAPVE cases undertaken at GOSH. The operative technique and spring design used at GOSH were detailed and explained. Results showed that the majority of patients underwent SAPVE to treat raised ICP, and this was done successfully. A minority underwent SAPVE for correction of abnormal head shape. Significant increases in ICV were achieved by SAPVE when undertaken at any age and in any diagnosis. Larger absolute and percentage volume increases were achieved when SAPVE was undertaken

at an earlier age. Patients who required their first SAPVE at a younger age and those with Apert or Crouzon-Pfeiffer syndrome were significantly more likely to require a repeat PVE. Comparison of patients requiring a single or two SAPVE showed no difference in percentage ICV increase. This would suggest that age at first procedure and syndromic diagnosis are more important factors in deciding which patients will require a repeat procedure. In summary, this chapter showed that:

1. At GOSH most SAPVE were undertaken to ameliorate raised ICP
2. Mean age at spring insertion was 20.6 months
3. 20% of patients had additional procedures at the time of spring removal with the majority being FOA
4. Most patients completed their SAPVE journey with no complications, where complications occurred, they were mostly surgical site infections with 17 patients requiring earlier than planned removal of springs
5. 19 patients required a repeat vault expanding procedure and these were more likely to be patients in zero-one age group at first procedure
6. Patients with Apert syndrome were the most likely to require repeat expansion
7. Mean percentage ICV increase due to SAPVE was 19.1%
8. Age at first SAPVE and syndromic diagnosis appear to be the most important factors in whether or not a patient will require a repeat PVE.

8.2.4 Chapter 6 – Optic nerve sheath diameter: Relationship to ICV and potential use as a non-invasive measure of intracranial pressure

Chapter 6 investigated the potential use of ONSD as a proxy for invasive measurement of ICP in children with craniosynostosis. It also attempted to correlate the

post-operative change in ONSD to the ICV change achieved through SAPVE. 148 pre and post-operative ONSD measurements and 74 pre and post-operative ICV measurements were performed. Invasive ICP monitoring results were available for 11 of the 75 patients studied. In patients undergoing SAPVE to reduced raised ICP and over the age of one at time of surgery, a significant post-operative decrease in ONSD was observed. A decrease in ONSD was also observed in the patients under the age of one at SAPVE however this did not reach significance. Ten out of 11 patients with concomitant ONSD measurements and invasive ICP monitoring results showed agreement when using thresholds for raised ICP of 4mm for those patients under one year, over 4.5mm for one to four-year-old patients and over 5mm for patients over four years of age. No significant correlation was seen between the relative or absolute volume increase and the relative or absolute change in ONSD following SAPVE. In summary:

1. Following SAPVE a significant reduction in ONSD was seen
2. ONSD measurements were in agreement with invasively monitored ICP results in ten out of the eleven patients studied
3. No significant correlation was seen between ONSD change and ICV change

8.2.5 Chapter 7 – A two centre comparison of three techniques for posterior vault expansion in syndromic craniosynostosis

Chapter 7 took a direct approach to comparison of three different surgical techniques used to expand the cranial vault. This was achieved through a two centre collaborative project between GOSH and SCH. Patients with Apert or Crouzon syndrome undergoing SAPVE, PCVR or PVDO were analysed and compared from a clinical and a volumetric perspective. Broadly speaking, clinical and volumetric results were similar

across the three groups, however SAPVE was found to be undertaken at an older age and to require less blood to be transfused. PVDO also required less blood to be transfused however this did not reach significance, although it would indicate reduced surgical trauma from the dynamic techniques. There was no significant difference in length of inpatient hospital or ICV expansion. All PCVR patients and 50% of PVDO patients underwent FOA at a later date. 1 SAPVE patient (7%) required further vault expanding surgery by means of a PCVR and two went on to have fronto-facial procedures 8 years following their initial SAPVE. To summarise:

1. Clinical and volumetric results were similar across the three groups
2. SAPVE is undertaken at a significantly older age in Crouzon children
3. SAPVE required significantly less blood to be transfused than PCVR and PVDO
4. Fewer PVDO and SAPVE patients required further vault expanding procedures

8.3 Limitations and future directions

8.3.1 Sample size and data

In any single centre study of rare syndromes, small sample sizes are a limitation. This was experienced when using the GOSH data for Chapters 3 to 6. Despite attempting to overcome this by expanding the study to include data from SCH in Chapter 7, the sample size remained small. To provide further evidence for the findings in this thesis would require prospective large-cohort studies and overall standardisation of data acquisition protocols. This would necessitate large scale sharing of information across international boundaries, which in itself holds data sharing problems. Chapter 3 has shown that CT scan data with reduced sampling rate can be useful and should, therefore,

not be excluded. Combining multi-centre data and including data with a reduced sample rate could facilitate the suggested larger-scale studies.

An added difficult to the rarity of the syndromes and therefore small sample size studied here is the reliance on data produced by ionising CT scans and the understandably conservative imaging protocols followed by most craniofacial institutions. Exposure to ionising radiation is kept to a minimum with CT scans taken preoperatively to aid surgical assessment and planning, but at GOSH, follow-up CT scans are often not taken unless complications arise or it is thought that the patient may require further surgery, thus skewing our data set. The lack of follow up imaging or an unacceptable time lag between operative procedure and post-operative imaging led to the exclusion of a number of patients. The advent of ultra-low dose 3D CT scanning and black bone MRI protocols could ameliorate these problems (Eley, Watt-Smith, Sheerin, & Golding, 2014). However, the problem of repeated general anaesthesia in the developing child remains. Volumetric studies using 3D surface scans have been performed, they have a fast acquisition time and good patient compliance; unfortunately they cannot generate ICV, but rather generate an overall head volume (Beaumont et al., 2017).

Throughout this thesis, patients with various craniofacial syndromes were investigated. Children with Apert syndrome were included throughout. Chapters 4, 5 and 6 widened the scope of syndromes studied by including all patients undergoing cranial vault expansion. Patients were grouped by diagnosis where possible; however, with some of the syndromes studied being very rare, a cohort of ‘other’ diagnoses was created.

8.3.2Limitations

In addition to sample size, there were a number of other limitations to this study. The mixed 'other' cohort contained a range of different syndromes and therefore a heterogenous cohort. This alongside the wide spectrum of phenotypes within the other diagnoses undoubtably leads to a degree of error within the chapters. Children with Apert syndrome were studied throughout this thesis, they were included as one cohort and not divided into the two main genetic cohorts of Ser252Trp or Pro253Arg, given the phenotypic variation shown by these diagnoses this presents a further limitation to the work presented. Unfortunately, this then flows through from chapter 4 in the growth normalisation equations used to estimate growth volume. 7% of patients studied in chapter 4 later required a shunt procedure to treat hydrocephalus, they were not excluded from the data collection, nor were those patients whose CT scan showed a degree of hydrocephalus. The growth curves may therefore have been skewed by the presence of hydrocephalus. Chapter 7 illustrated the limitation of using growth curves to normalise for growth between operation and post-operative CT scan. One patient returned a negative ICV expansion following PVDO. This patient was very young at the time of their first CT scan, suggesting a severe phenotype and had a considerable (given their age at presentation) time lag between their preoperative imaging and PVDO. The rapid increase in ICV of the neonatal calvarium appears to be accounted for poorly by the chapter 4 growth curves. This is due to the limited number of data points in very young patients.

The variability in surgical technique must be taken into account. Chapter 7 purposefully compared different surgical techniques; however, there were variations in surgical techniques used within the separate procedural cohorts. This is driven by patient

(syndrome, severity of syndromic features) and operator characteristics. Craniofacial teams are large in terms of multidisciplinary members but contain few surgeons, who, whilst mostly following similar techniques will certainly have a degree of difference in their surgical methodology. To include the greatest number of subjects all operating surgeons were included.

The clinical data used in chapters 5 and 7 was taken from hospital records. Analysis of this data was performed diligently; however, it is limited by the accuracy of the primary recording.

8.4 Conclusions

The principal aim of this thesis was to provide an understanding of whether cranial vault expansion lowers ICP and use this understanding to provide information as to the optimal patient specific volume expansion, thereby improving surgical outcomes and patient quality of life. A multidisciplinary, two centred approach to achieving this aim has been presented. In the over ones, cranial vault expansion has been shown to reduce ONSD in patients with syndromic craniosynostosis and through this, it is inferred that cranial vault expansion lowers ICP. By studying 172 SAPVE cases, age at first SAPVE and syndromic diagnosis are important factors in whether or not a patient will require a repeat PVE. SAPVE required significantly less blood to be transfused than PCVR and PVDO, however differing operative protocols at the two institutions studied nullify this finding. Both SAPVE and PVDO required fewer secondary vault expanding procedures. The heterogenicity of the syndromes studied makes providing patient specific suggestions difficult, however it appears that postponing first vault expansion until the patient is over

the age of one year may reduce the need for further cranial vault expansion. It is of course not always possible or safe to defer vault expanding surgery until a patient is over one year of age. Raised ICP is known to have a detrimental effect on the optic nerve. When children with syndromic craniosynostosis show obvious signs of raised ICP they are operated on (after the exclusion of hydrocephalus and airway occlusion) to alleviate this. Insidiously raised ICP may well also have a deleterious effect on the optic nerve and it is for this reason that many craniofacial centres opt for prophylactic vault expansion in these patients. Given the findings of chapters 5 and 7, PVE is a relatively safe procedure whether undertaken by SAPVE, PVDO or PCVR. It would therefore seem sensible to offer a prophylactic vault expansion before the age of one year, in the knowledge that a second (as evidenced by the findings in chapter 5), cranial vault expanding procedure is likely to be required at a later date. Having this evidence will aid in the counselling of parents and in the planning of the patients' surgical journey. The data provided in this thesis could also be used to prewarn clinicians of those patients at risk for early and / or repeated vault expanding procedure and council family accordingly. The microscopic effect of insidiously raised ICP on the optic nerve is at present unknown. Animal models could be employed to assess damage caused and potentially add weight to the recommendation of early surgery.

That raised ICP can be treated successfully through expansion of the cranial vault cannot be explained by volume expansion alone. This is indicated by the fact that children with Apert syndrome are as likely as other children with craniosynostosis to suffer from raised ICP, despite having significantly larger intracranial volumes. Further work is required here. Firstly, studies in which the Apert cohort is subdivided into those children with Ser252Trp or Pro253Arg mutations is needed. These studies could include

volumetric work as well as clinical review, both in an attempt to illustrate which patients benefit most from PVE and at what age they are likely to require it. Given the data collected during this work, these studies are intended to follow on from this thesis. Secondly, it would be of great interest to know what the constitutes the brain volume of children with syndromic craniosynostosis. Children with Apert syndrome present with such a markedly larger ICV, what is it that fills this volume? Further work to delineate the brain volume into grey matter, white matter and CSF is possible using similar automated ICV calculating tools described in chapter 3. It will be interesting to see if, and how the distribution of these constituents changes following cranial vault expansion. Thirdly, further work into non-invasive methods of measuring ICP in children is required. The use of ONSD via ocular ultrasound is widely published in the adult population, however this may not be practical in paediatric patients, a study to further investigate the practicality of this would be of great use, as ONSD measurements via ocular ultrasound could provide immediate, non-invasive proxy ICP measurements. Currently ONSD as measured from CT imaging is more suited to being a research tool.

The title of this thesis asked, 'What volume increase is needed for the management of raised intracranial pressure in children with craniosynostosis?', whilst an increase in ICV does appear to allow the ICP to reduce, the reasons for that reduction are not clear and I don't believe an answer to that question can be inferred from this work. The percentage increase in ICV did not appear to alter the efficacy of cranial vault expansion. To my mind there is a degree of splinting of the intracranial contents which is released by the expansion of the calvarium, this may then allow CSF or blood to flow out of the cranial vault more freely. This is another exciting area for future research. In 2001 Taylor et al. investigated children with syndromic craniosynostosis and showed that in 18

angiography studies either a 51 to 99% stenosis, or no flow at all could be observed in the sigmoid–jugular sinus complex bilaterally or unilaterally (Taylor et al., 2001). The proposed 'splinting' of the intracranial contents may have led to this aberrant venous drainage (and may also force the formation of collateral venous networks found in children with syndromic craniosynostosis) and following cranial vault expansion, the relaxion of the tissues allows for normal flow to resume. A follow up study to that of Taylor et al. investigating venous outflow pre and post-operatively may help validate this thinking. Arterial spin labelling could be used to assess cerebral blood flow in these children which may be a more powerful methodology that an angiogram study. Whether or not the morphology of the skull base changes post PVE would make an interesting additional study. The diameter of the jugular foramen has been shown to be reduced in children with syndromic craniosynostosis (De Jong et al., 2015), but the shape of the jugular foramen could also be different and this may have an effect on venous outflow, a study to investigate this would be of intrigue.

Chapter 7 investigated three different surgical techniques and found them to offer mostly similar results. Given these findings perhaps it is now possible for the surgical team to recommend surgical technique based on patient parameters. In an older child who has progressed through their first 2 years without needing PVE and may not need as much ICV expansion, a traditional PCVR can be offered. When not trying to achieve large ICV increases, skin closure becomes less of an issue and the child will only require one procedure. In younger children, one of the dynamic techniques could be employed. PVDO and SAPVE require less blood transfusion and are technically less traumatic, they will require a device removal procedure, however this could be combined with a FOA to avoid the need for further vault expansion. The control in both expansion velocity and

vector afforded by the distractors makes them an attractive technique, future device development could focus on fully covered and resorbable distractors that utilise external activators or make use of the body's natural fluid in a similar way to osmotic implants used in breast surgery, whether or not this is possible or feasible would be of great interest to discover. That the springs are intended to remain fully covered make them an attractive device also. Future design could focus on spring materials with less aggressive opening speeds, which would allow for a gradual expansion. This would more closely mirror the dynamics of the distractors. In essence however, both of the dynamic techniques achieve similar results (in this work), and the best outcome most likely comes from a well-practiced surgeon using the technique that they are most familiar with. If that surgeon or surgical team have all three techniques in their armamentarium then they are well placed to discuss the benefits and disadvantages of each with the patient's family, delivering a greater degree of patient / parent choice into this difficult clinical decision making process.

To conclude, this thesis has provided a freely available technique to automatically calculate ICV, usable equations to normalise ICV growth between two time points, syndrome specific OFC and ICV correlations, an in depth clinical and volumetric analysis of all SAPVE cases undertaken at GOSH, an investigation into the use of ONSD as a marker for ICP and a two centred, three technique comparison of cranial vault expansion. The suggestions made within can influence surgical and clinical decision making, improve family and surgeon dialogue both of which it is hoped will ultimately improve patient quality of life.

REFERENCES

Abbott, A., Netherway, D., Niemann, D., Clark, B., Yamamoto, M., Cole, J., … David, D. (2000). CT Determined Intracranial Volume for a Normal Population. *Journal of Craniofacial Surgery*.

Abu-Sittah, G. S., Jeelani, O., Dunaway, D., & Hayward, R. (2016). Raised intracranial pressure in Crouzon Syndrome: incidence, causes and management. *Journal of Neurosurgery. Pediatrics*, *17*(9), 469–475. https://doi.org/DOI: 10.3171/2015.6.PEDS15177.

Alperin, N. J., Lee, S. H., Loth, F., Raksin, P. B., & Lichtor, T. (2000). MR-intracranial pressure (ICP): A method to measure intracranial elastance and pressure noninvasively by means of MR imaging: Baboon and human study. *Radiology*, *217*(3), 877–885. https://doi.org/10.1148/radiology.217.3.r00dc42877

Anderson, P. J., Netherway, D. J., Abbott, A. H., Cox, T., Roscioli, T., & David, D. J. (2004). Analysis of intracranial volume in Apert syndrome genotypes. *Pediatric Neurosurgery*, *40*(4), 161–164. https://doi.org/10.1159/000081933

Apert, E. (1906). De l'acrocephalosyndactalie. *Bull Soc Med Hop Paris*, *23*, 1310.

Arab, K., Fischer, S., Bahtti-Softeland, M., Maltese, G., Kolby, L., & Tarnow, P. (2016). Comparison Between Two Different Isolated Craniosynostosis Techniques: Does It Affect Cranial Bone Growth? *The Journal of Craniofacial Surgery*, *27*(5), e454-7. https://doi.org/10.1097/SCS.0000000000002769

Arnaud, E., Marchac, A., Jeblaoui, Y., Renier, D., & Di Rocco, F. (2012). Spring-assisted posterior skull expansion without osteotomies. *Child's Nervous System*, *28*, 1545–1549. https://doi.org/10.1007/s00381-012-1843-4

Avery, R. A., Shah, S. S., Licht, D. J., Seiden, J. A., Huh, J. W., Boswinkel, J., … Liu, G. T. (2010). Reference range for cerebrospinal fluid opening pressure in children. *The New England Journal of Medicine*, *363*(9), 891–893. https://doi.org/10.1056/NEJMc1004957

Ballantyne, J., Hollman, A. S., Hamilton, R., Bradnam, M. S., Carachi, R., Young, D. G., & Dutton, G. N. (1999). Transorbital optic nerve sheath ultrasonography in

normal children. *Clinical Radiology*, *54*(11), 740–742. https://doi.org/10.1016/S0009-9260(99)91176-5

Beaumont, C. A. A., Knoops, P. G. M., Borghi, A., Jeelani, N. U. O., Koudstaal, M. J., Schievano, S., … Rodriguez-Florez, N. (2017). Three-dimensional surface scanners compared with standard anthropometric measurements for head shape. *Journal of Cranio-Maxillofacial Surgery*, *45*(6), 921–927. https://doi.org/10.1016/j.jcms.2017.03.003

Bekerman, I., Sigal, T., Kimiagar, I., Ben Ely, A., & Vaiman, M. (2016). The quantitative evaluation of intracranial pressure by optic nerve sheath diameter/eye diameter CT measurement. *American Journal of Emergency Medicine*, *34*(12), 2336–2342. https://doi.org/10.1016/j.ajem.2016.08.045

Bradley, J. ., Shahinian, H., Levine, J. P., Rowe, N., & Longaker, M. T. (2000). Growth restriction of cranial sutures in the fetal lamb causes deformational changes, not craniosynostosis. *Plastic and Reconstructive Surgery*, *105*(7), 2416–2423. Retrieved from http://ovidsp.ovid.com/ovidweb.cgi?T=JS&PAGE=reference&D=emed5&NEWS=N&AN=2000202868

Bray, P. F., Shields, D. W., Wolcott, G. J., & Madsen, J. A. (1969). Occipitofrontal head measure of intracranial. *The Journal of Pediatrics*, *75*(2), 303–305.

Breakey, W., Knoops, P. G. M., Borghi, A., Rodriguez-Florez, N., Dunaway, D. J., Schievano, S., & Jeelani, O. N. U. (2017). Intracranial Volume Measurement: A Systematic Review and Comparison of Different Techniques. *Journal of Craniofacial Surgery*, *28*(7). https://doi.org/10.1097/SCS.0000000000003929

Breik, O., Mahindu, A., Moore, M. H., Molloy, C. J., Santoreneos, S., & David, D. J. (2016). Apert syndrome: Surgical outcomes and perspectives. *Journal of Cranio-Maxillofacial Surgery*. https://doi.org/10.1016/j.jcms.2016.06.001

Brueton, L. A., Herwerden, L. Van, Chotai, K. A., & Winter, R. M. (1992). The mapping of a gene for craniosynostosis : evidence for linkage of the Saethre-

Chotzen syndrome to distal chromosome 7p. *J Med Genet*, *29*(Acs Iii), 681–685. https://doi.org/10.1136/jmg.29.10.681

Carinci, F., Pezzetti, F., Locci, P., Becchetti, E., Carls, F., Avantaggiato, A., … Bodo, M. (2005). Apert and Crouzon Syndromes: Clinical Findings, Genes and Extracellular Matrix. *Journal of Craniofacial Surgery*, *16*(3), 361–368. https://doi.org/10.1097/01.SCS.0000157078.53871.11

Choi, M., Flores, R. L., & Havlik, R. J. (2012). Volumetric Analysis of Anterior Versus Posterior Cranial Vault Expansion in Patients With Syndromic Craniosynostosis. *Journal of Craniofacial Surgery*, *23*(2), 455–458. https://doi.org/10.1097/SCS.0b013e318240ff49

Cinalli, G, Renier, D., Sebag, G., Sainte-Rose, C., Arnaud, E., & Pierre-Kahn, a. (1995). Chronic tonsillar herniation in Crouzon's and Apert's syndromes: the role of premature synostosis of the lambdoid suture. *Journal of Neurosurgery*, *83*(4), 575–582. https://doi.org/10.3171/jns.1995.83.4.0575

Cinalli, G, Sainte-Rose, C., Kollar, E. M., Zerah, M., Brunelle, F., Chumas, P., … Renier, D. (1998). Hydrocephalus and craniosynostosis. *Journal of Neurosurgery*, *88*(2), 209–214. https://doi.org/10.3171/jns.1998.88.2.0209

Cinalli, Giuseppe, Spennato, P., Sainte-Rose, C., Arnaud, E., Aliberti, F., Brunelle, F., … Renier, D. (2005). Chiari malformation in craniosynostosis. *Child's Nervous System*, *21*(10), 889–901. https://doi.org/10.1007/s00381-004-1115-z

Cohen, M M, & Kreiborg, S. (1996). A clinical study of the craniofacial features in Apert syndrome. *International Journal of Oral and Maxillofacial Surgery*, *25*(1), 45–53. https://doi.org/10.1016/S0901-5027(96)80011-7

Cohen, M Michael. (1993). Pfeiffer Syndrome Up date , Clinic Subtypes , and Guidelines for Differential Diagnosis. *American Journal of Medical Genetics*, *307*.

Cohen, M Michael, Kreiborg, S., Lammer, E. J., Cordero, J. F., Mastroiacovo, P., Erickson, J. D., … Martínez-Frías, M. L. (1992). Birth prevalence study of the apert syndrome. *American Journal of Medical Genetics Part A*, *42*(5), 655–659.

https://doi.org/10.1002/ajmg.1320450322

Collmann, H., Sörensen, N., & Krauß, J. (2005). Hydrocephalus in craniosynostosis: A review. *Child's Nervous System*, *21*(10), 902–912. https://doi.org/10.1007/s00381-004-1116-y

Cornejo-Roldan, L. R., Roessler, E., & Muenke, M. (1999). Analysis of the mutational spectrum of the FGFR2 gene in Pfeiffer syndrome. *Human Genetics*, *104*(5), 425–431. https://doi.org/10.1007/s004390050979

Costa, M. A., Ackerman, L. L., Tholpady, S. S., Greathouse, S. T., Tahiri, Y., & Flores, R. L. (2015). Spring-assisted cranial vault expansion in the setting of multisutural craniosynostosis and anomalous venous drainage: Case report. *Journal of Neurosurgery: Pediatrics*, *16*(1), 80–85. https://doi.org/10.3171/2014.12.PEDS14604

Cunningham, M. L., Seto, M. L., Ratisoontorn, C., Heike, C. L., & Hing, A. V. (2007). Syndromic craniosynostosis: From history to hydrogen bonds. *Orthodontics and Craniofacial Research*, *10*(2), 67–81. https://doi.org/10.1111/j.1601-6343.2007.00389.x

Czerwinski, M., Kolar, J. C., & Fearon, J. a. (2011). Complex craniosynostosis. *Plastic and Reconstructive Surgery*, *128*(4), 955–961. https://doi.org/10.1097/PRS.0b013e3182268ca6

De Jong, T., Rijken, B. F. M., Lequin, M. H., Van Veelen, M. L. C., & Mathijssen, I. M. J. (2012). Brain and ventricular volume in patients with syndromic and complex craniosynostosis. *Child's Nervous System*, *28*(1), 137–140. https://doi.org/10.1007/s00381-011-1614-7

De Jong, T., Rijken, B. F. M. M., Lequin, M. H., van Veelen, M.-L. L. C., Mathijssen, I. M. J. J., Fearon, J. A., … Johnson, D. (2015). Venous hypertension in syndromic and complex craniosynostosis: The abnormal anatomy of the jugular foramen and collaterals. *Plastic and Reconstructive Surgery*, *122*(1), 312–318. https://doi.org/10.1097/PRS.0b013e3181845a92

De Jong, T., Van Veelen, M. L. C., & Mathijssen, I. M. J. (2013). Spring-assisted posterior vault expansion in multisuture craniosynostosis. *Child's Nervous System*, *29*, 815–820. https://doi.org/10.1007/s00381-013-2033-8

Derderian, C. A., Bastidas, N., & Bartlett, S. P. (2012). Posterior cranial vault expansion using distraction osteogenesis. *Child's Nervous System*, *28*(9), 1551–1556. https://doi.org/10.1007/s00381-012-1802-0

Derderian, C. A., & Seaward, J. (2012). Syndromic Craniosynostosis. *Seminars in Plastic Surgery*, *26*, 64–75. https://doi.org/10.1016/j.fsc.2016.06.008

Derderian, C. A., Wink, J. D., McGrath, J. L., Collinsworth, A., Bartlett, S. P., & Taylor, J. A. (2015). Volumetric Changes in Cranial Vault Expansion. *Plastic and Reconstructive Surgery*, *135*(6), 1665–1672. https://doi.org/10.1097/PRS.0000000000001294

Dinomais, M., Celle, S., Duval, G. T., Roche, F., Henni, S., Bartha, R., … Annweiler, C. (2016). Anatomic Correlation of the Mini-Mental State Examination: A Voxel-Based Morphometric Study in Older Adults. *PloS One*, *11*(10), e0162889. https://doi.org/10.1371/journal.pone.0162889

Dominique Renier, M.D., Christian Sainte-Rose, M.D., Daniel Marchac, M.D., and Jean-Francois Hirsch, M. D. (1982a). Intracranial pressure changes in craniostenosis. *J*, *57*(9), 370–377. https://doi.org/10.3171/jns.1982.57.3.0370

Dominique Renier, M.D., Christian Sainte-Rose, M.D., Daniel Marchac, M.D., and Jean-Francois Hirsch, M. D. (1982b). Intracranial pressure in craniostenosis. *J Neurosurg*, *57*(9), 370–377. https://doi.org/10.3171/jns.1982.57.3.0370

Driessen, C., Bannink, N., Lequin, M., van Veelen, M.-L. C., Naus, N. C., Joosten, K. F. M., & Mathijssen, I. M. J. (2011). Are ultrasonography measurements of optic nerve sheath diameter an alternative to funduscopy in children with syndromic craniosynostosis? *Journal of Neurosurgery. Pediatrics*, *8*(September), 329–334. https://doi.org/10.3171/2011.6.PEDS10547

Driessen, C., Joosten, K. F. M., Bannink, N., Bredero-Boelhouwer, H. H., Hoeve, H. L.

J., Wolvius, E. B., … Mathijssen, I. M. J. (2013). How does obstructive sleep apnoea evolve in syndromic craniosynostosis? A prospective cohort study. *Archives of Disease in Childhood*, *98*(7), 538–543. https://doi.org/10.1136/archdischild-2012-302745

Edler, R., Abd Rahim, M., Wertheim, D., & Greenhill, D. (2010). The use of facial anthropometrics in aesthetic assessment. *Cleft Palate-Craniofacial Journal*. https://doi.org/10.1597/08-218.1

Eide, P. K., Helseth, E., Due-Tønnessen, B., & Lundar, T. (2002). Assessment of continuous intracranial pressure recordings in childhood craniosynostosis. *Pediatric Neurosurgery*, *37*(6), 310–320. https://doi.org/10.1159/000066311

el Ghouzzi, V., Le Merrer, M., Perrin-Schmitt, F., Lajeunie, E., Benit, P., Renier, D., … Bonaventure, J. (1997). Mutations of the TWIST gene in the Saethre-Chotzen syndrome. *Nature Genetics*, *15*(1), 42–46. https://doi.org/10.1038/ng0197-42

Eley, K. A., Watt-Smith, S. R., Sheerin, F., & Golding, S. J. (2014). "Black Bone" MRI: a potential alternative to CT with three-dimensional reconstruction of the craniofacial skeleton in the diagnosis of craniosynostosis. *European Radiology*, *24*(10), 2417–2426. https://doi.org/10.1007/s00330-014-3286-7

Evans, J. D. (1996). *Straightforward statistics for the behavioural sciences. Pacific Grove, CA: Brooks/Cole Publishing*. Pacific Grove, CA: Brooks/Cole Publishing.

Faro, C., Benoit, B., Wegrzyn, P., Chaoui, R., & Nicolaides, K. H. (2005). Three-dimensional sonographic description of the fetal frontal bones and metopic suture. *Ultrasound in Obstetrics and Gynecology*, *26*(6), 618–621. https://doi.org/10.1002/uog.1997

Fearon, J. A. (2014). Evidence-Based Medicine: Craniosynostosis. *Plastic and Reconstructive Surgery*, *133*(5), 1261–1275. https://doi.org/10.1097/PRS.0000000000000093

Fearon, J. A., Kolar, J. C., & Munro, I. R. (1996). Trigonocephaly-associated hypoterlorism: Is treatment necessary? *Plastic and Resconstructive Surgery*.

Florisson, J. M. G., Barmpalios, G., Lequin, M., Van Veelen, M. L. C., Bannink, N., Hayward, R. D., & Mathijssen, I. M. J. (2015). Venous hypertension in syndromic and complex craniosynostosis: The abnormal anatomy of the jugular foramen and collaterals. *Journal of Cranio-Maxillofacial Surgery*, *43*(3), 312–318. https://doi.org/10.1016/j.jcms.2014.11.023

Fok, H., Jones, B. M., Gault, D. G., Andar, U., & Hayward, R. (1992). Relationship between intracranial pressure and intracranial volume in craniosynostosis. *British Journal of Plastic Surgery*, *45*(5), 394–397. https://doi.org/10.1016/0007-1226(92)90013-N

Foo, R., Guo, Y., McDonald-McGinn, D. M., Zackai, E. H., Whitaker, L. a, & Bartlett, S. P. (2009). The natural history of patients treated for TWIST1-confirmed Saethre-Chotzen syndrome. *Plastic and Reconstructive Surgery*, *124*(6), 2085–2095. https://doi.org/10.1097/PRS.0b013e3181bf83ce

Forrest, C. R., & Hopper, R. A. (2013). Craniofacial Syndromes and Surgery. *Plastic and Reconstructive Surgery*, *131*(1), 86e-109e. https://doi.org/10.1097/PRS.0b013e318272c12b

Francisca, B., Rijken, M., Ottelander, B. K. Den, Veelen, M. C. Van, Lequin, M. H., Margreet, I., & Mathijssen, J. (2015). The occipitofrontal circumference: reliable prediction of the intracranial volume in children with syndromic and complex craniosynostosis. *Neurosurgical Focus*, *38*(5: E9), 1–6. https://doi.org/10.3171/2015.2.FOCUS14846.Disclosure

Gault, D., Brunelle, F., Renier, D., & Marchac, D. (1988). The calculation of intracranial volume using CT scans. *Child's Nervous System : ChNS : Official Journal of the International Society for Pediatric Neurosurgery*, *4*(5), 271–273. https://doi.org/10.1007/BF00271922

Gault, D. T., Renier, D., Marchac, D., & Jones, B. M. (1992). Intracranial pressure and intracranial volume in children with craniosynostosis. *Plastic and Reconstructive Surgery*. https://doi.org/10.1097/00006534-199209000-00003

Geeraerts, T., Newcombe, V. F., Coles, J. P., Abate, M., Perkes, I. E., Hutchinson, P. J., … Menon, D. K. (2008). Use of T2-weighted magnetic resonance imaging of the optic nerve sheath to detect raised intracranial pressure. *Critical Care*, *12*(5), R114. https://doi.org/10.1186/cc7006

Glass, G. E., O'Hara, J., Canham, N., Cilliers, D., Dunaway, D., Fenwick, A. L., … Wilson, L. C. (2019). ERF-related craniosynostosis: The phenotypic and developmental profile of a new craniosynostosis syndrome. *American Journal of Medical Genetics, Part A*, *179*(4), 615–627. https://doi.org/10.1002/ajmg.a.61073

Goldstein, J. a, Paliga, J. T., Wink, J. D., Low, D. W., Bartlett, S. P., & Taylor, J. a. (2013). A craniometric analysis of posterior cranial vault distraction osteogenesis. *Plastic and Reconstructive Surgery*, *131*, 1367–1375. https://doi.org/10.1097/PRS.0b013e31828bd541

Gosain, a K., McCarthy, J. G., Glatt, P., Staffenberg, D., & Hoffmann, R. G. (1995). A study of intracranial volume in Apert syndrome. *Plastic and Reconstructive Surgery*. https://doi.org/10.1097/00006534-199502000-00008

Govender, P. V, Nadvi, S. S., & Madaree, A. (1999). The Value of Transcranial Dopple Ultrasonography in Craniosynostosis. *The Journal of Craniofacial Surgery*, *10*(3), 260–263.

Governale, L. S. (2015). Craniosynostosis. *Pediatric Neurology*, *53*(5), 394–401. https://doi.org/10.1016/j.pediatrneurol.2015.07.006

Graham, J. M., deSaxe, M., & Smith, D. W. (1979). Sagittal craniostenosis: Fetal head constraint as one possible cause. *The Journal of Pediatrics*, *95*(5 PART 1), 747–750. https://doi.org/10.1016/S0022-3476(79)80728-3

Graham, J. M., & Smith, D. W. (1980). Metopic Craniostenosis as a Consequence of Fetal Head Constraint: Two Interesting Experiments of Nature. *Pediatrics*, *65*(5), 1000–1002.

Greene, A. K., Mulliken, J. B., Proctor, M. R., Meara, J. G., & Rogers, G. F. (2008). Phenotypically unusual combined craniosynostoses: presentation and management.

Plastic and Reconstructive Surgery, *122*, 853–862. https://doi.org/10.1097/PRS.0b013e31817f45f0

Greives, M. R., Ware, B. W., Tian, A. G., Taylor, J. A., Pollack, I. F., & Losee, J. E. (2015). Complications in Posterior Cranial Vault Distraction. *Annals of Plastic Surgery*, *76*(2), 211–215. https://doi.org/10.1097/SAP.0000000000000518

Hackshaw, A., Rodeck, C., & Boniface, S. (2011). Maternal smoking in pregnancy and birth defects: A systematic review based on 173 687 malformed cases and 11.7 million controls. *Human Reproduction Update*. https://doi.org/10.1093/humupd/dmr022

Haredy, M., Zuccoli, G., Tamber, M., Davis, A., Nischal, K., & Goldstein, J. A. (2018). Use of neuroimaging measurements of optic nerve sheath diameter to assess intracranial pressure in craniosynostosis. *Child's Nervous System*.

Hayward, R. (2005). Venous hypertension and craniosynostosis. *Child's Nervous System*, *21*(10), 880–888. https://doi.org/10.1007/s00381-004-1114-0

Hayward, R. D., Britto, J., Dunaway, D., & Jeelani, O. (2016). Connecting raised intracranial pressure and cognitive delay in craniosynostosis: many assumptions, little evidence. *J Neurosurg Pediatr May*, *Neurosurgi*(May 13), 1–9. https://doi.org/10.3171/2015.6.PEDS15374.

Hayward, Richard, & Gonsalez, S. (2005). How low can you go? Intracranial pressure, cerebral perfusion pressure, and respiratory obstruction in children with complex craniosynostosis. *Journal of Neurosurgery*, *102*(1 Suppl), 16–22. https://doi.org/10.3171/ped.2005.102.1.0016

Heer, I. M. de, Klein, A. de, Ouweland, A. M. van den, Vermeij-Keers, C., Wouters, C. H., Vaandrager, J. M., … Hoogeboom, J. M. (2004). Clinical and Genetic Analysis of Patients with Saethre-Chotzen Syndrome. *Plastic and Reconstrustive Surgery*, *115*(7), 1894–1902. https://doi.org/10.1097/01.PRS.0000165278.72168.51

Helmke, K., & Hansen, H. C. (1996). Fundamentals of transorbital sonographic: Evaluation of optic nerve sheath expansion under intracranial hypertension. II.

Patient study. *Pediatric Radiology*, *26*(10), 706–710. https://doi.org/10.1007/BF01383384

Herring, S. W. (2008). Mechanical Influences on Suture Biology. *Frontier in Oral Biology*, *12*, 41–56. https://doi.org/10.1159/0000115031.Mechanical

Honnebier, M. B., Cabiling, D. S., Hetlinger, M., McDonald-McGinn, D. M., Zackai, E. H., & Bartlett, S. P. (2008). The natural history of patients treated for FGFR3-associated (Muenke-type) craniosynostosis. *Plastic and Reconstructive Surgery*, *121*(3), 919–931. https://doi.org/10.1097/01.prs.0000299936.95276.24

Hopper, R. A., Kapadia, H., & Morton, T. (2013). Normalizing facial ratios in apert syndrome patients with le fort ii midface distraction and simultaneous zygomatic repositioning. *Plastic and Reconstructive Surgery*, *132*(1), 129–140. https://doi.org/10.1097/PRS.0b013e318290fa8a

Hott, J., & Rekate, H. L. (2014). *Intracranial Pressure*. *Encyclopedia of the Neurosurgical Sciences (Second Edition)*. https://doi.org/10.1016/j.cxom.2015.05.003

Ibrahimi, O. A., Zhang, F., Eliseenkova, A. V., Linhardt, R. J., & Mohammadi, M. (2004). Proline to arginine mutations in FGF receptors 1 and 3 result in Pfeiffer and Muenke craniosynostosis syndromes through enhancement of FGF binding affinity. *Human Molecular Genetics*, *13*(1), 69–78. https://doi.org/10.1093/hmg/ddh011

Ibrahimi, O. a, Chiu, E. S., McCarthy, J. G., & Mohammadi, M. (2005). Understanding the molecular basis of Apert syndrome. *Plastic and Reconstructive Surgery*, *115*(1), 264–270. https://doi.org/10.1097/01.PRS.0000146703.08958.95

Ilizarov, G. A. (1990). Clinical Application of the Tension-Stress Effect for Limb Lengthening. *Clinical Orthopaedics and Related Research*, *250*, 8–26.

Iseki, S., Wilkie, A. O. M., & Morriss-Kay, G. M. (1999). Fgfr1 and Fgfr2 have distinct differentiation- and proliferation-related roles in the developing mouse skull vault. *Development*, *126*(24), 5611–5620.

Jabs, E. W., Müller, U., Li, X., Ma, L., Luo, W., Haworth, I. S., … Maxson, R. (1993). A mutation in the homeodomain of the human MSX2 gene in a family affected with autosomal dominant craniosynostosis. *Cell*, *75*(3), 443–450. https://doi.org/10.1016/0092-8674(93)90379-5

Jacobi, A. (1894). NON NOCERE. *Med Rec*, *45*, 609–618.

Jane, J. A., Edgerton, M. T., Futrell, J. W., & Park, T. S. (1978). Immediate correction of sagittal synostosis. *Journal of Neurosurgery*, *49*(5), 705–710. https://doi.org/10.3171/jns.1978.49.5.0705

Jeelani, N. (2019). Spring-Assisted Distraction : Principles and Techniques. In C. Di Rocco, D. Pang, & J. Rutka (Eds.), *Textbook of Pediatric Neurosurgery* (pp. 1–15). Springer, Cham.

Jentink, J., Loane, M. A., Dolk, H., Barisic, I., Garne, E., Morris, J. K., & de Jong-van den Berg, L. T. W. (2010). Valproic acid monotherapy in pregnancy and major congenital malformations. *The New England Journal of Medicine*, *362*(23), 2185–2193. https://doi.org/10.1097/OGX.0b013e3182021f65

Johnson, D., Horsley, S. W., Moloney, D. M., Oldridge, M., Twigg, S. R. F., Walsh, S., … Wilkie, A. O. M. (1998). A comprehensive screen for TWIST mutations in patients with craniosynostosis identifies a new microdeletion syndrome of chromosome band 7p21.1. *American Journal of Human Genetics*, *63*(5), 1282–1293. https://doi.org/10.1086/302122

Johnson, D., & Wilkie, A. O. M. (2011). Craniosynostosis. *European Journal of Human Genetics*, *19*(4), 369–376. https://doi.org/10.1038/ejhg.2010.235

Jones, B. M. (2008). Paul Louis Tessier: Plastic Surgeon who revolutionised the treatment of facial deformity. *Journal of Plastic, Reconstructive & Aesthetic Surgery*, *61*(9), 1005–1007. https://doi.org/10.1016/j.bjps.2008.07.001

Kamdar, M. R., Gomez, R. A., & Ascherman, J. a. (2009). Intracranial volumes in a large series of healthy children. *Plastic and Reconstructive Surgery*, *124*(6), 2072–2075. https://doi.org/10.1097/PRS.0b013e3181bcefc4

Killer, H. E., Jaggi, G. P., Flammer, J., Miller, N. R., Huber, A. R., & Mironov, A. (2007). Cerebrospinal fluid dynamics between the intracranial and the subarachnoid space of the optic nerve. Is it always bidirectional? *Brain*, *130*(2), 514–520. https://doi.org/10.1093/brain/awl324

Kirschner, R. E., Gannon, F. H., Xu, J., Wang, J., Karmacharya, J., Bartlett, S. P., & Whitaker, L. a. (2002). Craniosynostosis and altered patterns of fetal TGF-beta expression induced by intrauterine constraint. *Plastic and Reconstructive Surgery*, *109*(7), 2338–2346; discussion 2347-2354.

Klingelhöfer, J., Conrad, B., Benecke, R., Sander, D., & Markakis, E. (1988). Evaluation of intracranial pressure from transcranial Doppler studies in cerebral disease. *Journal of Neurology*, *235*(3), 159–162. https://doi.org/10.1007/BF00314307

Lajeunie, E., Heuertz, S., El Ghouzzi, V., Martinovic, J., Renier, D., Le Merrer, M., & Bonaventure, J. (2006). Mutation screening in patients with syndromic craniosynostoses indicates that a limited number of recurrent FGFR2 mutations accounts for severe forms of Pfeiffer syndrome. *European Journal of Human Genetics*, *14*(3), 289–298. https://doi.org/10.1038/sj.ejhg.5201558

Lakin, G. E., Sinkin, J. C., Chen, R., Koltz, P. F., & Girotto, J. A. (2012). Genetic and epigenetic influences of twins on the pathogenesis of craniosynostosis: A meta-analysis. *Plastic and Reconstructive Surgery*, *129*(4), 945–954. https://doi.org/10.1097/PRS.0b013e31824422a8

Lane, L. (1892). Pioneer craniectomy for relief of mental imbecility due to premature sutural closure and microcephalus. *JAMA*, *18*, 49–50.

Lannelongue, M. (1890). De la craniectomie dans la microcephalie. *CR Acad Sci*, *110*, 1382–1385.

Lauritzen, C. G. K., Davis, C., Ivarsson, A., Sanger, C., & Hewitt, T. D. (2008). The evolving role of springs in craniofacial surgery: the first 100 clinical cases. *Plastic and Reconstructive Surgery*, *121*, 545–554.

https://doi.org/10.1097/01.prs.0000297638.76602.de

Lauritzen, C., Sugawara, Y., Kocabalkan, O., & Olsson, R. (1998). Spring mediated dynamic craniofacial reshaping. *Scandinavian Journal of Plastic and Reconstructive Surgery and Hand Surgery*, *32*(3), 331–338. https://doi.org/10.1080/02844319850158697

Leikola, J., Koljonen, V., Heliövaara, A., Hukki, J., & Koivikko, M. (2014). Cephalic index correlates poorly with intracranial volume in non-syndromic scaphocephalic patients. *Child's Nervous System*, *30*(12), 2097–2102. https://doi.org/10.1007/s00381-014-2456-x

Levitt, M. R., Niazi, T. N., Hopper, R. A., Ellenbogen, R. G., & Ojemann, J. G. (2012). Resolution of syndromic craniosynostosis-associated Chiari malformation Type I without suboccipital decompression after posterior cranial vault release. *Journal of Neurosurgery: Pediatrics*, *9*(2), 111–115. https://doi.org/10.3171/2011.11.peds11268

Liasis, A, Nischal, K. K., Leighton, S., Yap, S., Hayward, R., & Dunaway, D. Adenoid-tonsillectomy to treat visual dysfunction in a child with craniosynostosis. *Pediatric Neurosurgery*, *41*(4), 197–200. https://doi.org/10.1159/000086561

Liasis, Alki, Nischal, K. K., Walters, B., Thompson, D., Hardy, S., Towell, A., … Hayward, R. (2006). Monitoring visual function in children with syndromic craniosynostosis: a comparison of 3 methods. *Archives of Ophthalmology*, *124*, 1119–1126. https://doi.org/10.1001/archopht.124.8.1119

Liasis, Alki, Thompson, D. A., Hayward, R., & Nischal, K. K. (2003). Sustained raised intracranial pressure implicated only by pattern reversal visual evoked potentials after cranial vault expansion surgery. *Pediatric Neurosurgery*, *39*(2), 75–80. https://doi.org/10.1159/000071318

Mangasarian, K., Li, Y., Mansukhani, A., & Basilico, C. (1997). Mutation associated with crouzon syndrome causes ligand-independent dimerization and activation of FGF receptor-2. *Journal of Cellular Physiology*, *172*(1), 117–125.

https://doi.org/10.1002/(SICI)1097-4652(199707)172:1<117::AID-JCP13>3.0.CO;2-9

Marucci, D. D., Dunaway, D. J., Jones, B. M., & Hayward, R. D. (2008). Raised intracranial pressure in Apert syndrome. *Plastic and Reconstructive Surgery*, *122*(4), 1162–1168; discussion 1169-1170. https://doi.org/10.1097/PRS.0b013e31818458f0

McCarthy, J. G., Schreiber, J., Karp, N., Thorne, C. H., & Grayson, B. H. (1992). Lengthening the human mandible by gradual distraction. *Plastic and Reconstructive Surgery*. https://doi.org/10.1097/00006534-199289010-00001

McGraw, P. V., Winn, B., Gray, L. S., & Elliott, D. B. (2000). Improving the reliability of visual acuity measures in young children. *Ophthalmic and Physiological Optics*, *20*(3), 173–184. https://doi.org/10.1016/S0275-5408(99)00054-X

Mehta, V. A., Bettegowda, C., Jallo, G. I., & Ahn, E. S. (2010). The evolution of surgical management for craniosynostosis. *Neurosurgical Focus*, *29*(6), E5. https://doi.org/10.3171/2010.9.FOCUS10204

Mizutani, T., Manaka, S., & Tsutsumi, H. (1990). Estimation of intracranial pressure using computed tomography scan findings in patients with severe head injury. *Surgical Neurology*, *33*(3), 178–184. https://doi.org/10.1016/0090-3019(90)90181-N

Morris, L. (2016). Management of craniosynostosis. *Facial Plastic Surgery*, *32*(2/2016), 123–132. https://doi.org/10.1097/01.PRS.0000056839.94034.47

Muehlmann, M., Koerte, I. K., Laubender, R. P., Steffinger, D., Lehner, M., Peraud, A., … Ertl-Wagner, B. (2013). Magnetic resonance-based estimation of intracranial pressure correlates with ventriculoperitoneal shunt valve opening pressure setting in children with hydrocephalus. *Investigative Radiology*, *48*(7), 543–547. https://doi.org/10.1097/RLI.0b013e31828ad504

Muenke, M, Gripp, K. W., McDonald-McGinn, D. M., Gaudenz, K., Whitaker, L. a, Bartlett, S. P., … Wilkie, a O. (1997). A unique point mutation in the fibroblast

growth factor receptor 3 gene (FGFR3) defines a new craniosynostosis syndrome. *American Journal of Human Genetics*, *60*(3), 555–564. Retrieved from http://eutils.ncbi.nlm.nih.gov/entrez/eutils/elink.fcgi?dbfrom=pubmed&id=9042914&retmode=ref&cmd=prlinks%5Cnfile:///Users/Joel/Documents/Library.papers3/Articles/1997/Muenke/Am. J. Hum. Genet. 1997 Muenke.pdf%5Cnpapers3://publication/uuid/F2F81EAD-5298-47

Muenke, Maximilian, Schell, U., Hehr, A., Robin, N. H., Losken, H. W., Schinzel, A., … Winter, R. M. (1994). A common mutation in the fibroblast growth factor receptor 1 gene in Pfeiffer syndrome. *Nature Genetics*, *8*(3), 269–274. https://doi.org/10.1038/ng1194-269

Muschelli, J., Ullman, N. L., Mould, W. A., Vespa, P., Hanley, D. F., & Crainiceanu, C. M. (2015). Validated automatic brain extraction of head CT images. *NeuroImage*, *114*, 379–385. https://doi.org/10.1016/j.neuroimage.2015.03.074

Nazir, S., O'Brien, M., Qureshi, N. H., Slape, L., Green, T. J., & Phillips, P. H. (2009). Sensitivity of papilledema as a sign of shunt failure in children. *Journal of AAPOS*, *13*(1), 63–66. https://doi.org/10.1016/j.jaapos.2008.08.003

Nowinski, D., Di Rocco, F., Renier, D., Sainterose, C., Leikola, J., & Arnaud, E. (2012). Posterior cranial vault expansion in the treatment of craniosynostosis. Comparison of current techniques. *Child's Nervous System*, *28*, 1537–1544. https://doi.org/10.1007/s00381-012-1809-6

O'Hara, J., Ruggiero, F., Wilson, L., James, G., Glass, G., Jeelani, O., … Dunaway, D. J. (2019). Syndromic craniosynostosis: Complexities of clinical care. *Molecular Syndromology*, *10*(1–2), 83–97. https://doi.org/10.1159/000495739

Padayachy, L. C., Padayachy, V., Galal, U., Gray, R., & Fieggen, A. G. (2016). The relationship between transorbital ultrasound measurement of the optic nerve sheath diameter (ONSD) and invasively measured ICP in children: Part I: repeatability, observer variability and general analysis. *Child's Nervous System*, *32*(10), 1769–1778. https://doi.org/10.1007/s00381-016-3067-5

Paganini, A., Bhatti-Söfteland, M., Fischer, S., Kölby, D., Hansson, E., O'Hara, J., … Kölby, L. (2019). In search of a single standardised system for reporting complications in craniofacial surgery: a comparison of three different classifications. *Journal of Plastic Surgery and Hand Surgery*, *0*(0), 1–7. https://doi.org/10.1080/2000656X.2019.1626736

Perlyn, C. A., Nichols, C., Woo, A., Becker, D., & Kane, A. A. (2009). Le Premier Siècle. *Journal of Craniofacial Surgery*, *20*(3), 801–806. https://doi.org/10.1097/SCS.0b013e3181843500

Persing, John A. M.D.; Jane, John A. M.D., Ph.D.; Shaffrey, M. M. D. (1989). Virchow and the Pathogenesis of Craniosynostosis: A Translation of His Original Work. *Plastic & Reconstructive Surgery*. https://doi.org/10.1097/00006534-198904000-00025

Pierre-Kahn, K., Hirsch, J. ., Renier, D., Metzger, J., & Maroteaux, P. (1980). Hydrocephalos in Achondroplasia. *Child's Brain*, *7*, 205–219.

Pivnick EK, Kerr NC, Kaufman RA, Jones DP, C. R. (1995). Rickets secondary to phosphate depletion. A sequela of antacid use in infancy. *Clin Pediatr (Phila)*, *34*(2), 73–78. https://doi.org/10.1177/000992289503400202

Rasmussen, S. A., Yazdy, M. M., Carmichael, S. L., Jamieson, D. J., Canfield, M. A., & Honein, M. A. (2007). Thyroid disease as a risk factor for craniosynostosis. *Obstetrics & Gynecology*, *110*(2), 369–377. https://doi.org/10.1097/01.AOG.0000270157.88896.76

Raybaud, C., & Rocco, C. (2007). Brain malformation in syndromic craniosynostoses, a primary disorder of white matter: A review. *Child's Nervous System*, *23*(12), 1379–1388. https://doi.org/10.1007/s00381-007-0474-7

Renier, D., Arnaud, E., Cinalli, G., Sebag, G., Zerah, M., & Marchac, D. (1996). Prognosis for mental function in Apert's syndrome. *Journal of Neurosurgery*, *85*(1), 66–72. https://doi.org/10.3171/jns.1996.85.1.0066

Rich, P. M., Cox, T. C. S., & Hayward, R. D. (2003). The jugular foramen in complex

and syndromic craniosynostosis and its relationship to raised intracranial pressure. *American Journal of Neuroradiology*, *24*(1), 45–51.

Rodgers, W., Glass, G. E., Schievano, S., Borghi, A., Rodriguez-Florez, N., Tahim, A., … Jeelani, N. U. O. (2017). Spring-Assisted Cranioplasty for the Correction of Nonsyndromic Scaphocephaly. *Plastic and Reconstructive Surgery*, *140*(1), 125–134. https://doi.org/10.1097/PRS.0000000000003465

Rollins, N., Booth, T., & Shapiro, K. (2000). MR venography in children with complex craniosynostosis. *Pediatric Neurosurgery*, *32*, 308–315. https://doi.org/10.1159/000028959

Rorden, C., Bonilha, L., Fridriksson, J., Bender, B., & Karnath, H. O. (2012). Age-specific CT and MRI templates for spatial normalization. *NeuroImage*, *61*(4), 957–965. https://doi.org/10.1016/j.neuroimage.2012.03.020

Roy, W. A., Iorio, R. J., & Meyer, G. A. (1981). Craniosynostosis in vitamin D-resistant rickets. A mouse model. *Journal of Neurosurgery*, *55*(2), 265–271. https://doi.org/10.3171/jns.1981.55.2.0265

Rutland, P., Pulleyn, L. J., Reardon, W., Baraitser, M., Hayward, R., Jones, B., … Wilkie, A. O. M. (1995). Idnetical mutations in the FGFR2 gene cause both Pfeiffer and Crouzon syndrome phenotypes. *Nature Genetics*, *9*(february), 173–176.

Saethre, M. (1931). Ein Beitrag zum Turmschiidelproblem (Pathogenese, Erblichkeit und Symptomatologie). . *Dtsch Z Nervenheilk*, *119*(September), 533–555.

Saiepour, D., Nilsson, P., Leikola, J., Enblad, P., & Nowinski, D. (2013). Posterior cranial distraction in the treatment of craniosynostosis - Effects on intracranial volume. *European Journal of Plastic Surgery*, *36*(11), 679–684. https://doi.org/10.1007/s00238-013-0874-8

Scolozzi, P., & Jaques, B. (2008). Computer-aided volume measurement of posttraumatic orbits reconstructed with AO titanium mesh plates: accuracy and reliability. *Ophthalmic Plastic and Reconstructive Surgery*, *24*(5), 383–389.

https://doi.org/10.1097/IOP.0b013e318185a72c

Selber, J. C., Brooks, C., Kurichi, J. E., Temmen, T., Sonnad, S. S., & Whitaker, L. A. (2008). Long-term results following fronto-orbital reconstruction in nonsyndromic unicoronal synostosis. *Plastic and Reconstructive Surgery*, *121*(5), 251–260. https://doi.org/10.1097/PRS.0b013e31816a9f88

Serlo, W. S., Ylikontiola, L. P., Lähdesluoma, N., Lappalainen, O. P., Korpi, J., Verkasalo, J., & Sàndor, G. K. B. (2011). Posterior cranial vault distraction osteogenesis in craniosynostosis: Estimated increases in intracranial volume. *Child's Nervous System*, *27*, 627–633. https://doi.org/10.1007/s00381-010-1353-1

Sgouros, S., Goldin, J. H., Hockley, a D., Wake, M. J., & Natarajan, K. (1999). Intracranial volume change in childhood. *Journal of Neurosurgery*, *91*, 610–616. https://doi.org/10.3171/jns.1999.91.4.0610

Sgouros, S., Goldin, J. H., Hockley, A. D., & Wake, M. J. C. (1996). Posterior skull surgery in craniosynostosis. *Child's Nervous System*, *12*(11), 727–733. https://doi.org/10.1007/BF00366158

Sgouros, S., Hockley, a D., Goldin, J. H., Wake, M. J., & Natarajan, K. (1999). Intracranial volume change in craniosynostosis. *Journal of Neurosurgery*, *91*, 617–625. https://doi.org/10.3171/jns.1999.91.4.0617

Simmons, D. R., & Peyton, W. T. (1947). Premature closure of the cranial sutures. *The Journal of Pediatrics*, *31*(5), 528–547. https://doi.org/10.1016/S0022-3476(47)80142-8

Skau, M., Milea, D., Sander, B., Wegener, M., & Jensen, R. (2011). OCT for optic disc evaluation in idiopathic intracranial hypertension. *Graefe's Archive for Clinical and Experimental Ophthalmology*, *249*(5), 723–730. https://doi.org/10.1007/s00417-010-1527-2

Smith, S. M. (2002). Fast robust automated brain extraction. *Human Brain Mapping*, *17*(3), 143–155. https://doi.org/10.1002/hbm.10062

Spruijt, B., Tasker, R. C., Driessen, C., Lequin, M. H., van Veelen, M. L. C., Mathijssen, I. M. J., & Joosten, K. F. M. (2016). Abnormal transcranial Doppler cerebral blood flow velocity and blood pressure profiles in children with syndromic craniosynostosis and papilledema. *Journal of Cranio-Maxillofacial Surgery*, *44*(4), 465–470. https://doi.org/10.1016/j.jcms.2016.01.001

Spruijt, Bart, Joosten, K. F. M., Driessen, C., Rizopoulos, D., Naus, N. C., van der Schroeff, M. P., … Mathijssen, I. M. J. (2015). Algorithm for the Management of Intracranial Hypertension in Children with Syndromic Craniosynostosis. *Plastic and Reconstructive Surgery*, *136*(2), 331–340. https://doi.org/10.1097/PRS.0000000000001434

Spruijt, Bart, Rijken, B. F. M., den Ottelander, B. K., Joosten, K. F. M., Lequin, M. H., Loudon, S. E., … Mathijssen, I. M. J. (2015). First vault expansion in Apert and Crouzon-Pfeiffer syndromes: Front or Back. *Plastic and Reconstructive Surgery*, 1. https://doi.org/10.1097/PRS.0000000000001894

Steinbacher, D. M., Skirpan, J., Puchała, J., & Bartlett, S. P. (2011). Expansion of the posterior cranial vault using distraction osteogenesis. *Plastic and Reconstructive Surgery*, *127*(2), 792–801. https://doi.org/10.1097/PRS.0b013e318200ab83

Sugawara, Y., Hirabayashi, S., Sakurai, A., & Harii, K. (1998). Gradual Cranial Vault Expansion for the Treatment of Craniofacial Synostosis: A Preliminary Report. *Ann Plast Surg*, *40*, 554–565.

Tamburrini, G., Caldarelli, M., Massimi, L., Santini, P., & Di Rocco, C. (2005). Intracranial pressure monitoring in children with single suture and complex craniosynostosis: A review. *Child's Nervous System*, *21*(10), 913–921. https://doi.org/10.1007/s00381-004-1117-x

Tay, T., Martin, F., Rowe, N., Johnson, K., Poole, M., Tan, K., … Gianoutsos, M. (2006). Prevalence and causes of visual impairment in craniosynostotic syndromes. *Clinical and Experimental Ophthalmology*, *34*(5), 434–440. https://doi.org/10.1111/j.1442-9071.2006.01242.x

Taylor, J. A., Derderian, C. A., Bartlett, S. P., Fiadjoe, J. E., Sussman, E. M., & Stricker, P. A. (2012). Perioperative Morbidity in Posterior Cranial Vault Expansion. *Plastic and Reconstructive Surgery*, *129*(4), 674e-680e. https://doi.org/10.1097/PRS.0b013e3182443164

Taylor, W. J., Hayward, R. D., Lasjaunias, P., Britto, J. a, Thompson, D. N., Jones, B. M., & Evans, R. D. (2001). Enigma of raised intracranial pressure in patients with complex craniosynostosis: the role of abnormal intracranial venous drainage. *Journal of Neurosurgery*, *94*(3), 377–385. https://doi.org/10.3171/jns.2001.94.3.0377

Ter Maaten, N. S., Mazzaferro, D. M., Wes, A. M., Naran, S., Bartlett, S. P., & Taylor, J. A. (2018). Craniometric Analysis of Frontal Cranial Morphology Following Posterior Vault Distraction. *Journal of Craniofacial Surgery*, *29*(5), 1169–1173. https://doi.org/10.1097/SCS.0000000000004473

Thomas, G. P. L., Wall, S. a., Jayamohan, J., Magdum, S. a., Richards, P. G., Wiberg, A., & Johnson, D. (2014). Lessons Learned in Posterior Cranial Vault Distraction. *The Journal of Craniofacial Surgery*, *25*(5), 1721–1727. https://doi.org/10.1097/SCS.0000000000000995

Thompson, D. N. ., Harkness, W. J., Jones, B. M., & Hayward, R. D. (1997). Aetiology of Herniation of the Hindbrain in Craniosynostosis. *Pediatric Neurosurgery*, *26*, 288–295.

Thompson, D. N., Harkness, W., Jones, B., Gonsalez, S., Andar, U., & Hayward, R. (1995). Subdural intracranial pressure monitoring in craniosynostosis: its role in surgical management. *Child's Nervous System : ChNS : Official Journal of the International Society for Pediatric Neurosurgery*, *11*(5), 269–275. https://doi.org/10.1007/BF00301758

Tng, T. T. H., Chan, T. C. K., Hagg, U., & Cooke, M. S. (1994). Validity of cephalometric landmarks . An experimental study on human skulls. *European Journal of Orthodontics*, *16*, 110–120.

Tuite, G. F., Chong, W. K., Evanson, J., Narita, A., Taylor, D., Harkness, W. F., … Hayward, R. D. (1996). The effectiveness of papilledema as an indicator of raised intracranial pressure in children with craniosynostosis. *Neurosurgery*, *38*(2), 272–278. https://doi.org/10.1097/00006123-199602000-00009

Twigg, S. R. F., & Wilkie, A. O. M. (2015). A Genetic-Pathophysiological Framework for Craniosynostosis. *American Journal of Human Genetics*, *97*(3), 359–377. https://doi.org/10.1016/j.ajhg.2015.07.006

Vesalius, A. (1552). *De Humani Corporis Fabrica*. Lugduni: Tornaesium.

Virchow, R. (1851). Ueber den cretinismus, namentlich in Franken: Und euber pathologische Schadelformen. *Verh Phys Med Gesane Wurzburg*, *2*, 230–71.

Wall, S. A., Goldin, J. H., Hockley, A. D., Wake, M. J. C., Poole, M. D., & Briggs, M. (1994). Fronto-orbital re-operation in craniosynostosis. *British Journal of Plastic Surgery*, *47*, 180–184.

Wang, Y., Nie, J., Yap, P. T., Li, G., Shi, F., Geng, X., … Shen, D. (2014). Knowledge-guided robust MRI brain extraction for diverse large-scale neuroimaging studies on humans and non-human primates. *PLoS ONE*, *9*(1), 1–23. https://doi.org/10.1371/journal.pone.0077810

Weinzweig, J., Kirschner, R. E., Farley, A., Reiss, P., Hunter, J., Whitaker, L. A., & Bartlett, S. P. (2003). Metopic synostosis: Defining the temporal sequence of normal suture fusion and differentiating it from synostosis on the basis of computed tomography images. *Plastic and Reconstructive Surgery*, *112*(5), 1211–1218. https://doi.org/10.1097/01.PRS.0000080729.28749.A3

White, N., Evans, M., Dover, S., Noons, P., Solanki, G., & Nishikawa, H. (2009). Posterior calvarial vault expansion using distraction osteogenesis. *Child's Nervous System*, *25*(2), 231–236. https://doi.org/10.1007/s00381-008-0758-6

Wiegand, C., & Richards, P. (2007). Measurement of intracranial pressure in children: a critical review of current methods. *Developmental Medicine and Child Neurology*, *49*(12), 935–941. https://doi.org/10.1111/j.1469-8749.2007.00935.x

Wilkie, a O., Tang, Z., Elanko, N., Walsh, S., Twigg, S. R., Hurst, J. a, … Maxson, R. E. (2000). Functional haploinsufficiency of the human homeobox gene MSX2 causes defects in skull ossification. *Nature Genetics*, *24*(4), 387–390. https://doi.org/10.1038/74224

Wilkie, A. O M. (1997). Craniosynostosis: Genes and mechanisms. *Human Molecular Genetics*, *6*(10 REV. ISS.), 1647–1656. https://doi.org/10.1093/hmg/6.10.1647

Wilkie, Andrew O M, Bochukova, E. G., Hansen, R. M. S., Taylor, I. B., Rannan-Eliya, S. V., Byren, J. C., … Lester, T. (2006). Clinical dividends from the molecular genetic diagnosis of craniosynostosis. In *American Journal of Medical Genetics, Part A* (Vol. 140, pp. 2631–2639). https://doi.org/10.1002/ajmg.a.31366

Xu, W., Gerety, P., Aleman, T., Swanson, J., & Taylor, J. (2016a). Noninvasive methods of detecting increased intracranial pressure. *Child's Nervous System*, *32*(8), 1371–1386. https://doi.org/10.1007/s00381-016-3143-x

Xu, W., Gerety, P., Aleman, T., Swanson, J., & Taylor, J. (2016b). Noninvasive methods of detecting increased intracranial pressure. *Child's Nervous System*, 1371–1386. https://doi.org/10.1007/s00381-016-3143-x

York, D. H., Pulliam, M. W., Rosenfeld, J. G., & Watts, C. (1981). Relationship between visual evoked potentials and intracranial pressure. *Journal of Neurosurgery*, *55*(6), 909–916. https://doi.org/10.3171/jns.1981.55.6.0909

Yushkevich, P. A., Piven, J., Hazlett, H. C., Smith, R. G., Ho, S., Gee, J. C., & Gerig, G. (2006). User-guided 3D active contour segmentation of anatomical structures: Significantly improved efficiency and reliability. *NeuroImage*, *31*(3), 1116–1128. https://doi.org/10.1016/j.neuroimage.2006.01.015

Appendix A **LIST OF PUBLICATIONS**

A.1 Peer reviewed journal articles directly related to this work

1. **Breakey, R. W. F.,** Knoops, P. G. M., Borghi, A., Rodriguez-Florez, N., Hayward, R., Dunaway, D. J., . . . Jeelani, N. U. O. (2017). Intracranial volume measurement: A systematic review and comparison of different techniques. *Journal of Craniofacial Surgery*, *28*(7), 1746-1751. https://doi.org/10.1097/SCS.0000000000003929

2. **Breakey, R. W. F.,** Knoops, P. G. M., Borghi, A., Rodriguez-Florez, N., O'Hara, J., James, G., … Jeelani, N. U. O. (2018). Intracranial Volume and Head Circumference in Children with Unoperated Syndromic Craniosynostosis. *Plastic and Reconstructive Surgery*, 142(5), 708e-717e. https://doi.org/10.1097/PRS.0000000000004843

A.2 Other peer reviewed journal articles

3. Misier, K. R. R. R., **Breakey, R. W. F.,** Caron, C. J. J. M., Schivano, S., Dunaway, D. J., Koudstaal, M. J., . . . Borghi, A. (2020). Correlation of intracranial volume with head surface volume in patients with multisutural craniosynostosis. *Journal of Craniofacial Surgery* [Online ahead of print] https://doi.org/10.1097/SCS.0000000000006372

4. Knoops, P. G. M., Papaioannou, A., Borghi, A., **Breakey, R. W. F.,** Wilson, A., Jeelani, N. U. O., . . . Schievano, S. (2019). A machine learning framework for automated computer-assisted diagnosis and planning in plastic and reconstructive surgery. *Scientific Reports, 9*, 13597. https://doi.org/10.1038/s41598-019-49506-1

5. Knoops, P. G. M., Borghi, A., **Breakey, R. W. F.**, Ong, J., Jeelani, N. U. O., Bruun, R., . . . Padwa, B. L. (2018). Three-dimensional soft tissue prediction in orthognathic surgery: A clinical comparison of Dolphin, ProPlan CMF, and

probabilistic finite element modelling. *International Journal of Oral & Maxillofacial Surgery 48*(4) 511-518. https://doi.org/10.1016/j.ijom.2018.10.008

6. Knoops, P. G. M., Beaumont, C. A. A., Borghi, A., Rodriguez-Florez, N., **Breakey, R. W. F.,** Rodgers, W., . . . Dunaway, D. J. (2017). Comparison of 3D scanners for craniomaxillofacial imaging. *Journal of Plastic, Reconstructive, and Aesthetic Surgery*, *70*(4), 441-449. https://doi.org/10.1016/j.bjps.2016.12.015

7. Knoops, P. G. M., Borghi, A., Ruggiero, F., Badiali, G., Bianchi, A., Marchetti, C., . . . Schievano S. (2018). A novel soft tissue prediction methodology for orthognathic surgery using probabilistic finite element modelling. *PLoS ONE*, *13*(5), e0197209. https://doi.org/10.1371/journal.pone.0197209

8. Sharma, J. D., O'Hara, J. L., Borghi, A., Rodriguez-Florez, N., **Breakey, W.,** Ong, J., . . . James, G. (2018). Results following adoption of a modified Melbourne technique of total scaphocephaly correction. *Journal of Craniofacial Surgery, 29*(5), 1117-1122. https://doi.org/10.1097/SCS.0000000000004593

9. Rodgers, W., Glass, G. E., Schievano, S., Borghi, A., Rodriguez-Florez, N., Tahim, A., . . . Jeelani, N. U. O. (2017). Spring assisted cranioplasty for the correction of non-syndromic scaphocephaly: A quantitative analysis of 100 consecutive cases. *Plastic and Reconstructive Surgery*, *140*(1), 125-134. https://doi.org/10.1097/PRS.0000000000003465

A.3 Peer reviewed conference publications directly related to this work

1. **Breakey, R. W. F.,** Knoops, P. G. M., Borghi, A., Rodriguez-Florez, N., Dunaway, D. J., . . . Jeelani, N. U. O. (2015, September 14-18). *Intracranial volume measurement: A systematic review and comparison of different techniques* [Oral presentation]. 15th Congress of the International Society of Craniofacial Surgery, Tokyo, Japan.

2. **Breakey, R. W. F.,** Knoops, P. G. M., Borghi, A., Rodriguez-Florez, N., O'Hara, J., James, G., . . . Jeelani, N. U. O. (2017, October 24-28). *Intracranial volume and head circumference in children with unoperated syndromic craniosynostosis* [Oral presentation]. 17th Congress of the International Society of Craniofacial Surgery, Cancun, Mexico.

3. van de Lande, L. S., **Breakey, R. W. F.,** Borghi, A., O'Hara, J., James, G., Ong, J. L., . . . Jeelani, N. U. O. (2019, October 4-6 and 20-24). *Posterior vault expansion using springs: A retrospective analysis of 177 consecutive cases* [Oral presentation]. 20th Biennial Meeting of the European Society of Craniofacial Surgery, Athens, Greece, and 47th Annual Meeting of the International Society for Paediatric Neurosurgery, Birmingham, UK.

4. **Breakey, R. W. F.**, Knoops, P. G. M., van de Lande, L. S., Borghi, A., O'Hara, J., James, G., . . . Jeelani, N. U. O. (2018, October 4-6). *Paediatric optic nerve sheath diameter measurements in 95 spring assisted posterior vault expansion cases* [Oral presentation]. 20th Biennial Meeting of the European Society of Craniofacial Surgery, Athens, Greece.

5. **Breakey, R. W. F.,** Mercan, E., van de Lande, L., Knoops, P., O'Hara, J., Birgfeld, C., . . . Hopper, R. (2019, September 16-19 and December 4-6). *A two-center comparison of three techniques for posterior cranial expansion in syndromic craniosynostosis* [Oral presentation]. 18th Biennial Meeting of the International Society of Craniofacial Surgery, Paris, France, and Winter Scientific Meeting of the British Association of Plastic, Aesthetic and Reconstructive Surgeons, Monte Carlo, Monaco.

Appendix B **COMMAND LINE SCRIPTS**

```
#!/bin/sh
  for filename in *.nii ; do
    fname=`$FSLDIR/bin/remove_ext ${filename}`
    echo $fname OPENED 1/9
    fslmaths ${fname} -thr 0.000 -uthr 100.000 ${fname}_thresh
    # mv ${fname}.nii ${fname}_norm.nii.gz
    echo $fname THRESHOLDED 2/9
# now smooth
 fslmaths ${fname}_thresh -s 1 ${fname}_thresh_smoothed
    echo $fname SMOOTHED 3/9
# rethreshold the smoothed file
   fslmaths ${fname}_thresh_smoothed -thr 0.000 -uthr 100.000 ${fname}_rethresh
   echo $fname RETHRESHOLDED 4/9
#BET
  bet ${fname}_rethresh  ${fname}_rethresh_bet -f 0.25 -R -B -m
echo $fname BET_PERFORMED 5/9
  fslmaths ${fname}_rethresh_bet -bin -fillh ${fname}_rethresh_bet_mask
echo $fname    BINARISED AND FILLED 5/9
 fslstats ${fname}_rethresh_bet_mask -V >> file.txt
echo $fname VOLUME CALCULATED AND WRITTEN TO TEXT FILE 9/9
     fslstats ${fname}_rethresh_bet_mask -V

done
```